THE CLOSING OF RESONANCE HORNS FOR PERIODICALLY FORCED OSCILLATORS

A THESIS
SUBMITTED TO THE FACULTY OF THE GRADUATE SCHOOL
OF THE UNIVERSITY OF MINNESOTA

BY

BRUCE BARTLETT PECKHAM

IN PARTIAL FULFILLMENT OF THE REQUIREMENTS
FOR THE DEGREE OF
DOCTOR OF PHILOSOPHY

1988

Acknowledgements

Several people were instrumental in my transition from a mathematical neophyte to a degree holder. Discussions with Dick Hall at the beginning, Yannis Kevrekidis in the middle, Rick Moeckel at the end, and Don Aronson and my advisor Dick McGehee throughout were especially helpful. Their interest in me and my work were as important to me as the many mathematical insights they provided. Dick McGehee, in particular, had a way of making his contributions feel like my own ideas.

I would also like to acknowledge the slow but persistent work done by the typist, Bruce B. Peckham.

This work was partially supported by NSF grants DMS 85-06634, DMS 86-01907, and DMS 87-03429.

Corrections:

p81 add strong stable mflds to #26

p83 #4 no inner circle

#8 add stable mflds

A2 add strong stable mflds

#7 add 2 arrows

p45 [AMKA] s/b [ACHA]

p31 Lemma 2 s/b Lemma 3.8

p79 label secondary hyp curve

p77 add arrows to unst. mflds on 12

p85 Add Gambaudo to ref list

p4 ± in sn. b.f.

p17 x = y

p [illegible] Figure 2 [illegible] Figure 3

p62 on 4th period doubling

p5 x s/b y in Bry unfolding

p86 in MSA Sond s/b Land

p69 reverse last 2 y arrows in q:1
add arrows to f^2 f^4

p79 relabel "s-n of inner curves" curve (Obtg of 445-28-9

Bruce Bartlett Peckham

Thesis Abstract

The Closing of Resonance Horns for Periodically Forced Oscillators

A two-parameter family of maps of the plane is generated by varying the forcing frequency ω and amplitude α of a planar oscillator with unforced frequency ω_0. For small forcing amplitude, resonance horns open into the first quadrant of the parameter plane from every point on the α=0 axis where ω_0/ω = p/q is rational. Inside the "p/q resonance horn," the corresponding phase portraits contain at least one period q orbit, with rotation number p/q. In this thesis, we investigate the continuation of resonance horns which terminate at some higher forcing amplitude, where the small amplitude theory is no longer applicable.

We define a "self rotation number" for an orbit that allows us to define a "p/q resonance surface" as a component of the closure of the set of period q points with self rotation number p/q. Its projection to the parameter space is a "p/q resonance horn." We show that the closure operation can add only fixed points with an eigenvalue $e^{2\pi ip/q}$ to the surface.

This enables us to enumerate all possible bifurcations associated with a p/q surface. The generic unfoldings of these surfaces imply that all such surfaces are two-manifolds. When the surfaces are compact, we classify them topologically. In addition, we show that if either the period is even, or the resonance surface is orientable, a compact resonance surface must have a fixed point associated with it.

The rest of the results of the thesis are concerned with the way these individual resonance surfaces and horns fit together to form a complete bifurcation picture. Except for the low period (strong resonance) cases, the resonance horns all tend to run from the zero forcing line to a Hopf bifurcation curve. Notable exceptions are the period-one and period-two horns, whose closings involve "breaks" in the Hopf bifurcation curve. These breaks allow the phase portraits to pass from an attracting invariant topological circle, that exists for small forcing amplitude, to an attracting fixed point at a high amplitude of forcing, without ever undergoing a Hopf bifurcation.

TABLE OF CONTENTS

1. INTRODUCTION

Phenomena which can be modelled by nonlinear forced oscillators occur in many fields of science and engineering. If one considers the amplitude and frequency of forcing as parameters, this parameter space can be divided up into regions in which the behavior of the forced oscillator is qualitatively the same. The local theory for such a bifurcation analysis, that is, the theory for small forcing amplitude, has been well developed: the parameter space is separated by "resonance horns" (entrainment regions, Arnol'd tongues) emanating from the frequency axis (zero forcing amplitude). This theory, obtained via circle map theory, is summarized in Sections 2.4 and 2.5 below. Section 2.2 includes a description of a similar situation in which resonance horns emanate from a Hopf bifurcation curve in a two-parameter space. The results presented in this paper provide a connection between these two "local" situations. Following the lead of Aronson, McGehee, Kevrekidis, and Aris [AMKA], we investigate the global structure of these resonance horns as they are continued beyond the region of small forcing amplitude where they are known to exist. As in [AMKA], we define "resonance surfaces" (surfaces of periodic points) in the phase×parameter space that project, at least for small forcing amplitude, to the "usual" resonance horns. Specifically we look at compact resonance surfaces. The corresponding resonance horns "close" or "terminate" at some amplitude of forcing. Some structure of the surfaces in the phase×parameter space is necessary for this phenomenon to occur. The completion of proofs of the conjectures introduced in [AMKA] are among the results introduced here.

Many of the results in this paper assume that, for positive amplitude of forcing, the family of maps generated by return maps of the forced planar oscillator flow are *generic*, smoothly varying (at least C^1 with respect to the parameters) two-parameter families of C^r diffeomorphisms of the plane. Therefore, only codimension-one and codimension-two bifurcations can occur. The generic unfoldings of such bifurcations, summarized in Section 2.2, tells us exactly what must be happening nearby in phase×parameter space. This local knowledge helps us piece together the global picture for the resonance surfaces.

Chapter 3 introduces the concept of the "self rotation number" of an orbit, a generalization of the "familiar" rotation number as defined in Section 2.3 for circle maps, annulus maps, and planar maps with a fixed point. The properties of this self

rotation number allow us to globally define a specific resonance surface whose projection to the parameter space will be a specific resonance horn. This self rotation number also aids us, in Section 3.4, to characterize all possible points on a resonance surface, and to classify all generic bifurcations associated with an individual resonance surface. Thus armed, we are able to topologically classify individual resonance surfaces (Section 3.5), and complete the proofs of results which include the conjectures of [AMKA] (Chapter 5).

Chapter 6 looks at typical bifurcation diagrams associated with each individual resonance surface, and pieces together the results to get some structure typical of the bifurcation diagram for any forced oscillator in the plane.

Many of the above results were suggested by numerical investigation of a specific two-parameter family of maps of the plane. In Chapter 4, we discuss this particular map, as well as the numerical techniques and theory we employed.

Chapter 7 indicates some extensions of results developed in this paper to applications other than forced oscillators.

2. PRELIMINARY THEORY - A SUMMARY OF KNOWN RESULTS

2.1 Continuous vs. Discrete Dynamics for Periodically Varying Vector Fields

Consider the following k-parameter family of nonautonomous differential equations

$$\frac{dx}{dt} = v(x,t,\mu),\ v \in C^1(M^n \times \mathbb{R} \times \mathbb{R}^k \rightarrow \mathbb{R}^n) \qquad \{2.1\}$$

where v is periodic with smoothly varying (C^1) period $T(\mu)$ in its second variable, t, and M^n is an n-dimensional manifold. Standard O.D.E. theory [Hale] implies the existence of a function $\phi \in C^1(M^n \times \mathbb{R} \times \mathbb{R} \times \mathbb{R}^k \rightarrow \mathbb{R}^n)$, called the flow of {2.1}, which satisfies the initial value problem:

$$\frac{\partial \phi(x_0,t_0,t,\mu)}{\partial t} = v(x,t,\mu), \qquad \phi(x_0,t_0,t_0,\mu) = x_0. \qquad \{2.2\}$$

The flow ϕ induces a C^1 family of orientation preserving diffeomorphisms, f_μ, of M^n via the "time $T(\mu)$ stroboscopic map" (equivalently, the "time $T(\mu)$ Poincare map") for any fixed value of t_0:

$$f_\mu(x) \equiv \phi(x,t_0,t_0+T(\mu),\mu) \qquad \{2.3\}$$

ϕ C^1 in all its arguments together implies $f_\mu(x)$ is C^1 in x and μ together.

Conversely, ϕ is called a "suspension" of the map(s) f_μ. Thus, for a fixed value of t_0, we have the choice of investigating the n+1+k dimensional continuous flow, ϕ, or the discrete n+k dimensional mapping, f.

Comments:

1. Among the relationships between f and ϕ, is the 1-1 correspondence between closed orbits of ϕ and the periodic orbits of f. The stability of the two corresponding orbits must also coincide.

2. For a fixed t_0, {2.3} uniquely defines the corresponding family of diffeomorphisms, f_μ, but, given a family of diffeomorphisms, "the" corresponding family of suspensions is not unique.

3. If we append the equation $\frac{dt}{dt} = 1$ to {2.1}, then we can think of the appended system as an autonomous vector field in the n+1 variables $(\mathbf{x}, t)$. (The μ variables are still parameters.) For each fixed μ, ϕ can then be viewed as a flow on $M^n \times \mathbb{S}$.

2.2 Local Fixed Point Bifurcations

Local bifurcation theory is built on the concepts of universal unfoldings and center manifold theory. Because we are interested in two-parameter families of maps of the plane, we describe the universal unfoldings for all local codimension-one and codimension-two bifurcations of fixed points for maps of the plane. Whenever we come across any of the following points in a generic two-parameter family of maps of the plane, then, in a neighborhood of such a point in phase × parameter space, the map we have must be topologically equivalent to the corresponding universal unfolding below. (In order to get the picture in the full four-dimensional space, we have added a parameter ε_2 to the codimension-one unfoldings: each slice corresponding to ε_2=constant is a copy of the one-parameter diagram. Points in the one-parameter diagram become lines and curves become two-dimensional surfaces. If the original bifurcation involves only a one-dimensional center manifold, we append the equation $f_\varepsilon(y)=2y$ or $\frac{1}{2}y$, depending on the stability of the nonsingular eigenvalue. Diagrams of recurrent sets are restricted to {y=0}, however, so they "look" the same as in the one-dimensional phase case.)

Codimension-one

Table 2.1

Name	Universal Unfolding	Ref's	Figure
Saddle-node	$f_\varepsilon(x) = x + \varepsilon \pm x^2$	Ar, GH	2.1
Period Doubling	$f_\varepsilon(x) = (\varepsilon\text{-}1)x \pm x^3$	Ar, GH	2.2

Hopf (nonresonant case)	$f_\varepsilon(r,\theta)=((1+\varepsilon)r \pm r^3, \theta+\omega)$ (ω is non resonant, i.e., $\omega \neq 2\pi p/q$)	Ar, GH	2.2,x=r

Codimension-two

Table 2.2

Name	Universal Unfolding	Ref's	Figure
Cusp (Saddle-node with a higher order degeneracy)	$f_\varepsilon(x)=\varepsilon_1 + (\varepsilon_2 + 1)x \pm x^3$	Ar, GH	2.3
Degenerate Period Doubling (w/ higher order degeneracy)	$f_\varepsilon(x)= (\varepsilon_1-1)x + \varepsilon_2 x^3 \pm x^5$	PK	2.4
Degenerate Hopf (w/ higher order degeneracy)	$f_\varepsilon(r,\theta)=((1+\varepsilon_1)r+\varepsilon_2 r^3 \pm r^5, \theta+\omega)$ (ω is nonresonant)	Ta2,GH	2.4,x=r

Hopf with Resonance: $\lambda_{1,2}=e^{\pm 2\pi i p/q}$. This is most complicated group of codimension-two bifurcations (with the possible exception of the degenerate Hopf, which we use very little in this paper). When $q \geq 3$, we can use complex coordinates: $z = x + iy$; the two parameters are represented by the complex parameter ε. When q=1 or 2, $y = \dot{x}$. In all the below cases, the "unfoldings" are not for the discrete map with the indicated resonant eigenvalues, but for the differential equation which approximates the q^{th} iterate of the map in the sense that, up to terms of degree q+1, the orbits of the q^{th} iterate of the map follow the flow lines of the differential equation.

$q \geq 5$	$\dot{z}= \varepsilon z + z\lvert z\rvert^2 A(\lvert z\rvert^2) + B\bar{z}^{q-1}$	Ar,Ta	2.5
q=4	$\dot{z} = \varepsilon z + Az\lvert z\rvert^2 + \bar{z}^3$	Ar,Ta	
q=3	$\dot{z} = \varepsilon z + Az\lvert z\rvert^2 + \bar{z}^2$	Ar,Ta	2.6
q=2 (Double -1)	$\ddot{x} = \varepsilon_1 x + 2\varepsilon_2 y \pm x^3 - 2x^2 y$	Ar,Ta	2.7
q=1 (Bogdanov)	$\ddot{x}= \varepsilon_1 + \varepsilon_2 \dot{x} + x^2 \pm xy$	Ar,Ta	2.8

Note the following about the resonant Hopf cases:

1. If $q \geq 5$, $\varepsilon = \mathbf{0}$ lies on a Hopf bifurcation line in the parameter space and is the tip of a "resonance horn" opening on one side of the Hopf line. The boundaries of the horn are saddle-node bifurcations for the q^{th} iterate of the map which become tangent of order $\frac{q-2}{2}$ as we approach $\varepsilon = \mathbf{0}$.

2. If $q=3$, $\varepsilon = (0,0)$ lies on a Hopf bifurcation line, but the bifurcation involves only the three saddles, not q saddles and q sinks as is the case for $q \geq 5$. Also, the period three saddles exist for ε in a full punctured neighborhood of (0,0), not just in a horn emanating from (0,0) in the parameter space.

3. When $q=4$, we get the following two cases:
   A. $|\mathbf{A}|<1$. The bifurcation involves only a single period-four orbit of saddle points; they exist in a full punctured neighborhood of $\varepsilon = \mathbf{0}$. The phase portraits are analogous to the $q=3$ case.
   B. $|\mathbf{A}|>1$. The $\varepsilon = \mathbf{0}$ point is the tip of a "resonance horn" inside which there exist one period-four saddle orbit, and one period-four node orbit. These orbits coalesce in saddle-node bifurcations on the boundaries of the resonance horn. Thus, the periodic points behave analogously to the $q \geq 5$ case. The phase portraits, however, may or may not be analogous, depending more delicately on **A**; all cases are not completely known at this time. A further difference with the $q \geq 5$ case is that the sides of the resonance horn do not become tangent at $\varepsilon = \mathbf{0}$, but open at an angle between 0 and π.

4. The bifurcation diagrams given for the above differential equations are the same as for the corresponding map which we were investigating in the first place, with the following exception: curves in parameter space for the flow that represent coincidence of a stable and an unstable manifold, that is, a global bifurcation, such as the homoclinic or heteroclinic orbits in the $q=1,2,3$ cases, become regions of manifold crossings in the parameter space bifurcation diagram for the map.

Golubitsky and Schaeffer [GS] also treat all of the above bifurcations, but from a slightly different perspective.

Continuation Theory

Let $\{\mathbf{f}_\mu\}$ be a two-parameter family of C^r maps of the plane, varying smoothly (C^1) with respect to μ. Define

$$\Gamma(1) \equiv \{(\mathbf{x},\mu) \in \mathbb{R}^2 \times \mathbb{R}^2 : \mathbf{f}_\mu(\mathbf{x}) = \mathbf{x}\}$$

$$Z(1) \equiv \{(\mathbf{x},\mu) \in \Gamma(1) : D_\mathbf{x}\mathbf{f}_\mu(\mathbf{x}) \text{ has an eigenvalue equal to } 1\}$$

$$D(1) \equiv \{(\mathbf{x},\mu) \in \Gamma(1) : D_\mathbf{x}\mathbf{f}_\mu(\mathbf{x}) \text{ has an eigenvalue equal to } -1\} \qquad \{2.4\}$$

$$H(1) \equiv \{(\mathbf{x},\mu) \in \Gamma(1) : D_\mathbf{x}\mathbf{f}_\mu(\mathbf{x}) \text{ has eigenvalues } \lambda_1,\lambda_2 \text{ with } \lambda_1 \cdot \lambda_2 = 1\}$$

$$E(1) \equiv \{(\mathbf{x},\mu) \in (\Gamma(1) : D_\mathbf{x}\mathbf{f}_\mu(\mathbf{x}) \text{ has eigenvalues } \lambda_1,\lambda_2 \text{ with } \lambda_1 = \lambda_2\}$$

The implicit function theorem implies that, generically, each component of $\Gamma(1)$ is a smooth (C^r) two-dimensional surface, and each component of $Z(1)$, $D(1)$, $H(1)$, $E(1)$ is a smooth (C^{r-1}) curve without endpoints, all embedded in $\mathbb{R}^4$. (See {4.4} and {4.5} for the actual equations describing the above sets.) The loss of smoothness in the curves is due to an equation involving eigenvalues, and thus first derivatives with respect to phase variables, in the definition of each set.

Claim 2.1: Generically, $Z(1)$ consists of

1) Simple saddle nodes

2) Bogdanov points

3) Cusp points

Sketch of Proof: The universal unfoldings of the simple saddle node (in either GH or A) give three nondegeneracy conditions, all generically holding in a one-parameter family. With two parameters, any one of these degeneracies may now exist. The Bogdanov point (a second eigenvalue on the unit circle) and the cusp point (a zero in a higher order term) are two of these. The third type involves a degeneracy with respect to a parameter. Because we have two parameters, however, a degeneracy with respect

to one parameter does not change the bifurcation. We can simply use the other parameter as our "continuation" parameter. In two-parameter families, at least one of the parameters will be "nondegenerate."

By similar arguments, we see that, generically, D(1) consists of

1) Simple period doublings

2) Double -1 eigenvalue points

3) Degenerate period doubling points

and H(1) consists of

1) Simple, nonresonant Hopf bifurcations

2) Degenerate (generalized) nonresonant Hopf bifurcations

3) Resonant Hopf bifurcations

4) Saddle points (not bifurcation points)

E(1) is not a true bifurcation set, only a curve separating nodes from foci. We will have no need to characterize its points as we have done with the other sets.

When dealing with periodic points of period $q \geq 2$, we can work with f_μ^q instead of just f_μ. The symmetry introduced implies:

1) When all points on an orbit are distinct, and any of the above bifurcations occurs for f_μ^q, the same bifurcation occurs simultaneously at each point on the orbit of the bifurcation point. Copies of the universal unfoldings for the fixed point bifurcations occur in a neighborhood of each point on the "bifurcation orbit."

2) When point(s) on an orbit do interact, the symmetries involved typically make the generic bifurcation different from the corresponding fixed point case. Heureristically, this can be explained with two comments. First, the q copies of the bifurcation now interact, so we shouldn't expect to obtain anything similar to the a fixed point bifurcation. Second, arbitrary perturbations of f_μ^q

3. $\rho(x,f) = p/q$ if and only if f has a periodic orbit of period q.

Annulus Maps

We can define rotation numbers for annulus maps $f:A\to A$, $A=I\times\mathbb{S}$, where I is an interval of the real line (with or without endpoints). Simply "lift" f to a degree one map $\tilde{f}$ ($\pi_\theta(\tilde{f}(a,\theta+2\pi)) = \pi_\theta(\tilde{f}(a,\theta)) + 2\pi$, where π_θ is the projection onto the second coordinate) of the universal covering space $I\times\mathbb{R}$ of A. Define

$$\rho(x,f) \equiv \lim_{k\to\infty} \frac{\pi_\theta(\tilde{f}^k(x)) - \pi_\theta(x)}{2\pi k} \qquad \{2.6\}$$

where $x = (a,\theta)$.

Maps of the Plane

For circle maps and annulus maps the "center" of the circle or annulus is a natural point around which to measure rotation. For maps of the plane, there exists no such center point. Whenever a planar map has a fixed point x_0, however, we can use it as a reference point. Any other point x in the plane can be written in the polar coordinates $(a,\theta)\in(0,\infty)\times\mathbb{S}$ defined by

$$x = x_0 - \begin{pmatrix} a\cos\theta \\ a\sin\theta \end{pmatrix} \qquad \{2.7\}$$

For $a \neq 0$, these coordinates make the planar map an annulus map, so {2.6} serves as a definition for the rotation number of points in the plane "around x_0."

We will return to further generalizations of the rotation number later in the paper. See, in particular, Sections 3.1 and 3.3.

Caution: Unlike rotation numbers for diffeomorphisms of the circle, the limits used in defining rotation numbers for annulus and planar maps do not always exist.

2.4 Two-parameter Families of Circle Maps

In order to set the stage for the primary object of study in this paper, the periodically forced planar oscillator, we now discuss a two-parameter family of circle maps that are perturbations of rigid rotations of the circle. [Hall]

Let $f:\mathbb{S}\rightarrow\mathbb{S}$ be defined by

$$f(\theta) = \theta + 2\pi\omega_0 + \alpha g(\theta) \qquad \{2.8\}$$

where ω_0 and α are scalar parameters which we group for convenience as $\mu=(\omega_0,\alpha)$, and $g(\theta)$ satisfies

1. $g\in C^1$, $|g'(\theta)| \leq 1$
2. For all $\theta\in\mathbb{R}$, $g(\theta+2\pi) = g(\theta)$ $\qquad \{2.9\}$
3. $\int_0^{2\pi} g(\theta)\, d\theta = 0$

The standard theory implies the existence of "resonance horns," similar to those associated to the Hopf bifurcations with resonance for $q\geq 5$, in the μ parameter space. Assumption 1 above on g implies that f_μ is a homeomorphism as long as $\alpha<1$. The uniqueness of rotation numbers for homeomorphisms implies that these resonance horns cannot overlap in the region where $\alpha<1$. The horns emanate from every point on the ω_0 axis where ω_0 is rational: $\omega_0 = p/q$, $(p/q) = 1$. Inside these horns, the phase portrait of $f_\mu{}^q$ is a "circle in resonance," containing a period q attracting orbit alternating with a period q repelling orbit. Figure 2.9 shows a typical horn with corresponding one-parameter families of phase trajectories and manifolds for $f_\mu{}^q$, $q=3$, on a one parameter cut α=constant, across the horn. (Let $\omega = 1$ for the diagram.) Ignore the manifolds and orbits off the invariant circle in the phase diagrams; they will be used in the next section. Compare Figure 2.9 with Figure 2.5. Figure 2.10 shows the locus of period-three points corresponding to the same one-parameter cut α=constant of Figure 2.9, along with its projection to the phase plane. Again, we have embedded $\mathbb{S}$ in the

plane so we can refer to the same diagram in the next section. The labels will also be explained later.

General Horn Comments

1. Horns exist for $q \geq 1$ with the circle map, but only for $q \geq 5$ with the Hopf bifurcation.

2. Circle map horn boundaries are wedge-shaped, while Hopf horn boundaries are tangent of order $(q-2)/2$ (for $q \geq 5$). Recall that for the $q=4$ Hopf bifurcation, when a resonance horn exists, it is wedge shaped. This is consistent with the $(q-2)/2$ contact order. Typically, in both cases, the horn width decreases as q increases.

2.5 Forced Planar Oscillators: Small Forcing Amplitude

Forced oscillators are the main object of study in this paper. We will start our basic forced oscillator model from the system

$$\frac{d\mathbf{x}}{dt} = \mathbf{F}(\mathbf{x}(t)) \ , \quad \mathbf{F}: \mathbb{R}^2 \to \mathbb{R}^2 \quad , \mathbf{F} \in C^1(\mathbb{R}^2) \qquad \{2.10\}$$

which we assume to have a normally hyperbolic stable closed orbit C_0 of frequency ω_0. Consider the two-parameter family of forced oscillations

$$\frac{d\mathbf{x}}{dt} = \mathbf{F}(\mathbf{x}) + \alpha\, \mathbf{G}(\mathbf{x}, \omega t) \quad , \omega \neq 0 \qquad \{2.11\}$$

where $G \in C^1(\mathbb{R}^2 \times \mathbb{R})$ has period 1 in its second variable. The amplitude of forcing, α, and the frequency of forcing, ω, are the two parameters. This equation is a special form of equation {2.1}. In particular, $\mu=(\omega,\alpha)$. The period of the forcing $T(\mu)=1/\omega$, which is certainly smoothly dependent on μ as long as $\omega \neq 0$. The family of maps we wish to study is:

$$\mathbf{x} \to \mathbf{f}_\mu(\mathbf{x}), \quad \mathbf{f}_\mu: \mathbb{R}^2 \to \mathbb{R}^2, \quad \mu=(\omega,\alpha) \in \mathbb{R}^2 \qquad \{2.12\}$$

where $\mathbf{f}_{(\omega,\alpha)}(\mathbf{x})\equiv\phi(\mathbf{x},t_0, t_0+1/\omega, (\omega,\alpha))$, for some fixed value of t_0. ϕ is the flow of {2.11} as defined in section 2.1.

The attracting orbit C_0 of the unforced system {2.10} ensures that C_0 is an attracting invariant circle for {2.12} if $\alpha=0$. Moreover, $\alpha=0$ implies that $\mathbf{f}_\mu$ restricted to C_μ is a rigid rotation. For small $\alpha>0$, normal hyperbolicity causes this invariant circle $C_{(\omega,\alpha)}$ to persist. Thus, for small $\alpha>0$, $\mathbf{f}_\mu|_{C_\mu}$ is a perturbation of a rigid rotation to which the theory of the previous section applies. For $\alpha=0$, the unforced period $1/\omega_0$ cycle, strobed at a time interval of $1/\omega$ to obtain $\mathbf{f}_\mu|_{C_\mu}$, $\mu=(\omega,0)$, results in a rotation number of ω_0/ω. This ratio turns out to be a more convenient parameter than ω. Consequently, we will let $\mu = (\omega_0/\omega,\alpha)$ from now on. For small $\alpha>0$, we again have horns in the parameter space emanating from every point on the ω_0/ω axis where ω_0/ω = p/q. Inside these horns, the phase portrait of $\mathbf{f}_\mu^q$ restricted to C_μ is a "circle in resonance," containing a period q attracting orbit alternating with a period q saddle orbit. Both orbits have a rotation number p/q, as do all points on C_μ. See Figure 2.9 again for the one-parameter cut $\{\alpha=\alpha_0\}$.

Note:

1. In Figure 2.9, the phase portraits are not restricted to C_μ, so the attractor-repeller pair on C_μ becomes a node-saddle pair in $\mathbb{R}^2$.

2. Except for the tip, the boundary of the horn consists of saddle-node bifurcations.

3. In Figure 2.10, we see the saddle-node pairing of $\mathbf{f}_\mu^q$ changes as we cross the horn. The saddle s_1 is paired with node n_1 on the left boundary, n_3 on the right boundary. We will exploit this change in pairing in Chapter 6.

4. G a generic two-parameter family of vector fields makes us expect $\mathbf{f}_\mu$ to be a generic two-parameter family for $\alpha>0$, which would, in turn, make $\mathbf{f}_\mu$ restricted to C_μ a generic two-parameter family of circle maps for $\alpha>0$. For $\alpha=0$ $\mathbf{f}_\mu$ is the time T map of a flow, which is definitely not generic.

5. As $\mu \rightarrow$ tip of the horn from "inside" the horn, the forced oscillator invariant circle in resonance, C_μ, approaches the unforced oscillator circle, C_0, while the Hopf invariant circle in resonance, C_μ, shrinks to a point.

4. The differences in the unfoldings of the local normal forms for the Hopf bifurcation for each period q=1, 2, 3, 4, or ≥5, is consistent with the vast differences in the global structure of the corresponding horns, as seen later in this paper.

3. RESONANCE SURFACES

3.0 Motivation

Let us return to the forced oscillator of Section 2.5. We were considering the family of time $1/\omega$ Poincare return maps generated by

$$\frac{dx}{dt}=F(x) + \alpha\, G(x,\omega t) \qquad \{2.11\}$$

We have seen that, for small forcing α, the persistence of the attracting invariant circle makes it natural to define the rotation number of orbits. The angle of rotation is measured with respect to the "center" of the circle. This gives us a way of distinguishing certain period q orbits from others.

As we move higher into the horn (away from the tip), however, this circle in resonance typically breaks and more complicated recurrent sets and attractors form. Consequently, it becomes more difficult to consistently assign a rotation number to a given orbit. Even if, for each parameter value with a periodic orbit, an appropriate "center" phase point can always be found around which to measure a rotation number, there is no guarantee that such points will vary continuously with the parameter. This comment applies to the theory of Matsuoka [Mat], which guarantees a "linked" fixed point corresponding to every periodic orbit. The fixed point, however, is not necessarily unique, nor does it vary continuously with parameter. Because of these problems, and in order to at least postpone invoking the (considerable) theory of Matsuoka, as well as for other reasons enumerated later on in this section, we use a generalization of the definition of rotation number of an orbit to include the point about which the rotation is measured. A special case of this generalized rotation number, the self rotation number, $\rho_s(x,f_\mu)\equiv\rho_s(x,\mu)$, depending only on the orbit itself, will, for us, be the most useful by-product of this construction.

Note that whenever both the point whose rotation number we are measuring and the point around which we are measuring the rotation are periodic points, our construction will give us a pair of knotted periodic orbits, an elementary concept in knot theory. See [Mat] or [BW] for more general ideas in knot theory. Our definition of rotation number, however, does not require the orbit under consideration to be periodic.

In order to keep the development as general as possible, we will not require our families of diffeomorphisms to be generated by Poincare return maps of three dimensional flows such as {2.11}. Unless specifically stated otherwise, in the remainder of Chapter 3, $\{f_\mu\}$ will be a family of orientation preserving C^r, $r \geq 1$, diffeomorphisms of $\mathbb{R}^2$ varying continuously in the C^1 topology as μ varies in a neighborhood of $\mathbb{R}^k$.

No generic assumptions are made in this chapter until section 3.5.

3.1 Self Rotation Number

The family $\{f_\mu\}$ induces a map $g: \mathbb{R}^2\times\mathbb{R}^2\times\mathbb{R}^k \to \mathbb{R}^2$ by

$$g(x,y,\mu) \equiv f_\mu(x) - f_\mu(y) \qquad \{3.1\}$$

By a slight abuse of notation, we write

$$g^j(x,y,\mu) \equiv f^j_\mu(x) - f^j_\mu(y) \qquad \{3.2\}$$

For any fixed value of $(y,\mu)\in \mathbb{R}^2\times\mathbb{R}^k$, {3.1} defines a diffeomorphism $g_{y,\mu}$ that is just a translate of f_μ. In this case, we can make the polar coordinate changes defined by

$$\begin{pmatrix} a\cos\theta \\ a\sin\theta \end{pmatrix} = x-y = g^0(x,y,\mu);\ \begin{pmatrix} A_{y,\mu}\cos\Theta_{y,\mu} \\ A_{y,\mu}\sin\Theta_{y,\mu} \end{pmatrix} = f_\mu(x) - f_\mu(y) = g^1(x,y,\mu) \qquad \{3.3\}$$

Because these coordinate changes are nonsingular for $x\neq y$ ($x\neq y$ implies $f_\mu(x)\neq f_\mu(y)$, also), $(A_{y,\mu},\Theta_{y,\mu})$: $(a,\theta) \in (0,\infty)\times\mathbb{S} \to (0,\infty)\times\mathbb{S}$ is an orientation preserving C^1 diffeomorphism varying continuously in the C^1 topology as μ varies. We define a function $R:(0,\infty)\times\mathbb{S}\times\mathbb{R}^2\times\mathbb{R}^k \to \mathbb{S}$ by

$$R(a,\theta,y,\mu) \equiv R_{a,\theta,y,\mu}(1) \equiv \Theta_{y,\mu}(a,\theta) - \theta \qquad \{3.4\}$$

By embedding $\mathbb{S}$ as the unit circle in the plane, we can write (via the change of coordinates {3.3})

$$\theta = \frac{x - y}{|x - y|} = \frac{g^0(x,y,\mu)}{|g^0(x,y,\mu)|};\ \Theta_{y,\mu}(a,\theta) = \frac{f_\mu(x) - f_\mu(y)}{|f_\mu(x) - f_\mu(y)|} = \frac{g^1(x,y,\mu)}{|g^1(x,y,\mu)|} \qquad \{3.5\}$$

Let Δ denote the diagonal of $\mathbb{R}^2\times\mathbb{R}^2$: $\Delta\equiv\{x,y\in \mathbb{R}^2 \mid x=y\}$.

Claim 3.1: θ and $\Theta_{y,\mu}(a,\theta)$ are C^1 functions of (x,y,μ) from $\{(\mathbb{R}^2\times\mathbb{R}^2)\backslash\Delta\}\times\mathbb{R}^k \to \mathbb{S}$.

Proof: The assumed C^1 topology on our function space implies that $(x,\mu)\to f_\mu(x)$ is C^1 in both x and μ. The other operations in the definitions of {3.5} are algebraic operations (including division by a nonzero scalar) and the norm operation: $z\to|z|$ for

$z \neq 0$; all such "other" operations are analytic. So the composition of operations defining θ and $\Theta_{y,\mu}(a,\theta)$ is at least C^1. □

Corollary 3.2: θ and $\Theta_{y,\mu}(a,\theta)$ are C^1 functions of (a,θ,y,μ) from $(0,\infty)\times\mathbb{S}\times\mathbb{R}^2\times\mathbb{R}^k \to \mathbb{S}$.

Proof: This is immediate from Claim 3.1 and the nonsingular coordinate change {3.3}.□

Using these relationships, we can see that the function R defined in {3.4} is equivalent to a function $r : \{(\mathbb{R}^2\times\mathbb{R}^2)\backslash\Delta\}\times\mathbb{R}^k \to \mathbb{S}$, which we will call the "rotation of x around y under f_μ," defined by

$$r(x,y,\mu) \equiv r_{x,y,\mu}(1) \equiv \frac{f_\mu(x) - f_\mu(y)}{|f_\mu(x) - f_\mu(y)|} - \frac{x - y}{|x - y|} \qquad \{3.6\}$$

$$= \frac{g^1(x,y,\mu)}{|g^1(x,y,\mu)|} - \frac{g^0(x,y,\mu)}{|g^0(x,y,\mu)|},$$

Note: On the right hand side of {3.6} we have identified the unit circle of $\mathbb{R}^2$ with $\mathbb{S}$; the subtraction of the two above "vectors," however, is performed in $\mathbb{S}$, not in $\mathbb{R}^2$.

R and r are related by

$$R(a,\theta,y,\mu) = r\left(y + \begin{pmatrix} a\cos\theta \\ a\sin\theta \end{pmatrix}, y, \mu\right). \qquad \{3.7\}$$

Corollary 3.3: Both R and r are C^1 on their respective domains.

Proof: This is a direct consequence of Claim 3.1, Corollary 3.2, and the definitions of R and r. □

The map R induces a map $\tilde{R}$ between the universal covering spaces of its domain and range in the following way. The domain covering map $p_d:(0,\infty)\times\mathbb{R}\times\mathbb{R}^2\times\mathbb{R}^k \to (0,\infty)\times\mathbb{S}\times\mathbb{R}^2\times\mathbb{R}^k$ is defined by $(a, \tilde{\theta}, y, \mu) \to (a, \theta, y, \mu)$, where $\theta = \tilde{\theta} \bmod (2\pi)$. The covering map of the range is $p_r:\mathbb{R}\to\mathbb{S}$ is defined by $\tilde{\theta}\to\theta$, where again, $\theta = \tilde{\theta} \bmod (2\pi)$. The general lifting lemma [Mu, p. 390] now implies that

specifying the image of a single point w_0 under $\tilde{R}$ (subject, of course, to the restriction $p_r \circ \tilde{R}(w_0) = R \circ p_d(w_0)$) uniquely defines a continuous lift of $R \circ p_d$ which we will call $\tilde{R}$:

$$\begin{array}{ccc} & \tilde{R} & \\ (0,\infty)\times\mathbb{R}\times\mathbb{R}^2\times\mathbb{R}^k & \longrightarrow & \mathbb{R} \\ \downarrow p_d & & \downarrow p_r \\ (0,\infty)\times\mathbb{S}\times\mathbb{R}^2\times\mathbb{R}^k & \xrightarrow{\quad R \quad} & \mathbb{S} \end{array}$$

Claim 3.4: $\tilde{R}(a,\tilde{\theta}+2\pi k,y,\mu) = \tilde{R}(a,\tilde{\theta},y,\mu)$, $k \in \mathbb{Z}$

Proof: We saw above that $(A_{y,\mu},\Theta_{y,\mu})$ is a diffeomorphism from the open annulus $(0,\infty)\times\mathbb{S}$ to itself for every fixed y and μ. When we "lift" such a map $(A_{y,\mu},\Theta_{y,\mu})$ as in the above construction to a map $(\tilde{A}_{y,\mu},\tilde{\Theta}_{y,\mu})$ of the covering space $(0,\infty)\times\mathbb{R}$, it satisfies the condition $\tilde{\Theta}_{y,\mu}(a,\tilde{\theta}+2\pi k) = \tilde{\Theta}_{y,\mu}(a,\tilde{\theta}) + 2\pi k$. ($f_\mu$ being a diffeomorphism implies $\tilde{\Theta}_{y,\mu}$ is a degree ± 1 map in its second variable; orientation preservation and f_μ mapping neighborhoods of x to neighborhoods of $f_\mu(x)$ implies the degree is $+1$.) Lifting both sides of equation {3.4} (by fixing the same value to ensure the lifted functions are equal)

$$\tilde{R}(a,\tilde{\theta}+2\pi k,y,\mu) = \tilde{\Theta}_{y,\mu}(a,\tilde{\theta}+2\pi k) - (\tilde{\theta}+2\pi k) = \tilde{\Theta}_{y,\mu}(a,\tilde{\theta}) + 2\pi k - (\tilde{\theta}+2\pi k)$$

$$= \tilde{\Theta}_{y,\mu}(a,\tilde{\theta}) - \tilde{\theta} = \tilde{R}(a,\tilde{\theta},y,\mu) \qquad \square$$

Note: This claim implies $\tilde{R} \circ p_d^{-1}$ is a well defined lift of R. By identifying $\tilde{R} \circ p_d^{-1}$ with $\tilde{R}$, we can think of $\tilde{R}$ as a lift of either R or $R \circ p_d$: let $\tilde{R}(a,\theta,y,\mu) \equiv \tilde{R}(a,\tilde{\theta},y,\mu)$ for any $\tilde{\theta} \in \mathbb{R}$ with $\tilde{\theta} \bmod (2\pi) = \theta \in \mathbb{S}$.

Claim 3.5: There exists a lift $\tilde{r}$ of r (not of $r \circ p_d$) that satisfies $\tilde{r}(x,y,\mu) = \tilde{r}(y,x,\mu)$.

Proof: Claim 3.4 implies the lift $\tilde{r}$ exists. Note that {3.6} implies $r(x,y,\mu)=r(y,x,\mu)$. To prove $\tilde{r}(x,y,\mu) = \tilde{r}(y,x,\mu)$, fix a point (x_0,y_0,μ_0) and define a path

$\gamma(t)=(x(t),y(t),\mu(t))$ in $(\{\mathbb{R}^2\times\mathbb{R}^2\}\backslash\Delta)\times\mathbb{R}^k$ by $x(t)=\frac{x_0+y_0}{2}+\begin{pmatrix}b\cos(\phi+t)\\ b\sin(\phi+t)\end{pmatrix}$, $y(t)=\frac{x_0+y_0}{2}$ $+\begin{pmatrix}b\cos(\phi+t+\pi)\\ b\sin(\phi+t+\pi)\end{pmatrix}$, $\mu(t)\equiv\mu_0$, where (b,ϕ) are chosen to satisfy $\frac{x_0-y_0}{2}=\begin{pmatrix}b\cos\phi\\ b\sin\phi\end{pmatrix}$. Along this path we can monitor $r(\gamma(t))$. $r(\gamma(t)) = r(x(t),y(t),\mu(t)) = r(y(t),x(t),\mu(t)) = r(\gamma(t+\pi))$. From this and the continuity of $\tilde{r}$ and γ, it follows that $\tilde{r}(\gamma(t)) - \tilde{r}(\gamma(0)) - [\tilde{r}(\gamma(t+\pi)) - \tilde{r}(\gamma(\pi))] \equiv 2k\pi$ for some integer value of k. Evaluating this expression at $t=0$ gives us $k=0$. At $t=\pi$, we get $2[\tilde{r}(\gamma(\pi)) - \tilde{r}(\gamma(0))] = 0$. (Recall $\tilde{r}$ is well defined, so $\tilde{r}(\gamma(t+2\pi)) = \tilde{r}(\gamma(t))$.) By using the definition of γ, we see that this is precisely $2[\tilde{r}(y,x,\mu) - \tilde{r}(x,y,\mu)] = 0$. □

We now are in a position to inductively define $\tilde{r}_{x,y,\mu}(k)$, $k\in\mathbb{Z}^+$, the <u>total rotation of x around y in k iterates of the map f_μ</u>:

$$\tilde{r}_{x,y,\mu}(k) \equiv \tilde{r}_{x,y,\mu}(k-1) + \tilde{r}(f^{k-1}(x),f^{k-1}(y),\mu)$$

$$= \sum_{j=0}^{k-1} \tilde{r}(f^j(x),f^j(y),\mu) \qquad \{3.8\}$$

Define the average rotation rate of x around y after k iterates, the <u>k^{th} iterate frequency of rotation of x around y:</u>

$$\frac{\tilde{r}_{x,y,\mu}(k)}{2\pi k}$$

Finally, for $x\neq y$, define the <u>rotation number of x around y</u>, i.e., the frequency of rotation of x around y per iterate of f_μ:

$$\rho(x,y,f_\mu) \equiv \rho(x,y,\mu) \equiv \lim_{k\to\infty} \frac{\tilde{r}_{x,y,\mu}(k)}{2\pi k},\ k\in\mathbb{Z}^+, \text{ whenever this limit exists} \qquad \{3.9\}$$

As a special case of this rotation number, for $x\neq f_\mu(x)$, define the <u>self rotation number of x:</u>

$$\rho_S(x,\mu) \equiv \rho(f_\mu(x),x,\mu).$$

The rotation, frequency of rotation, and rotation number for backward iterates are defined analogously, but are not needed for the problems treated in this paper.

When the family of diffeomorphisms f_μ is generated as a return map of a flow $\phi(x,t_0,t,\mu)$ of a differential equation such as in {2.11}, we can define $\tilde{r}$ uniquely. The flow is a natural suspension which uniquely determines choice for a lift of r. We saw in Section 2.5, we saw that the maps, $f_\mu(x)$, are defined as $\phi(x,t_0,t_0+\frac{1}{\omega},\mu)$, for a fixed t_0 are a family of orientation preserving diffeomorphisms of $\mathbb{R}^2$ varying continuously in the C^1 topology as μ varies in $\mathbb{R}^k$. Paralleling the above treatment (and dropping reference to the fixed value of t_0), we define

$$r_{x,y,\mu}: [0,\infty)\to\mathbb{S}^1 \text{ by } t\to \frac{\phi(x,t/\omega,\mu) - \phi(y,t/\omega,\mu)}{|\phi(x,t/\omega,\mu) - \phi(y,t/\omega,\mu)|} - \frac{\phi(x,0,\mu) - \phi(y,0,\mu)}{|\phi(x,0,\mu) - \phi(y,0,\mu)|}$$

$$\left(= \frac{\phi(x,t/\omega,\mu) - \phi(y,t/\omega,\mu)}{|\phi(x,t/\omega,\mu) - \phi(y,t/\omega,\mu)|} - \frac{x-y}{|x-y|}\right) \qquad \{3.10\}$$

(Recall that the subtraction is performed in $\mathbb{S}$, not in $\mathbb{R}^2$.)

The direction of the arrows in Figure 3.1 represents $\frac{\phi(x,t/\omega,\mu) - \phi(y,t/\omega,\mu)}{|\phi(x,t/\omega,\mu) - \phi(y,t/\omega,\mu)|}$ at each time t.

Let $\tilde{r}_{x,y,\mu}(t)$ be the unique lift of $r_{x,y,\mu}(t)$, $r:\{(\mathbb{R}^2\times\mathbb{R}^2)\backslash\Delta\}\times\mathbb{R}^k\times\mathbb{R}\to\mathbb{S}$ (it exists by the same construction as above) from $\mathbb{S}$ to $\mathbb{R}$ that is continuous in (x,y,μ,t) and satisfies $\tilde{r}_{x,y,\mu}(0)=0$. (Note that $\tilde{r}_{x,y,\mu}$ is defined on $(-\infty,\infty)$ and that, because we have rescaled time in the flow by a factor of $T_\mu=1/\omega$, this definition coincides on its common domain of definition, $\mathbb{Z}^+$, with the definition in {3.8}, assuming the arbitrary lift was "properly" chosen to define {3.8}. $\tilde{r}(x,y,\mu) \equiv \tilde{r}_{x,y,\mu}(1)$ is now determined by the flow ϕ; the arbitrary addition of a multiple of 2π has been eliminated.

The rotation number of x around y is now defined as in {3.9}. (Again, backward time rotation numbers are defined analogously, but are not used in this paper.)

Note the following properties involving the rotation number of $\mathbf{x}$ around $\mathbf{y}$:

1. The rescaling of time in {3.10} by the factor of $T_\mu=1/\omega$ means that $\tilde{r}$ is really the ratio of the frequency of rotation of $\mathbf{x}$ around $\mathbf{y}$ to the frequency of forcing, ω.

2. If $\mathbf{x}$ and $\mathbf{y}$ are both periodic of period q for some fixed μ, i.e., $\mathbf{f}_\mu^q(\mathbf{x})=\mathbf{x}$ and $\mathbf{f}_\mu^q(\mathbf{y})=\mathbf{y}$, then $r_{\mathbf{x},\mathbf{y},\mu}(q)=r_{\mathbf{x},\mathbf{y},\mu}(0)=0$, so $\rho_S(\mathbf{x},\mu) = \dfrac{\tilde{r}_{\mathbf{x},\mathbf{y},\mu}(q)}{2\pi q}$. Because the quantity $\dfrac{\tilde{r}_{\mathbf{x},\mathbf{y},\mu}(q)}{2\pi q}$ is defined by flowing for a finite time $qT(\mu)$ which varies smoothly with μ, property 1 implies $\rho(\mathbf{x},\mathbf{y},\mu)$ is C^1 when restricted to the submanifold defined by $\{\mathbf{f}_\mu^q(\mathbf{x})=\mathbf{x}\} \cap \{\mathbf{f}_\mu^q(\mathbf{y})=\mathbf{y}\} \cap \{\mathbf{x}\neq\mathbf{y}\}$, for some fixed t_0. This property will be extremely useful to us in later sections.

3. In Section 3.3, we show $\tilde{r}_{\mathbf{x},\mathbf{y},\mu}(t)$ can be extended to include cases when $\mathbf{x}=\mathbf{y}$. This will allow us in turn to define $\rho_S(\mathbf{x},\mathbf{f}_\mu)$ for fixed points of $\mathbf{f}_\mu$.

4. For circle maps, the usual rotation number $\rho(x,f_\mu)$ of $x\in\mathbb{S}$ is included in our definition by embedding $\mathbb{S}$ as the unit circle in $\mathbb{R}^2$. $\rho(x,f_\mu)=\rho(\mathbf{x},\mathbf{y},\mathbf{f}_\mu)$ where on the right hand side we think of $x\in\mathbb{S}\subset\mathbb{R}^2$ and $\mathbf{y}=\mathbf{f}_\mu^j(\mathbf{y})=(0,0)$ for all j, and $\mathbf{f}_\mu|_{\mathbb{S}}=f_\mu$.

5. For maps of the plane, computing the rotation number of $\mathbf{x}$ around a fixed point $\mathbf{y}_0$ of $\mathbf{f}_\mu$, $\rho(\mathbf{x},\mathbf{y}_0,\mathbf{f}_\mu)$, is also included in our generalized rotation number. In this case, however, the interpretation is simpler: $\tilde{r}_{\mathbf{x},\mathbf{y},\mu}(k)$ is the total change in the (lifted) second coordinate of the single annulus map $(A_{\mathbf{y},\mu},\Theta_{\mathbf{y},\mu})$ in k iterates. (See {3.3} and {3.8}.) When $\mathbf{y}_0$ is not a fixed point, the full development described in this section is necessary: evaluating $\tilde{r}_{\mathbf{x},\mathbf{y},\mu}(k+1) - \tilde{r}_{\mathbf{x},\mathbf{y},\mu}(k)$ involves the change in the (lifted) second coordinate of the annulus map $(A_{\mathbf{z},\mu},\Theta_{\mathbf{z},\mu})$ where $\mathbf{z}=\mathbf{f}_\mu^k(\mathbf{y})$.

6. We can compute rotation numbers for orbits without having to locate a fixed point around which the orbit rotates.

7. If we know, or can assume, the angle traversed between consecutive iterates, $\tilde{r}_{x,y,\mu}(i+1) - \tilde{r}_{x,y,\mu}(i)$, is eventually in some fixed interval of length 2π, then the actual flow ϕ need not be used. This is because $\tilde{r}_{x,y,\mu}(i+1) - \tilde{r}_{x,y,\mu}(i)$ is always defined mod (2π). This is especially useful in computing rotation numbers for flows whose Poincare maps have a closed form and for maps not generated as a return map of a flow.

Claim 3.6: For a circle homeomorphism, the standard rotation number of x under Θ, $\rho(x,\Theta)$, is equivalent to the self rotation number, $\rho_s(x,\Theta)$.

Proof: Let $\tilde{\Theta}$ be a lift of Θ. Embed $\mathbb{S}$ as the unit circle in $\mathbb{R}^2$ as above. Set f be any homeomorphism of $\mathbb{R}^2$ that fixes the origin and satisfies $f|_{\mathbb{S}} = \Theta$. What we need to check is that $\rho(x,0,f)=\rho(f(x),x,f)$ for all $x \in \mathbb{S} < \mathbb{R}^2$. Geometrically, in $\mathbb{R}^2$, $\tilde{r}(f^j(x),f^j(0),f) = \tilde{r}(f^j(x),0,f)$ measures the change in the angle of the vectors from the origin to $f^j(x)$ as j increases. That is, $\tilde{r}(f^j(x),f^j(0),f) = \tilde{\Theta}^{j+1}(x) - \tilde{\Theta}^j(x)$. Similarly, we can think of $\tilde{r}(f(x),x,\mu)$ as measuring the change in the angle of the vectors $f^{j+1}(x) - f^j(x)$ as j increases. Equivalently, we could measure the change in the angle of the perpendiculars to these secants of the unit circle. The perpendicular to $f^{j+1}(x) - f^j(x)$ is $\frac{1}{2}(\tilde{\Theta}^{j+1}(x) + \tilde{\Theta}^j(x))$, being the bisector of the sector swept out between $\tilde{\Theta}^{j+1}(x)$ and $\tilde{\Theta}^j(x)$. So $\tilde{r}(f^{j+1}(x),f^j(x),\mu) = \frac{1}{2}(\tilde{\Theta}^{j+2}(x) + \tilde{\Theta}^{j+1}(x)) - \frac{1}{2}(\tilde{\Theta}^{j+1}(x) + \tilde{\Theta}^j(x))$. Consequently

$$\tilde{r}_{x,0,\mu}(k) - \tilde{r}_{f(x),x,\mu}(k) = \{\tilde{\Theta}^{k+1}(x) - \tilde{\Theta}^0(x)\}$$

$$- \{\frac{1}{2}(\tilde{\Theta}^{k+1}(x) + \tilde{\Theta}^k(x) - \frac{1}{2}(\tilde{\Theta}^1(x) + \tilde{\Theta}^0(x))\}$$

$$= \frac{1}{2}(\tilde{\Theta}^{k+1}(x) - \tilde{\Theta}^k(x)) \mp \frac{1}{2}(\tilde{\Theta}^1(x) - \tilde{\Theta}^0(x))$$

$$\leq \max_{x \in \mathbb{S}} | \tilde{r}_{x,0,\mu}(1) |$$

Therefore, $\rho(x,0,f)=\rho(f(x),x,f)$. □

3.2 Resonance Surfaces and Regions: Definitions and Justifications

We now define and proceed to identify various components of the two dimensional surface of period q points:

$$\Gamma(q) \equiv \{(\mathbf{x},\mu)\in \mathbb{R}^2\times\mathbb{R}^2 : \mathbf{f}_\mu^q(\mathbf{x})=\mathbf{x}\}, \text{ where } q \text{ is fixed } \geq 1 \qquad \{3.11\}$$

The following two lemmas which will help us to determine the structure of $\Gamma(q)$.

Lemma 3.7: Let $\{\mathbf{f}_\mu\}$ be a family of orientation preserving diffeomorphisms of $\mathbb{R}^2$ varying continuously in the C^1 topology as μ varies in a neighborhood of $\mathbb{R}^k$. Then $\rho_s(\mathbf{x},\mathbf{f}_\mu)$ is constant over components of

$$\Gamma(q)\backslash\{\text{fixed points of } \Gamma(q)\}. \quad (q\geq 2)$$

Proof: Because all points of Γ (and their iterates) satisfy $\mathbf{f}_\mu^q(\mathbf{x})=\mathbf{x}$, then $q\rho_s(\mathbf{x},\mathbf{f}_\mu) = \frac{\tilde{r}_{\mathbf{f}_\mu(\mathbf{x}),\mathbf{x},\mu}(q)}{2\pi}$ is well defined, continuous, and integer valued on $\Gamma(q)\backslash\{\text{fixed points on } \Gamma(q)\}$. Therefore ρ_s must be constant. □

Note: In Section 3.3, we will define ρ_s on the fixed points of $\Gamma(q)$ as well.

Lemma 3.7 allows us to define the following objects for $q\geq 2$:

$$\Gamma^{p/q} \equiv \{(\mathbf{x},\mu)\in \mathbb{R}^2\times\mathbb{R}^2 : \mathbf{x} \text{ is a true period } q \text{ point of } \mathbf{f}_\mu \text{ with self rotation number } p/q\} \qquad \{3.12\}$$

$(\mathbf{x},\mu)\in \Gamma^{p/q} \equiv$ a <u>p/q point</u> on a <u>p/q orbit</u>

Component of $\overline{\Gamma^{p/q}} \equiv$ <u>p/q resonance surface</u>

Projections of resonance surfaces to the μ parameter plane ≡ <u>p/q resonance regions</u>.

Lemma 3.8: <u>Let</u> $\{\mathbf{f}_\mu\}$ be as in Lemma 3.7. Suppose, in addition, $(p,q) = 1$, $q\geq 2$, and $(\mathbf{x}_0,\mu_0) \in \overline{\Gamma^{p/q}} \setminus \Gamma^{p/q}$. Then $\mathbf{x}_0$ is a fixed point of $\mathbf{f}_{\mu_0}$.

Proof: Choose a sequence $(\mathbf{x}_i,\mu_i)$ in $\Gamma^{p/q}$ that approaches (x_0,μ_0). Continuity of $\mathbf{f}_\mu{}^q(\mathbf{x})$ in $\mathbf{x}$ and μ implies $\mathbf{f}_{\mu_0}{}^q(\mathbf{x}_0)=\mathbf{x}_0$. If the orbit at μ_0 is not a fixed point, then the only other possibility is a periodic orbit of period r, $1<r<q$. The self rotation number of (x_0,μ_0) would then exist and equal n/r for some $n\in\mathbb{Z}$. Continuity of the self rotation number implies p/q=n/r. This contradicts (p,q)=1. Therefore, $\mathbf{x}_0$ must be a fixed point of $\mathbf{f}_{\mu_0}$. □

Note that all points on the orbit of $\mathbf{x}_i$ coalesce to $\mathbf{x}_0$ by the continuity of $\mathbf{f}_\mu(\mathbf{x})$ with respect to $\mathbf{x}$ and μ:

$$\mathbf{x}(t)\to\mathbf{x}_0 \Rightarrow \mathbf{f}^j_{\mu(t)}(\mathbf{x}(t)) \to \mathbf{f}^j_{\mu(0)}(\mathbf{x}(0)) = \mathbf{x}_0,\ j=0,\ldots,q-1.$$

Lemma 3.8 says that if (p,q)=1, the closure operation can add to $\Gamma^{p/q}$ only fixed points where p/q orbits "coalesce." In Section 3.4 we will see that the eigenvalues of these fixed points will also be (at least partially) determined.

3.3 Self Rotation Number of Fixed Points

In the previous section, we made two polar coordinate changes (see {3.3}) to define the diffeomorphism $(A_{y,\mu},\Theta_{y,\mu})\ (a,\theta) : (0,\infty)\times\mathbb{S} \to (0,\infty)\times\mathbb{S}$ from f_μ. We begin by extending this function, and then as a consequence, $R(a,\theta,y,\mu)$: $(0,\infty)\times\mathbb{S}\times\mathbb{R}^2\times\mathbb{R}^k\to\mathbb{S}$, to a=0. The extended function R we will still be able to lift. This will enable us to define rotation numbers for a=0. By showing these rotation numbers are independent of θ, we will define the rotation of a point around itself, and thus the self rotation number of a fixed point.

Lemma 3.10: Let f_μ be a family of C^1 orientation-preserving diffeomorphisms of $\mathbb{R}^2$, varying continuously in the C^1 topology with respect to $\mu\in\mathbb{R}^k$. Then the diffeomorphisms $(A_{y,\mu}(a,\theta),\Theta_{y,\mu}(a,\theta))$ of $(0,\infty)\times\mathbb{S}$, induced by f_μ by the change of coordinates defined in {3.3}, can be uniquely extended to homeomorphisms of $[0,\infty)\times\mathbb{S}$.

Proof: We will first determine the proper extension of $(A_{y,\mu}(a,\theta),\Theta_{y,\mu}(a,\theta))$ to a = 0. {3.3} implies

$$A_{y,\mu}(a,\theta) = |f_\mu(x) - f_\mu(y)|; \quad \Theta_{y,\mu}(a,\theta) = \frac{f_\mu(x) - f_\mu(y)}{|f_\mu(x) - f_\mu(y)|} \qquad \{3.13\}$$

and

$$a=|x-y|; \qquad \theta=\frac{x-y}{|x-y|} \qquad \{3.14\}$$

As $a\to0$, $x\to y$, $f_\mu(x) \to f_\mu(y)$, so $A_{y,\mu}(a,\theta)\to0$. Therefore define

$$A_{y,\mu}(0,\theta) \equiv 0 \qquad \{3.15\}$$

To find the extension for $\Theta_{y,\mu}(a,\theta)$, we start with Taylor's theorem:

$$f_{\mu_0}(x) = f_{\mu_0}(y) + Df_{\mu_0}(y)\begin{pmatrix}a\cos\theta\\ a\sin\theta\end{pmatrix} + o(a).$$

From {3.13}:

$$\Theta_{y,\mu}(a,\theta) = \frac{Df_{\mu_0}(y_0)\begin{pmatrix}a\cos\theta\\ a\sin\theta\end{pmatrix} + o(a)}{\left|Df_{\mu_0}(y_0)\begin{pmatrix}a\cos\theta\\ a\sin\theta\end{pmatrix} + o(a)\right|} = \frac{Df_{\mu_0}(y_0)\begin{pmatrix}\cos\theta\\ \sin\theta\end{pmatrix} + o(1)}{\left|Df_{\mu_0}(y_0)\begin{pmatrix}\cos\theta\\ \sin\theta\end{pmatrix} + o(1)\right|} \text{ as } a\to 0$$

Because each f_μ is a diffeomorphism, $Df_{\mu_0}(y)$ always exists and is nonsingular. Therefore, we can define

$$\Theta_{y,\mu}(0,\theta) \equiv \lim_{a\to 0} R(a,\theta,y_0,\mu_0) = \frac{Df_{\mu_0}(y_0)\begin{pmatrix}\cos\theta\\ \sin\theta\end{pmatrix}}{\left|Df_{\mu_0}(y_0)\begin{pmatrix}\cos\theta\\ \sin\theta\end{pmatrix}\right|} \qquad \{3.16\}$$

$Df_{\mu_0}(y_0)$ nonsingular also implies that $\Theta_{y,\mu}(0,\theta)$ is continuous in θ and bijective as a function only of θ. So {3.15} and {3.16} define $(A_{y,\mu}(a,\theta),\Theta_{y,\mu}(a,\theta))$ as a bijective continuous map of the compact space $[0,\varepsilon]\times\mathbb{S}$ and its image in $[0,\infty)\times\mathbb{S}$. Such a map is necessarily a homeomorphism. Combining this with the overlapping diffeomorphism $(A_{y,\mu}(a,\theta),\Theta_{y,\mu}(a,\theta))$ on $(0,\infty)\times\mathbb{S}$, we obtain $(A_{y,\mu}(a,\theta),\Theta_{y,\mu}(a,\theta))$ as a homeomorphism of the extended space $[0,\infty)\times\mathbb{S}$.

Lemma 3.11: $\Theta_{y,\mu}(a,\theta)$ is continuous in a neighborhood of $(0,\theta_0,y_0,\mu_0)$ in $[0,\infty)\times\mathbb{S}\times\mathbb{R}^2\times\mathbb{R}^k$.

Proof: Note first that for each component of $f_\mu=(f_\mu^1, f_\mu^2)$

$$f_\mu^j\left(y+\begin{pmatrix}a\cos\theta\\ a\sin\theta\end{pmatrix}\right) - f_\mu^j(y) = f_\mu\left(y+\begin{pmatrix}a\cos\theta\\ a\sin\theta\end{pmatrix}\right) - f_\mu^j\left(y+\begin{pmatrix}0\\ a\sin\theta\end{pmatrix}\right)+f_\mu^j\left(y+\begin{pmatrix}0\\ a\sin\theta\end{pmatrix}\right) - f_\mu^j(y)$$

$$= \frac{\partial f_\mu^j}{\partial x_1}\left(y+\begin{pmatrix}c_1^j\\ a\sin\theta\end{pmatrix}\right)* a\cos\theta + \frac{\partial f_\mu^j}{\partial x_2}\left(y+\begin{pmatrix}0\\ c_2^j\end{pmatrix}\right)* a\sin\theta \qquad \{3.17\}$$

$$\equiv a*X^j$$

where c_1^j is between 0 and $a\cos\theta$, c_2^j is between 0 and $a\sin\theta$, j=1,2, by the mean value theorem. Our assumptions on the C^1 continuity of **f** with respect to μ imply that the partial derivatives in {3.14} vary continuously as a function of μ and the evaluation points. Because the $c_i^j \to 0$ as $r \to 0$ uniformly in (θ,y,μ), the evaluation points of the partial derivatives $\to y_0$ as $(a,y)\to(0,y_0)$ uniformly in (θ,μ). So $\frac{\partial f_\mu^j}{\partial x_1}\left(y+\begin{pmatrix} c_1^j \\ a\sin\theta \end{pmatrix}\right)$, and $\frac{\partial f_\mu^j}{\partial x_2}\left(y+\begin{pmatrix} 0 \\ c_2^j \end{pmatrix}\right)$ are continuous functions of (a,θ,y,μ) in a neighborhood of a=0. Consequently, each X^j is a continuous function of (a,θ,y,μ) in a neighborhood of a=0. Furthermore, since we have factored out an a from {3.14} in defining X^j, and because the linear part of a diffeomorphism is never singular, i.e., $|(X^1,X^2)|$ is never zero, we have $\frac{(X^1,X^2)}{|(X^1,X^2)|}$ is a continuous function of (a,θ,y,μ) in a neighborhood of a=0. Therefore, $\frac{(X^1,X^2)}{|(X^1,X^2)|}$ (which equals $\Theta_{y,\mu}(a,\theta)$ by {3.14}) is a continuous function of (a,θ,y,μ) in a neighborhood of a=0. Together with the "automatic" continuity of $\Theta_{y,\mu}(a,\theta)$ away from a=0, we obtain the continuity of $\Theta_{y,\mu}(a,\theta)$ on the full space, $[0,\infty)\times\mathbb{S}\times\mathbb{R}^2\times\mathbb{R}^k$. □

Note: Although we don't need the fact here, $A_{y,\mu}(a,\theta)$ is also continuous on the full space, $[0,\infty)\times\mathbb{S}\times\mathbb{R}^2\times\mathbb{R}^k$, so the extended annulus diffeomorphisms $(A_{y,\mu}(a,\theta), \Theta_{y,\mu}(a,\theta))$ vary continuously in the C^0 topology with respect to y and μ.

Corollary 3.12: Let f_μ be a family of C^1 orientation-preserving diffeomorphisms of $\mathbb{R}^2$, varying continuously in the C^1 topology with respect to $\mu\in\mathbb{R}^k$. Then $R(a,\theta,y,\mu)$ can be uniquely extended to a continuous function $R: [0,\infty)\times\mathbb{S}\times\mathbb{R}^2\times\mathbb{R}^k\to\mathbb{S}$.

Proof: This is immediate from Corollary 3.11 since $R(a,\theta,y,\mu)$ is defined in {3.4} as $\Theta_{y,\mu}(a,\theta) - \theta$. □

Because $R(a,\theta,y,\mu)$ can be extended to a=0, so can its lift $\tilde{R}(a,\tilde{\theta},y,\mu)$. Thus, we can extend our definition of rotation number in {3.9} to a=0 (depending on θ):

$$P(a,\theta,y,\mu) \equiv \lim_{t\to\infty} \frac{\tilde{R}_{a,\theta,y,\mu}(k)}{2\pi k},\ k\in \mathbb{Z}^+, \text{ whenever this limit exists} \quad \{3.18\}$$

As in {3.7},

$$P(a,\theta,y,\mu) = \rho(y+\begin{pmatrix} a\cos\theta \\ a\sin\theta \end{pmatrix}, y, \mu), \qquad \text{for } a\neq 0 \quad \{3.19\}$$

Corollary 3.13: Let f_μ be a family of C^1 orientation-preserving diffeomorphisms of $\mathbb{R}^2$, varying continuously in the C^1 topology with respect to $\mu\in\mathbb{R}^k$. Then $\rho_s(y,f_\mu)$ has a natural extension to the fixed points of f_μ which always exists.

Proof: We saw above in the proof of Lemma 3.10, that $\Theta_{y,\mu}(0,\theta)$ is a homeomorphism of $\mathbb{S}$. When y is a fixed point, we iterate the same annulus map $\Theta_{y,\mu}(0,\theta)$ instead of a different map $\Theta_{z,\mu}(0,\theta)$, $z=f_\mu^j(y)$, at each iterate. Consequently, the self rotation number of a fixed point is the self rotation number of a circle homeomorphism. Such homeomorphisms have a unique (independent of θ) rotation number which always exists. By an argument similar to that in the proof of Claim 3.6, this rotation number equals $P(a,\theta,y,\mu)$ for each $\theta\in\mathbb{S}$. Thus, $P(0,\theta,y,\mu)$ always exists and is independent of θ. So

$$\rho(y,y,\mu) \equiv P(0,\theta,y,\mu), \text{ for any choice of } \theta\in\mathbb{S} \quad \{3.20\}$$

is a natural definition for the $\rho(y,y,\mu)$ □

3.4 Fixed Points of Resonance Surfaces

In Section 3.2, we showed that, when $q \geq 2$, $(p,q)=1$, a p/q resonance surface $\Gamma^{p/q}$ consists of period q points $\Gamma^{p/q}$, and fixed points $\overline{\Gamma^{p/q}} \setminus \Gamma^{p/q}$. We can use the machinery of the previous section to determine at least one, if not both, of the eigenvalues of these fixed points.

Lemma 3.14: The self rotation number $\rho_s(\mathbf{x},\mathbf{f}_\mu)$ exists and is identically equal to p/q for all points on a p/q resonance surface. (Compare with lemma 3.7)

Proof: All points $(\mathbf{x},\mu) \in \overline{\Gamma^{p/q}}$ satisfy $\mathbf{f}_\mu^q(\mathbf{x})=\mathbf{x}$. If $(\mathbf{x},\mu)$ is not a fixed point, then Lemma 3.7 tells us that $\rho_s(\mathbf{x},\mathbf{f}_\mu) = p/q$. If $(\mathbf{x},\mu)$ is a fixed point, then we can choose a sequence in $\Gamma^{p/q}$: $(\mathbf{x}_i,\mu_i) \to (\mathbf{x},\mu)$. $\mathbf{x}_i$ is a period q point of $\mathbf{f}_{\mu_i}$ with self rotation number p/q. Define (a_i,θ_i) by $\mathbf{f}_{\mu_i}(\mathbf{x}_i) - \mathbf{x}_i = \begin{pmatrix} a_i\cos\theta_i \\ a_i\sin\theta_i \end{pmatrix}$. Pick a point θ_0 in the ω-limit set of $\{\theta_i\}$ and a subsequence (which we will still call $\{\theta_i\}$) such that $\theta_i \to \theta_0$. By the above comments, $\tilde{R}_{a_i,\theta_i,x_i,\mu_i}(q) \equiv p$. Continuity of $\tilde{R}$ implies $\tilde{R}_{0,\theta_0,x,\mu}(q) \equiv p$. That is, $P(0,\theta_0,x,\mu) = p/q$. So by {3.18}, $\rho_s(\mathbf{x},\mathbf{f}_\mu) = \rho(\mathbf{f}_\mu(\mathbf{x}),\mathbf{x},\mathbf{f}_\mu) = P(0,\theta_0,\mathbf{y},\mu) = p/q$. □

Theorem 3.15: Let $\mathbf{f}_\mu$ be a two parameter family of orientation preserving diffeomorphisms of $\mathbb{R}^2$ varying continuously in the C^1 topology w.r.t. μ. Suppose, in addition, $(\mathbf{x}_0,\mu_0) \in \overline{\Gamma^{p/q}} \setminus \Gamma^{p/q}$, $(p,q) = 1$, $q \geq 2$. Then $\mathbf{x}_0$ is a fixed point of $\mathbf{f}_{\mu_0}$, and:

1. If $q \geq 3$, then $D\mathbf{f}_{\mu_0}(\mathbf{x}_0) \sim \begin{pmatrix} \cos(2\pi p/q) & -\sin(2\pi p/q) \\ \sin(2\pi p/q) & \cos(2\pi p/q) \end{pmatrix}$

2. If $q=2$, then $D\mathbf{f}_{\mu_0}(\mathbf{x}_0)$ has a -1 eigenvalue

Proof: $Df^q_{\mu_0}(x_0)$ must have an eigenvalue 1 or the q points on the orbit could be uniquely continued above μ_0 to preserve the p/q orbit above μ_0. Therefore $Df_{\mu_0}(x_0)$ must have an eigenvalue λ where $\lambda^q=1$. That is, $\lambda=e^{2\pi ij/q}$, j=0,...,q-1 mod (1). In Lemma 3.9 (2), we proved that x_0 is a fixed point at which all points on the orbit of x(t) coalesce. Therefore, all we have left to prove are statements 1 and 2. We begin by enumerating the possible self rotation numbers for the fixed point x_0.

Case 1: λ is complex (j/q≠0 or 1/2 mod(1)). Then $\Theta_{x_0,\mu_0}(0,\theta):\mathbb{S}\to\mathbb{S}$ is conjugate to a rigid rotation by $2\pi j/q$ mod(1). So there exists an integer m such that for every θ, the rotation number $P(0,\theta,x_0,\mu_0) = \rho_s(x_0,f_{\mu_0}) = j/q + m$.

Case 2: $\lambda = -1$ (j/q = 1/2 mod(1)). There exists an eigenvector corresponding to this -1 eigenvalue. This means that there exists a θ_{-1} such that $\Theta_{x_0,\mu_0}(0,\theta_{-1}) = \theta_{-1}+\pi$, and $\Theta_{x_0,\mu_0}(0,\theta_{-1}+\pi) = \theta_{-1}$. So there exists an integer m such that $P(0,\theta_{-1},x_0,\mu_0) = 1/2 + m$. Thus, for every θ, the rotation number $P(0,\theta,x_0,\mu_0) = \rho_s(x_0,f_{\mu_0}) = 1/2 + m$.

Case 3: $\lambda = 1$ (j/q = 0 mod (1)). There exists an eigenvector corresponding to this 1 eigenvalue. This means that there exists a θ_1 such that $\Theta_{x_0,\mu_0}(0,\theta_1) = \theta_1$. So there exists an integer m such that $P(0,\theta_1,y,\mu) = m$. Thus, for every θ, the rotation number $P(0,\theta,x_0,\mu_0) = \rho_s(x_0,f_{\mu_0}) = m$.

Lemma 3.14, however, says that $\rho_s(x_0,f_{\mu_0})$ must be p/q. So p/q = j/q mod (1). (p,q) = 1 implies (j,q) =1. q≥3 implies $\lambda = e^{2\pi ij/q} = e^{2\pi ip/q}$ is complex, so the eigenvalues of $Df_{\mu_0}(x_0)$ are complex conjugates and $Df_{\mu_0}(x_0)$ is therefore conjugate to

$$\begin{pmatrix} \cos(2\pi j/q) & -\sin(2\pi j/q) \\ \sin(2\pi j/q) & \cos(2\pi j/q) \end{pmatrix} = \begin{pmatrix} \cos(2\pi p/q) & -\sin(2\pi p/q) \\ \sin(2\pi p/q) & \cos(2\pi p/q) \end{pmatrix}$$

q=2 implies $\lambda=e^{2\pi i(1/2+m)} = -1$. □

3.5 The Topology of Generic Resonance Surfaces

Viewed strictly as a differentiable manifold in the phase×parameter space M^4, we see that the implicit function theorem guaranties that $\Gamma(q) = \{(x,\varepsilon) \in \mathbb{R}^2 \times \mathbb{R}^2 : f_\varepsilon^q(x)=x\}$ is a smooth two-dimensional manifold in the neighborhood of any point (x,ε) with the 2×4 Jacobian matrix $D_{x,\varepsilon}(f_\varepsilon^q)(x) - (Id_{2\times2}|0_{2\times2})$ has rank 2. The same is evidently true for $\overline{\Gamma^{p/q}} \subset \Gamma(q)$, $q\geq2$. Define the p/q singular set:

$$Z^{p/q} \equiv \{(x,\mu) \in \overline{\Gamma^{p/q}} : D_x f_\mu^q(x) \text{ has an eigenvalue equal to one}\} \quad \{3.21\}$$

Near the nonsingular points, $\overline{\Gamma^{p/q}}$ can be expressed as a function of ε. Near the singular points, this is impossible. We can, however, explicitly solve for two of the four variables $(x, y, \varepsilon_1, \varepsilon_2)$ in terms of the other two in the universal unfoldings of the various singular bifurcation points. The following chart is obtained directly from the universal unfoldings of Section 2.2. Except for the normal forms given in complex coordinates, the resonance surfaces of periodic points described by the equations below were already pictured in Figures 2.1, 2.3, and 2.4. For the Hopf cases with $q\geq2$, we find zeroes of the associated vector field away from the origin $(x,y) = (0,0)$, because the origin represents a fixed point of the associated map, not a period q point.

Table 3.1

Name	Independent Var's	Explicit form of $\overline{\Gamma^{p/q}}$
Saddle-node	x,ε_2	$\varepsilon = \varepsilon_1 = x^2$, $y = 0$
Period Doubling	x,ε_2	$\varepsilon = \varepsilon_1 = -\pm x^2$, $y = 0$
Cusp	x,ε_2	$\varepsilon_1 = -(\varepsilon_2 x \pm x^3)$, $y = 0$
Degenerate Per Dbling	x,ε_2	$\varepsilon_1 = -(\varepsilon_2 x^2 \pm x^4)$, $y = 0$

Hopf with Resonance:

$q\geq 5$	z	$\epsilon = -\lvert z\rvert^2 A(\lvert z\rvert^2) - B\frac{\bar{z}^{q-1}}{z}$
$q=4$	z	$\epsilon = -A\lvert z\rvert^2 - \frac{\bar{z}^3}{z}$
$q=3$	z	$\epsilon = -A\lvert z\rvert^2 - \frac{\bar{z}^2}{z}$
$q=2$	x,ϵ_2	$\epsilon_1 = -\pm x^2,\ y=0$
$q=1$ (Bogdanov)	x,ϵ_2	$\epsilon_1 = -\pm x^2,\ y=0$

Although the actual equations at a given singularity can differ from the above equations, the contact order doesn't. For instance, in the saddle node, the general form is $\epsilon=ax^2$, for some nonzero a. We can always, however, solve in terms of the two indicated independent variables listed in the above chart. Consequently, in a neighborhood of any of the above singularities, $\overline{\Gamma^{p/q}}$ is a two-dimensional manifold.

The smoothness of the resonance surfaces requires some closer inspection. Away from the bifurcation set, the surface is as smooth as the original system, $\{f_\mu\}$. On the bifurcation set, we need to consider the explicit formulas in the above table. Except for the Hopf cases q=3, q=4, $q\geq 5$, the above expressions are analytic. Consequently, for a particular application, the surface will be as smooth as the normal form (not truncated), which is as smooth as the original system. For q=4 and $q\geq 5$ the surfaces defined in the table are C^1 but not C^2. The q=3 surface is continuous and all directional derivatives exist, but due to the linear term $\bar{z}^2/z$, it is not differentiable at the bifurcation point.

Theorem 3.16: A component of $\overline{\Gamma^{p/q}}$ (that is, a resonance surface) with $q\geq 2$, $(p,q) = 1$, is generically a two-dimensional manifold without boundary in M^4. If $q\neq 3$, the manifold is at least C^1.

Proof: Let (x_0,μ_0) be a point of $\overline{\Gamma^{p/q}}$.

Case 1: $Df^q_{\mu_0}(x_0)$ has no eigenvalue equal to 1.

The implicit function theorem gives us $\mathbf{x}$ as a smooth (C^r where each f_μ is assumed to be C^r) function of μ.

Case 2: $Df^q_{\mu_0}(\mathbf{x}_0)$ has an eigenvalue equal to 1, and x_0 is a true period q point of f_{μ_0}.

Because the orbit points are not interacting, the only possible bifurcations are q-fold copies of fixed point bifurcations. Thus, a saddle-node, a cusp, and a Bogdanov bifurcation for $f^q_{\mu_0}$ are the only possibilities. (See Claim 2.1 in Section 2.2.) Table 3.1 shows all such points are smooth (at least C^1) manifold points.

Case 3: $Df^q_{\mu_0}(\mathbf{x}_0)$ has an eigenvalue equal to 1, and x_0 is not a true period q point of f_{μ_0}.

Theorem 3.15 says x_0 must be fixed point with eigenvalues $e^{2\pi ip/q}$. Table 3.1 again treats all such points. As discussed above, except when q=3, the manifold is at least C^1 at such points. □

Corollary 3.17 The set of all fixed points $\Gamma(1)$ is generically a smooth (as smooth as the original system) two dimensional manifold without boundary in M^4.

Proof: This is immediate from Theorem 3.16 by ignoring case 3.

Whenever we can assume, as we do in Chapter 5, that a resonance surface is compact, then it can be topologically classified by its genus and orientability.

In the process of proving Theorem 3.16 (Cases 2 and 3) we proved

Corollary 3.18: Generically, for (p,q) = 1, $Z^{p/q}$ consists of

1) q copies of simple saddle-node bifurcations of period q points of f_μ
2) q copies of cusp bifurcation points of period q points of f_μ
3) q copies of Bogdanov bifurcation points of period q points of f_μ
4) A Hopf bifurcation of a fixed point of f_μ with resonant eigenvalues $e^{2\pi ip/q}$

4. NUMERICAL EXPERIMENTS

4.1 A Forced Oscillator Caricature

The following example, given to the author in 1985, was devised by R. P. McGehee as a caricature of a forced oscillator, tractable to computer simulations and experiments.

$$\mathbf{x}_{n+1} = \mathbf{F}_\mu(\mathbf{x}_n) \text{ for } (\mathbf{x},\mu) = (\omega_0,\alpha,x,y) \in \mathbb{R}^2\times\mathbb{R}^2 \qquad \{4.1\}$$

where $\mathbf{F}_\mu$ is the composition $\mathbf{g}_\alpha \bullet \mathbf{f}_{\omega_0}$.

$\mathbf{f}_{\omega_0}$ is defined as the time one map of the flow described by

$$\frac{dr}{dt} = \frac{r(1-r^2)}{1+r^2}, \quad \frac{d\theta}{dt} = 2\pi\omega_0 + \frac{1-r^2}{1+r^2}, \ \omega_0 \in \mathbb{R} \qquad \{4.2\}$$

$$\mathbf{g}_\alpha \equiv (1 - \alpha)((x,y) - (1,0)) + (1,0), \ \alpha \in [0,1] \qquad \{4.3\}$$

The vector field described by {4.2} has the unit circle as a globally attracting invariant set which serves as our "unforced" oscillator. By composing the two maps, we perturb the flow of {4.2} by "kicking" the system toward (1,0) every second, according to {4.3}. (Thus, the forcing frequency ω is always 1.) This type of composition has been called "impulse forcing" by others. [SDCM]

Note that $\mathbf{g}_0$ is the identity. Thus, for small α, we can think of the composition as a perturbation of the unforced oscillator {4.2}. This means that the theory of section 2.5 for forced oscillators with small forcing amplitude should apply for small α. We should be able to find (given good enough numerical techniques) resonance horns emanating from each point $(\omega_0/\omega,\alpha) = (\omega_0,\alpha) = (p/q,0)$ on the ω_0 axis into the $\alpha>0$ region.

$\mathbf{g}_1$ on the other hand maps every point to (1,0). Consequently, for large α (near 1), $\mathbf{F}_\mu$ is a perturbation of a map with a globally attracting fixed point. This is important because one of the objects of investigation is resonance horns that "close." Being a perturbation of a map with a globally attracting fixed point means that for α near 1, no periodic points other than fixed points should exist. That is, each p/q resonance horn must close when α approaches 1.

The specific form of the vector field {4.2} was chosen because it has an explicit solution obtainable by separation of variables. This saves us hours of computing time by allowing us to find a closed form for the time 1 map of {4.2}, instead of requiring a numerical integration to evaluate each iterate of $\mathbf{F}_\mu$.

4.2 Numerical Techniques

Several standard "continuation" packages currently exist for following equilibria of differential equations, and fixed points of discrete maps. [DK] All seem to use a Newton-Raphson iterative scheme to converge in the full phase×parameter space to the desired points. Some small additions allow continuation of periodic points of discrete maps with period larger than 1. These periodic points are precisely the points on the resonance surfaces that we are investigating.

Ideas originating with R. P. McGehee led to continuation techniques which turned out to be similar to "standard" pseudo arc length continuation methods. [Do] Our algorithms are tailored specifically for a four-dimensional system (two parameters, two phase variables), however, so their versatility is somewhat restricted. All our Newton-Raphson iterations are performed on a four-dimensional (no larger augmented systems) system of equations, two of which are always

$$\mathbf{F}_\mu^q(\mathbf{x}) - \mathbf{x} = \mathbf{0} \qquad \{4.4\}$$

The remaining two equations depend on the situation, although one of the two is always chosen to ensure that the vector from the original guess to the point on the resonance surface to which we converge is perpendicular to a second vector. This second vector is usually chosen to be at least an approximation to a tangent vector to the resonance surface at the starting guess or at the previously found point on the resonance surface. The fourth equation is chosen in one of the following two manners:

1. Same as the third equation, but with a different (independent) tangent vector. The two tangent vectors to the resonance surface can be chosen by the user, approximated numerically from nearby points on the resonance surface, or constrained to lie in a certain three-dimensional slice of the phase×parameter space, such as μ_2=constant.

2. To ensure a codimension-one (bifurcation) curve is followed ($A = D_x f_\mu q(x)$):

Equation	Description	{4.5}
A. $Tr(A) - Det(A) - 1 = 0$	Saddle-node bif.; an eigenvalue = 1	
B. $Tr(A) + Det(A) + 1 = 0$	Period doubling bif.; an eigenvalue = -1	
C. $Det(A) - 1 = 0$	Hopf bifurcation; the product of the eigenvalues =1	
D. $[Tr(A)]^2 - 4Det(A) = 0$	The eigenvalues are equal	

Although the last curve is not a bifurcation curve, it does indicate the boundary between nodes and foci, which helps to determine the phase metamorphoses in the bifurcation diagrams.

A note of comparison with standard continuation routines such as AUTO [Do]: the above method for continuing codimension-one curves does not require the augmentation of the original system with an equation for the eigenvector (eg., for the saddle-node: $A\phi = \phi$). For this reason, it may be considered more efficient, although we lose the distinguishing feature of the eigenvector. This can cause a convergence problem because we can have points, all close to each other on the resonance surface, that satisfy the same set of four equations, but have different eigenvectors.

Note that the condition for a Hopf bifurcation we use can be satisfied not only for a Hopf bifurcation, but also for a saddle point whose real eigenvalues multiply to get one. Thus, our routines don't stop at double 1 or double -1 eigenvalue points in the Hopf continuation. We do, however, have a curve which continues indefinitely; this provides a nice way to get from one true Hopf bifurcation curve to another.

4.3 Experimental Phenomena: Compact Resonance Surfaces

The resonance surfaces of the system described in Section 4.1 do turn out to be compact for $q \geq 2$. One parameter cuts for constant $\alpha > 0$ give us cross sections of the various p/q resonance surfaces. Small α always yields slices analogous to Figure 2.10. Following the saddle-node curves gives us the boundaries of the resonance surfaces, with the exception of the period two horns, whose boundary includes period doubling curves, as well. The combination of cross sections and bifurcation curves allows us to get an idea of what the complete resonance surfaces are like, both topologically and geometrically.

For most of the p/q resonance horns (period $q \geq 5$), the cross sections are the same topologically from the small α cross sections near the bottom tip of the resonance horn, to the cross sections approaching the Hopf bifurcation point (with resonant eigenvalues $e^{\pm 2\pi i p/q}$) which mark the closing of the p/q resonance horn. The orientation near the Hopf point depends on whether the Hopf bifurcation point is supercritical or subcritical. See Figure 4.1. The cross sections for the strong resonance cases (q=1,2,3) are indicated along with q=5 in Figure 4.2. We have attempted to draw in the actual three-dimensional space $\{\alpha=\alpha_0\}$. Note the "$\sqrt[q]{1}$" point for q=3, 5. These are Hopf bifurcation points with resonance: $\lambda_1, \lambda_2 = e^{\pm 2\pi i p/q}$.

From the small forcing amplitude theory, we know each p/q resonance surface projecting to a resonance horn near zero forcing amplitude has as a boundary, C_0, the original unforced oscillator, lying above (p/q,0) in the (ω_0,α) parameter plane. Thus, each such compact resonance surface is a compact two-manifold with a single topological circle as its boundary. We can use either Morse theory or combinatorial construction to identify each surface.

We will pursue the Morse theory first. [Mi] Temporarily identifying the points on this circle to a point, leaves us with all p/q resonance surfaces with $q \geq 2$ as compact two-manifolds without boundary. We can then use Morse theory to determine the particular two-manifold represented by each resonance surface. We use as our Morse function, projection onto the parameter variable α. For $q \geq 3$, the resonance surfaces have two critical points, and so must be spheres. The p/2 horns all have three critical

points; they are therefore projective planes. By reopening the holes we closed to apply the Morse theory, we see that the p/q resonance surfaces are disks for $q \geq 3$, a mobius strip for $q=2$, and a cylinder for $q=1$.

The fixed point surface $\Gamma(1)$ is quite different, because it extends to all parameter values. The triangular curves of period-one saddle-node fixed point bifurcations mark folds in the fixed point surface rather than the boundaries of period-one "resonance horns." Inside the triangles, there exist three fixed points; outside there exists only one. Since the parameter space is the strip $\mathbb{R}\times[0,1]$, and the folds don't change the topology, $\Gamma(1)$ must also be a closed strip with a hole (C_0).

The combinatorial construction of these surfaces corroborates the Morse theory results just stated. [Ma] In all cases, the boundary circle C_0 is represented by a cross section "near" the tip. (Cross sections "A" in Figure 4.2) This circle is divided by the saddle-node bifurcation points into q "node" components (n_i) alternating with q "saddle" components (s_i). (Recall Figure 2.10.) For $q=1$, we cut the fixed point surface on either side of the triangular "resonance region" in order to use the combinatorial approach, valid for compact surfaces. The various cross sections of Figure 4.2 determined the pairings and corresponding edge identifications to use in Figure 4.3. Dick Hall first suggested a figure similar to parts of the $q=3$ diagram; Dick McGehee and Rick Moeckel suggested other parts of the $q=3$ diagram and the $q \geq 5$ diagram.

Figure 4.4 pictures several of the p/q resonance horns with some selected phase portraits. These phase portraits were chosen to show the various routes from the attracting invariant circle C_0 to the unique attracting fixed point for large α. (The 4/5's horn pictured is a hedge to limit the number of phase protraits we needed to draw. The actual change from super to subcritical Hopf bifurcations occurs somewhere between the the 4/5 and 1/1 horns.) Figure 4.5 is actual computer output of a three-dimensional version of Figure 4.4: the q copies of the saddle-node curves demark the "edges" of the various p/q resonance surfaces while several cross sections (α=constant) have been included as an aid to visualize the structure of the entire surface. We projected the actual surface into the three-dimensional $(x,\varepsilon_1,\varepsilon_2)$ space for Figure 4.4. Dealing with the fourth dimension requires even more imagination.

Some more detailed typical bifurcation diagrams are included in Chapter 5.

4.4 Experimental Phenomena: A Bifurcation Overview

Return to Figure 4.4's picture of several of the p/q resonance horns together. They all appear to run from α=0 to (roughly) the Hopf bifurcation curve. A naive description of the full bifurcation picture is that of a globally attracting invariant circle surrounding an unstable fixed point at α=0, shrinking around the unstable fixed point to form a globally attracting fixed point as α increases toward 1. The natural way for this to happen is via a Hopf bifurcation. The Hopf curve, however, has breaks in both the period-two and period-one horns. As the selected phase portraits from Figure 4.4 show, these breaks allow radically different paths in the parameter space from the bottom (with respect to α) to the top.

In the period-two horn, the unstable fixed point undergoes a first period "undoubling" to become a saddle, and then a second to become a stable fixed point. In the period-one horn, the saddle point, which is paired with a stable node along the sides of the resonance horn, switches loyalties at a top corner cusp to be paired with what used to be the center unstable fixed point. Above the top of the triangle, the only remaining fixed point is the stable fixed point. Note that the only codimension-two point which supports three fixed points is the cusp. It occurs, however, in a single phase dimension. The Bogdanov points and the associated Hopf bifurcation are necessary in order for the three fixed points to be able to line up in that one dimension. As we discuss in Chapter 6, this is the reason the cusps and Bogdanov points must be part of the period-one saddle-node curves.

To avoid misleading anyone about the complexity of the full bifurcation problem, we mention that, even though the resonant surfaces of fixed points turn out to be standard topological surfaces, the complete picture of phase portraits will never be simple. This is mostly due to the existence of global bifurcations: manifold crossings and corresponding regions of "chaos." Such regions are known to necessarily exist near codimension-two local bifurcation points with manifold crossings. In particular, the list includes Bogdanov points, double -1 points, and Hopf points with period-three resonance. See Chapter 6 for a more complete discussion of the "typical" bifurcation diagrams.

5. COMPACT RESONANCE SURFACES--BIFURCATION STRUCTURE

5.0 Introduction

In section 3.5, we treated our resonance surfaces as topological objects in the phase×parameter space, M^4. In the process we considered the singular set

$$Z^{p/q} \equiv \{(\mathbf{x},\mu) \in \overline{\Gamma^{p/q}} : D_{\mathbf{x}} f_{\mu}^{q}(\mathbf{x}) \text{ has an eigenvalue equal to one}\} \quad \{3.21\}$$

We determined that even points in the singular set are manifold points of $\overline{\Gamma^{p/q}}$. We now consider the question of determining what singular points and/or curves actually exist on any given resonance surface. In particular, we consider the specific resonance surfaces that we know exist for forced planer oscillators with small forcing amplitude. (Recall sections 2.2 and 2.5.)

We define these resonance surfaces for $q \geq 2$ as

$$\Gamma_0^{p/q} \equiv \text{the component of } \overline{\Gamma^{p/q}} \text{ containing } C_0 \times \mu_{tip}, \text{ where } \mu_{tip} = (p/q,0) \quad \{5.1\}$$

$$\equiv \underline{\text{the}} \text{ p/q resonance surface}$$

$$A_0^{p/q} \equiv \pi_{\mu}(\Gamma_0^{p/q}) \text{ where } \pi_{\mu} \text{ is the projection onto the parameter space} \quad \{5.2\}$$

$$\equiv \text{the } \underline{\text{p/q Arnol'd Resonance Horn}} \text{ we wish to investigate.}$$

If we let

$$\Gamma^{p/1} \equiv \Gamma(1) \text{ for every p} \quad \{5.3\}$$

then $\overline{\Gamma^{p/1}} = \Gamma^{p/1}$, and q=1 can also fit into definitions {5.1} and {5.2}.

Caution: $(\mathbf{x},\mu) \in \Gamma^{p/1}$ does not imply $\rho_S(\mathbf{x},f_{\mu})=p$. The role of p in {5.1} for q=1 is only to determine a certain component of $\Gamma(1)$.

Continuing:

$$Z_0^{p/q} \equiv Z^{p/q} \cap \overline{\Gamma_0^{p/q}} \qquad \{5.4\}$$

The first question we ask is : "How simple can the resonance surfaces be?" From the small forcing amplitude theory we know that $\Gamma_0^{p/q}\,|_{\{0<\alpha_0<\alpha\}}$ is composed of true period-q points. All examples of "closed" resonance horns, however, appear to have a point where the period-q orbit sitting "above" it on the resonance surface coalesces to a fixed point. This leads to the following conjecture, which we are not able to prove in its full generality. A *generic* resonance surface is one that arises from a generic two-parameter family of forced oscillations of the plane as in {2.11}).

<u>Conjecture 5.0</u>: Let $\Gamma_0^{p/q}$, q≥2, be a generic p/q resonance surface. If $\Gamma_0^{p/q}$ is compact, then it has a fixed point with eigenvalue $e^{2\pi ip/q}$.

Typically, this fixed point occurs along a saddle-node bifurcation curve for q≥5 (the q saddle-node curves coalesce to a fixed point), and on the interior of the resonance horn for q=3. When q=4, either may occur. A whole curve (a period doubling curve) of fixed points will exist for q=2, while q=1 is altogether a different case.

5.1 The Actual Theorem

We begin, as usual, with some new notation. We define a quotient manifold $[\Gamma_0^{p/q}]$ by $[\Gamma_0^{p/q}] \equiv \Gamma_0^{p/q} / \sim$ where $(x,\mu) \sim \vec{f}(x,\mu)$ $(= (\mathbf{f}_\mu^j(x),\mu))$ for any integer j. If $\Gamma_0^{p/q}$ has no fixed points then the natural projection $\pi_\sim: \Gamma_0^{p/q} \to [\Gamma_0^{p/q}]$ is a q-fold covering map.

Theorem 5.1: Let $\Gamma_0^{p/q}$, q≥2, be a generic p/q resonance surface. If $\Gamma_0^{p/q}$ is compact, and either q is even or $[\Gamma_0^{p/q}]$ is orientable, then it has a fixed point with eigenvalue $e^{2\pi ip/q}$.

Proof: Assume $\Gamma_0^{p/q}$ has no fixed points.

Because we are working with the specific resonance horn $\Gamma_0^{p/q}$ for the rest of the proof, we will drop the subscript 0 and superscript p/q.

The small forcing amplitude theory implies that $\partial(\Gamma) = \Gamma\big|_{\{\alpha=0\}} = C_0$ is a topological circle, which covers $\partial[\Gamma] = [C_0]$ q times. The same is true of any slice $\{\alpha=\alpha_0\}$ for small enough α_0. Thus, Γ is topologically equivalent to $\Gamma\big|_{\{\alpha\geq\alpha_0\}}$ for α_0 sufficiently small (retract the cylinder $\Gamma\big|_{\{0\leq\alpha\leq\alpha_0\}}$ onto the circle $C_{\alpha_0} \equiv \Gamma\big|_{\{\alpha=\alpha_0\}}$, so we may work directly with $\{\alpha \geq \alpha_0\}$. We shall still refer to the "truncated" manifold as Γ.

C_{α_0} (see Figure 2.10) is divided by 2q saddle-node points (a period-q orbit on the left side of the resonance horn and a period-q orbit on the right side) into segments which alternate between node segments and saddle segments. We label them $s_1, ..., s_q$; $n_1, ..., n_q$. $[C_{\alpha_0}]$ has two corresponding segments in the quotient manifold which we will label [s] and [n].

Because $[\Gamma]$ is a two-manifold with a single hole, it has a combinatorial normal form as in Figure 5.1. [Ma] The outside curve consists of edges identified in pairs. Furthermore, the normal form allows all outside vertices to be the same point P.

Without fixed points, $\pi_{\sim}: \Gamma \to [\Gamma]$ is a q-fold covering map. For each oriented closed curve $[\gamma] \in [\Gamma]$, we can define an index $I([\gamma]) \in \mathbb{Z}/q$ by lifting $[\gamma]$ to Γ. Because $\pi_{\sim}$ is a covering map, this lift is uniquely determined by fixing a starting point $\mathbf{u}_0 \in \Gamma$. The ending point $\mathbf{u}_1 \in \Gamma$ is necessarily an iterate of the $\mathbf{u}_0$. ($\mathbf{u}_0, \mathbf{u}_1 \in \pi_{\sim}^{-1}[\mathbf{u}]$ for some $[\mathbf{u}] \in [\Gamma]$. Say $\mathbf{u}_1 = \mathbf{f}^j(\mathbf{u}_0)$, $j \in \mathbb{Z}/q$. We define $I([\gamma])$ to be j. This index is well defined independent of the choice of base point in $[\Gamma]$ and of the corresponding starting point of the lift in Γ.

We now consider the specific path $[\gamma] \in [\Gamma]$ indicated in Figure 5.1. Since it is obviously contractible to a point, the lifting lemma [Mu] implies $I([\gamma])$ is zero. Consequently, $I([C_{\alpha_0}]) + I([\text{the outside curve}])$, with orientations on these two curves induced by the indicated arrows on $[\gamma]$, is zero.

Furthermore, the small forcing amplitude theory implies that the action of **f** on C_{α_0} is conjugate to a rigid rotation by $2\pi p/q$. By following any s_i and then the n_j to which it connects (or vice verse), we see that a lift of $[C_{\alpha_0}]$ ends up an angle of $2\pi/q$ away from its starting point. Thus the index $I([C_{\alpha_0}]) = k$, where $pk=\pm 1 \in \mathbf{Z}/q$. Equivalently,

$I([C_{\alpha_0}])$ and q are relatively prime. {5.5}

To compute I([the outside curve]), we use the fact that, in its combinatorial form, this outside curve consists of pairs of identified edges. Each edge, because all vertices are identified, is a closed curve in $[\Gamma]$, and thus has an index. If $[\Gamma]$ is orientable, one of each pair will point clockwise, and the other will point counterclockwise. In this case, the indices of the two will cancel each other and the index all the way around will be zero. This contradicts {5.5}. If $[\Gamma]$ is not orientable, noncancelable indices will occur in pairs, forcing the "outside" index to be even. If q is even, this will again contradict {5.5}. □

Note to readers of [AMKA]: The above theorem is sufficient to prove the Conjectures stated in that publication. Their restriction to a Γ which projects to a "simple disklike region" is more than strong enough to ensure that, except possibly for fixed points, $[Z_0^{p/q}]\big|_{\{\alpha>0\}}$ consists of only the single component $[CSN^{p/q}]$, which we define to be the component containing the (identified) saddle-node orbit we know exists for small forcing amplitude. $[\Gamma_0^{p/q}] \setminus [Z_0^{p/q}]\big|_{\{\alpha>0\}}$ consists of two components which we label [S] and [N] for the Saddle and Node surfaces we know exist near the tip of the surface, each necessarily orientable by overlapping coordinate systems that are all projections to the parameter plane, and each with a single hole consisting of $[CSN^{p/q}]$ and either [s] or [n]. (With our notation, $[s] = [S]\big|_{\{\alpha=\alpha_0\}}$ and $[n] = [N]\big|_{\{\alpha=\alpha_0\}}$.) When the two components are sewn together along their common boundary, $[CSN^{p/q}]$, the resulting manifold $[\Gamma]$ is necessarily orientable.

6. TYPICAL FORCED OSCILLATOR BIFURCATION DIAGRAMS

6.0 Introduction

So far, we have described, in Chapter 4, some of the resonance surfaces and other bifurcation structure associated with a particular example. We developed some machinery in Chapter 3 in order to enable us to prove in Chapter 5 some results about the structure of certain resonance surfaces. The questions we now ask are:

1) How reasonable are the assumptions of our theorems? Can we expect to see in practice examples of the fixed points that appear in our theorems?

2) How close to "typical" is the example of Chapter 4? What features are most likely to vary from case to case?

We will begin by considering each resonance horn individually. Comparisons are facilitated by existing numerical examples in the existing literature: a periodically forced CSTR [KAS], a periodically forced Brusselator [KT, AMKA], a forced bimolecular surface reaction model [MSA], and two impulse forcing models [SDCM], similar to our example. The last two, [MSA] and [SDCM] offer the best view of the complete parameter space bifurcation diagrams of which we are aware at this time. ~~[AMKA]~~ has the most detail of possible bifurcations inside a single horn.
[ACHA]

6.1 Assumptions on the system

Assumption 1: $\Gamma_0^{p/q}$ is compact.

As mentioned in Chapter 4, for small forcing amplitude we can consider the system

$$\frac{dx}{dt} = F(x) + \alpha G(x,\omega t)\,, \quad \omega \neq 0 \qquad \{2.11\}$$

as a perturbation of the unforced system $\frac{dx}{dt} = F(x)$, and for large forcing amplitude as a perturbation of the "forcing system," $\frac{dx}{dt} = G(x,\omega t)$. If, as happened in our example, both equations have recurrence restricted to a bounded region of phase space, then we would expect the same to hold for all α. If the time $1/\omega$ map of $\frac{dx}{dt} = G(x,\omega t)$ has a unique attracting fixed point, then for large enough α, we expect any individual $\Gamma_0^{p/q}$, $q \geq 2$, to cease to exist. Because the second parameter controls the self rotation number of an orbit, which is constant on a given $\Gamma_0^{p/q}$, that resonance surface should exist only in a finite interval of ω_0/ω's.

Caution: For $\omega=0$, the resulting planar map will usually exhibit nongeneric behavior, besides having a restricted physical interpretation. Furthermore, as $\omega \to 0$, integration of return maps can become very expensive. We avoided this problem in our caricature by varying ω_0 instead of ω. In addition, the integrability of the unforced oscillator system allowed us to completely avoid any numeric integration.

Assumption 2: $[\Gamma_0^{p/q}]$ is orientable.

The the comments after the proof of Theorem 5.1 gives us a hint of how "messy" the system must be in order to obtain a nonorientable $[\Gamma_0^{p/q}]$. We note that we are aware of no example in the literature where $[Z_0^{p/q}]$ consists of anything other than $[CSN^{p/q}]$ and possibly a fixed point bifurcation. If $\Gamma_0^{p/q}$ has a fixed point bifurcation, then we already have what we want, while without any further components of $[Z_0^{p/q}]$, $[\Gamma_0^{p/q}]$ is always orientable. The least complicated way to form a nonorientable manifold is with three components of $[\Gamma_0^{p/q}] \setminus [Z_0^{p/q}]$, each with two holes, one identified with each of the other two components. This would form a Klein bottle. In general, we need a chain of components of $[\Gamma_0^{p/q}] \setminus [Z_0^{p/q}]$: $[X_1]$, ..., $[X_M]$, each connected to its

neighbors, with $[X_1] = [S]$, and $[X_M] = [N]$, and orientations arranged so that all boundary pairs don't cancel each other.

The most "reasonable" complications we would expect to see are:

1. A Handle: a saddle-node boundary curve (not [CSN]) along which [S] and [N] are identified to make a "handle" on $[\Gamma_0^{p/q}]$. See Figure 6.1.

2. An Interior Fold: a saddle-node boundary curve between one of [S] or [N] (say [S]) and a third component, [X], is caused by an extra fold which appears on [S]. See Figure 6.2.

3. A Boundary Fold: This is similar to the interior fold just described, except that the extra fold occurs at the "edge" of the surface, involving both the [S] and [N] surfaces.

A handle adds a new singular component (in addition to $[CSN^{p/q}]$) but no new surfaces to the component "chain." An interior fold adds a surface component, but the chain terminates after that addition. When this happens, [X] is a topological disk. If the index of the saddle-node curve along which it attaches to [S] is not zero, then X would necessarily have a fixed point. Thus, adding such a fold cannot change the index of $[C_{\alpha_0}]$ or the orientability of $[\Gamma_0^{p/q}]$. A boundary fold adds neither a singular component nor a surface component. (Neither fold changes the topology of $\Gamma_0^{p/q}$.) In all three cases, $[\Gamma_0^{p/q}]$ remains orientable, so the corresponding resonance surfaces must all have fixed points associated with them.

Note the cubic nature of the cross sections at the beginning and end of the fold in Figures 6.2 and 6.3, slice B. Such folds can only occur in conjunction with the two corresponding cusps. Studying Figure 6.3 shows why the two cusps must occur on the interior of the horn for the boundary fold. The self intersection point P in the parameter space must generically correspond to two different phase points. Thus four distinct surfaces exist that project to the interior of our loop. They are paired by the saddle-node bifurcations, say surface 1 with 2 and 3 with 4. As we travel around the loop, this

pairing must change from 1 with 2 at one end to 3 with 4 at the other. If no fixed points are involved, the only local codimension-two bifurcation that involves more than two periodic orbits is the cusp bifurcation, which involves three. Consequently, two cusps are needed in order to make the exchange. In our example, we first exchange 3 for 1, and then 4 for 2.

Both [MSA] and [SDCM] have found examples of boundary folds, but we are not aware of examples of the other two "complications."

Assumption 3: The (pseudo) Hopf Curve (which exists by Assumption 1) is unique, and the self rotation number varies monotonically along the curve.

This assumption, which has not been used to obtain any of the results in this paper so far, can be thought of as a "reasonableness of parameter dependence" assumption. Although one can easily imagine systems in which there exist more than one Hopf bifurcation curve, this assumption (which appears to be satisfied by all the examples cited above) severely limits the possibilities for the full bifurcation structure. This monotonicity assumption, which also appears to be satisfied in all the examples cited in the chapter introduction, while not expected to hold for arbitrary two-parameter families of maps, *will* tend to hold for forced oscillator bifurcation diagrams, because by construction, one of the parameters is effectively a rotation number. Thus we expect rotation numbers to increase in general as the rotation number parameter is increased. This, along with the expectancy of crossing the Hopf curve as one increases the forcing amplitude, causes the Hopf curve to roughly run parallel to the rotation number axis.

With assumptions 1 and 3, the $\Gamma_0^{p/q}$ resonance surfaces for q even (and > 2), have only one road to follow: from the bottom tip of the horn to the Hopf point with rotation number p/q. Furthermore, because the rational numbers with q even are dense in the reals, it would require an extremely nonlinear map to allow the "odd" surfaces to go anywhere but to the appropriate point on the Hopf bifurcation curve next to their well-behaved even brothers. In fact, by the same arguments used for the resonance surfaces emanating from the zero forcing axis, the only way for the tips of a p/q

resonance horn to fail to connect is to have both corresponding quotient surfaces be distinct nonorientable surfaces. With assumption 2, of course, this is not an issue.

6.2 Individual Resonance Horns

Modulo the folds and handles that were mentioned under the assumption 2 discussion above (which could be eliminated by a broader monotonicity assumption than Assumption 3), the topological character of the resonance horns must be the same as in our example for $q \geq 3$: $\Gamma_0^{p/q}$ is a topological disk.

For $q \geq 5$, the bifurcation structure can have any of the complicated internal structure described in [ACHM], although the larger the period q, the narrower the resonance horn, and the less "room" for complications to develop. For instance, the first step in the breakup of the invariant circle C_0, the changing of the sink eigenvalues from real to complex, doesn't even appear to occur in our examples. The invariant circle appears to persist throughout the entire resonance horn.

We have seen that for q=3, the "$\sqrt[3]{1}$" point must occur as an isolated singular point. The "$\sqrt[4]{1}$" point may be an isolated point, or it may appear as do all other "$\sqrt[q]{1}$" points: at the intersection point of the 2q saddle-node rays as in Figure 4.3 for q=5.

As promised, Figures 6.4, 6.5, and 6.6 show some rather detailed bifurcation diagrams for typical period 1, 2, and 3 horns, respectively. We believe these to be complete bifurcation diagrams modulo the following equivalences.

1. We have indicated both local and global codimension-one bifurcations by curves in the parameter space. The global bifurcations, of course, because they involve manifold crossings, typically occur in a region of parameter space, not on a curve. In some but not all cases, we have included the vector field approximation to these global bifurcations: manifolds are shown as coincident. The actual manifolds for the map generically cross each other infinitely many times, but are not coincident. In regions of homoclinic crossings, for

instance, it is known that there is an infinity of topologically inequivalent maps. We have conveniently identified them as a single equivalence class.

2. In the p/q resonance horn, all self rotation numbers are typically very close to p/q. We think of q as our "base period" and require equivalent maps to all have the same number, orientation, and stability of period q orbits. The basins of attraction and stability for other recurrent sets should be the same, but these recurrent sets, not being of our base period, we do not require to be topologically equivalent. This comment applies to any of the period q = 1, 2, or 3 phase portraits in which a nontrivial invariant curve appears, with a (self) rotation number other than p/q. Phase locking at different frequencies on these "other" invariant curves makes these phase diagrams topologically inequivalent. We treat them, however as equivalent.

We will make some brief comments on the bifurcation diagrams, indicating what features are typical of period q resonance surfaces, and indicating what features are most likely to vary from system to system. All local bifurcation curves we have been able to confirm using our continuation techniques. The knowledge of global bifurcation curves which originate at local codimension-two bifurcation points comes from the corresponding unfolding. The orientation of the global curves when they interact with codimension-one local curves is the feature of which we are least certain. See, for example, the point on the period doubling curve in the period-two horn where almost all the dashed global lines converge. Symmetry, some suggestions from [ACHM], and some (hopefully) educated guesses all played roles in determining these curves.

q=3

All bifurcation curves and points necessarily appear except possibly the equal eigenvalue curve, inside which the period-three sink becomes complex. If this equal eigenvalue curve were larger, it could intersect the saddle-node curve to give a Bogdanov point. Stability arguments imply the Bogdanov points always occur in pairs. If the equal eigenvalue curve were smaller, it might not intersect the global stable manifold crossings bounding the bottom of regions 4 and 6, respectively, in Figure 6.6. These two crossing "curves" could then connect with each other to form the top boundary of region 2.

q=2

Assumption 3 implies there are exactly two double -1 points with self rotation number p/2. The unfoldings of these points imply the existence of period doubling curves through each. The generic unfoldings of period doubling curves imply each component is a closed curve. Stability arguments (period doubling of a saddle or a node) imply both double -1 points must lie on the same period doubling curve.

The gap in the Hopf bifurcation curve between the two double -1 points allows routes from the attracting invariant circle C_0 for the unforced oscillator to the globally attracting fixed point for large amplitude of forcing that don't involve a Hopf bifurcation of the fixed point. Typically, this route involves the period-two saddle "undoubling" as we enter the period doubling circle from the bottom, and the period-two sink undoubling as we leave the period doubling circle at the top. (Recall Figure 4.4.) This is possible only if there exist two degenerate period doubling points where the period doubling bifurcation changes from supercritical to subcritical: on the "bottom half" we undouble on the way into to period doubling circle; on the top half we undouble on the way out of the circle. The resulting "ice cream cone" period-two resonance horn is therefore typical.

Note that Arnol'd has split the q=2 unfoldings into two cases (Figure 2.7), depending on whether the period-two orbit which appears is a saddle or a node/focus. In Figure 6.5, the right hand side double -1 is the former; the left hand side double -1 is the latter. The Bogdanov point B_2 (Figure 6.5) for the period-two orbit appears in conjunction with the node/focus double -1 point; the secondary Hopf bifurcation curve runs between these two points. If the double -1 points were both of the "saddle" type or both of the "node/focus" type, the period-two Bogdanov point wouldn't necessarily appear.

q=1

Assumption 3 implies there are exactly two Bogadanov points with self rotation number p/1. Saddle-node curves pass through each. The generic unfoldings of saddle-node curves imply each component other than $CSN^{p/1}$ is a closed curve. Stability arguments imply both Bogdanov points must lie on the same saddle-node component.

All $CSN^{p/1}$ resonance horns we have seen bound a triangular regions (with cusp points at the top two corners) and do, in fact, contain two Bogdanov points (with self rotation number p/1).

If there are no other saddle-node curves with self rotation number p/1, then the two cusps and two Bogdanov points will always appear on the $CSN^{p/1}$. This is because the gap in the Hopf bifurcation curve between the Bogdanov points allows a route in the parameter space from the bottom to the top without ever encountering a Hopf bifurcation. Because the self rotation numbers will all tend to be near p/1, no period doubling curves will be involved either. The only remaining bifurcation is the saddle-node.

Inside the triangle, we have, for the most part (at least near the bottom tip) one saddle, one stable node/focus, and one unstable node/focus. (Figure 4.4, again) In order to be left with the stable node/focus at the "top" of the parameter space, the saddle-node bifurcation along the top of the saddle-node curve must involve the saddle and the unstable node/focus (originally the "center" fixed point in low forcing amplitude phase portraits) instead of the saddle and the stable node/focus which we know interact at the sides of the horn near its bottom tip. The two cusp points are where this exchange takes place, while the change in the stability of the node is the saddle-node bifurcation takes place at the Bogdanov points. Note that the cusp bifurcations can take place only between a saddle and two nodes which have the same stability. In Figure 6.4, both nodes are sources in the top left corner of the triangle, while both are sinks in the top right corner.

The relative position of the cusps and the Bogdanov points also determines the criticality of the Hopf bifurcation curve emanating from the Bogdanov points. In the top left corner, we have a subcritical Hopf bifurcation curve. The corresponding bifurcation diagrams are more complicated than those for the region near the supercritical Hopf bifurcation in the top right corner of the horn.

6.3 Global Global Theory

We have discussed above, some global aspects of individual resonance surfaces and resonance horns. Figure 4.4 shows how the global horns fit together to form the

global global picture for our example. From the above comments, we consider this figure to be typical of resonance horns when they do all close.

Because we have only pictured a few of the resonance horns in Figure 4.4, one aspect we have failed to address is the overlapping of these horns. As mentioned in the previous section, phase portraits corresponding to the p/q resonance horn with $q \geq 5$ (as far as we could determine) always had a globally attracting invariant circle. In such cases, we know the resonance horns cannot overlap. On the other hand, when an invariant curve is part of a phase portrait (as we saw several times in the period 1, 2, and 3 bifurcation diagrams), we expect regions of overlapping horns. Because these invariant curves occur in the universal unfoldings of codimension-two points such as the Bogdanov point, the double negative one point, and the period-three resonant Hopf bifurcation point, near these points we will always have overlapping resonance horns. Figure 6.7 shows the placement of some of these resonance horns in the full bifurcation picture.

By following "curves" of homoclinic orbits, which again exist in the neighborhood of the same three codimension-two points, we can identify regions of chaotic behavior. These "curves" are labelled $\underline{h}$ in Figure 6.7.

Our caricature example had one additional codimension-two bifurcation point: a degenerate Hopf bifurcation. This bifurcation is roughly similar to the degenerate period doubling bifurcation described in Section 2.2. At this point, the Hopf bifurcations change between supercritical and subcritical. Because the Hopf bifurcations at the "left hand" Bogdanov point are subcritical, and the Hopf bifurcations at the right hand double negative one are supercritical, there must be at least one point along the Hopf bifurcation line connecting the two points where the criticality changes. Chenciner [Ch] has discussed this bifurcation in great detail, although the complicated nature of the resonances involved in the problem make a complete description virtually impossible.

7. PARTING COMMENTS

The applicability of the tools and results developed in this paper is not limited to the forced oscillator problem. We list a few of them here.

7.1 Hopf Bifurcation Resonance Horns

The cross sections of resonance surfaces near the Hopf bifurcation tip are topologically the same as cross sections near the "unforced oscillator" tip for $q \geq 5$. Thus most of the global theory derived above for horns emanating from a line in the parameter space representing an unforced oscillator can be applied to horns emanating from a line of Hopf bifurcations. In particular, if in section 3.2, we redefined

$\Gamma_0^{p/q} \equiv$ the component of $\Gamma^{p/q}$ containing the point at the Hopf bifurcation line with linearization $e^{2\pi ip/q}$

then in order to close, these surfaces must encounter a second Hopf bifurcation point. Topologically, these surfaces would typically be spheres instead of disks, because the unforced oscillator "hole" for the forced oscillator resonance surfaces does not appear.

7.2 $(p,q) \neq 1$

Throughout this paper, we have assumed we were working with p/q resonance surfaces with $(p,q)=1$. If this is not the case, the surface can be thought of as a "secondary" bifurcation surface. Such a surface can still have period q orbits and fixed points, but it may also have period r orbits for any r that divides both p and q. A classification of all possible bifurcation points for this surface must include these nonfixed points as well. When r is the lowest period of an orbit involved in a bifurcation, r copies of a bifurcation of f^r will appear.

7.3 Orientation at Coalescence of Orbits with Real Eigenvalues

The continuity of $\tilde{R}_{a,\theta,x,\mu}(q)$, including $\{a=0\}$, as used in the proof of Lemma 3.14, gives us an interesting way to corroborate the orientation of the period-two points of Arnol'd's unfolding in Figure 2.7 for q=2. The period-two points all have $\tilde{R}_{a,\theta,x,\mu}(2) \equiv p$. At a=0, however, only $\theta = 0,\pi \bmod (2\pi)$, corresponding to the eigenvectors of -1 for the linear part of the normal form, have $\tilde{R}_{a,\theta,x,\mu}(2) \equiv p$. Consequently, as μ approaches the bifurcation value, the period-two points must coalesce to the fixed point tangent to the eigendirections. This does indeed happen, for the period-two points all lie in $\{y=0\}$.

We can get a similar result on the fixed point surface $\Gamma(1)$, although not quite as easily. The quantity $\tilde{R}_{a,\theta,x,\mu}(1) = \theta$, where $\lambda=e^{a+2\pi i\theta}$ is one of the eigenvalues of the fixed point. Consequently, the sets of fixed points with constant $\tilde{R}_{a,\theta,x,\mu}(1)$ are typically curves along the fixed point surface when the eigenvalues are complex, and full two-dimensional regions on the fixed point surface when the eigenvalues are real. As in the q=2 case in the above paragraph, the eigenvectors corresponding to the 1 eigenvalue are described by y=0. At the very least, the saddle, with its real eigenvalues, must approach the bifurcating fixed point (0,0) tangent to the x axis in the phase plane as the parameter approaches the Bogdanov bifurcation point. In the actual unfolding, both saddle and node fixed points, when they exist, occur with y=0.

7.4 Self Rotation Numbers for Fixed Points of Nondiffeomorphisms

In Section 3.3, we discussed the fact that for diffeomorphisms $\{f_\mu\}$, $Df_\mu(y)$ always exists and is nonsingular. This facilitated defining the self rotation number of a fixed point. If $Df_\mu(y)$ is singular, but nonzero, we can still define the self rotation number because $\Theta_{y,\mu}(0,\theta) \equiv \lim_{a\to 0} R(a, \theta, y_0, \mu_0)$ still exists even though it can no longer be expressed as $\dfrac{Df_{\mu_0}(y_0)\begin{pmatrix}\cos\theta\\ \sin\theta\end{pmatrix}}{\left|Df_{\mu_0}(y_0)\begin{pmatrix}\cos\theta\\ \sin\theta\end{pmatrix}\right|}$, as we did in {3.16}. If $Df_\mu(y)$ is zero,

then higher order terms must be considered to find an appropriate extension of the self rotation number to fixed points.

Figure 2.1

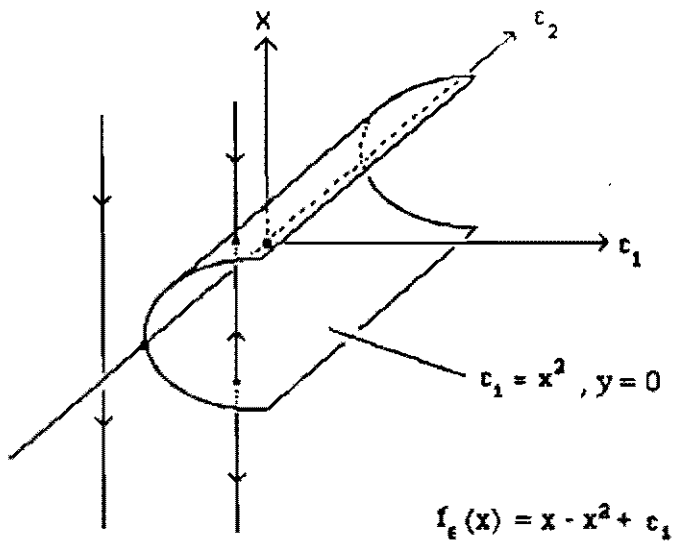

Figure 2.2

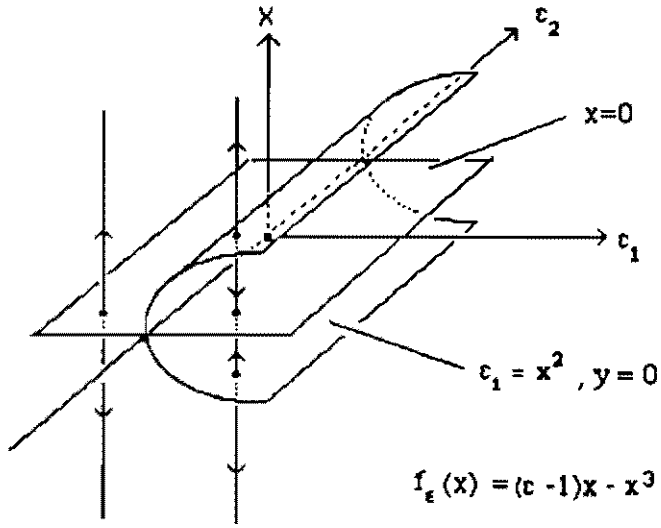

Figure 2.3

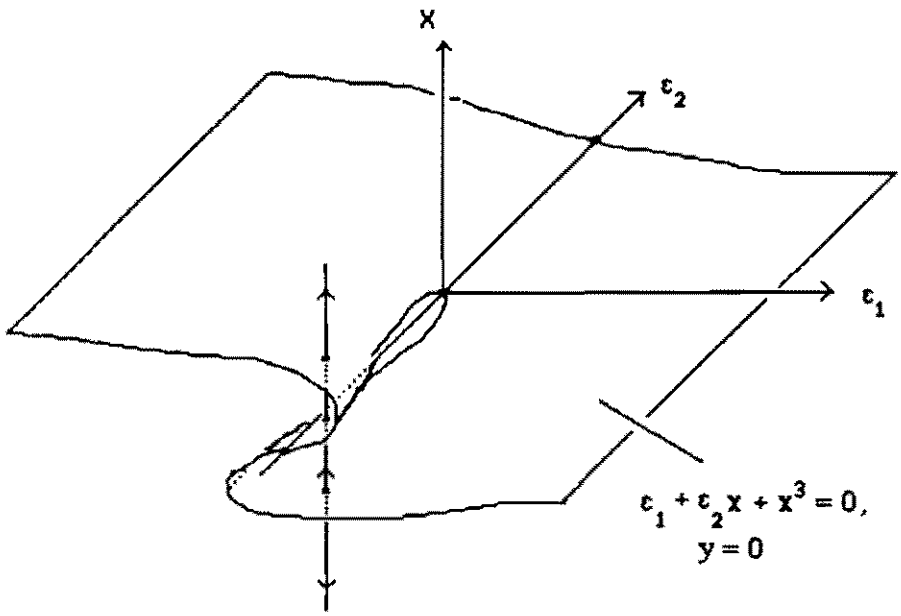

$$f_c(x) = c_1 + (c_2 + 1)x + x^3$$

Figure 2.4

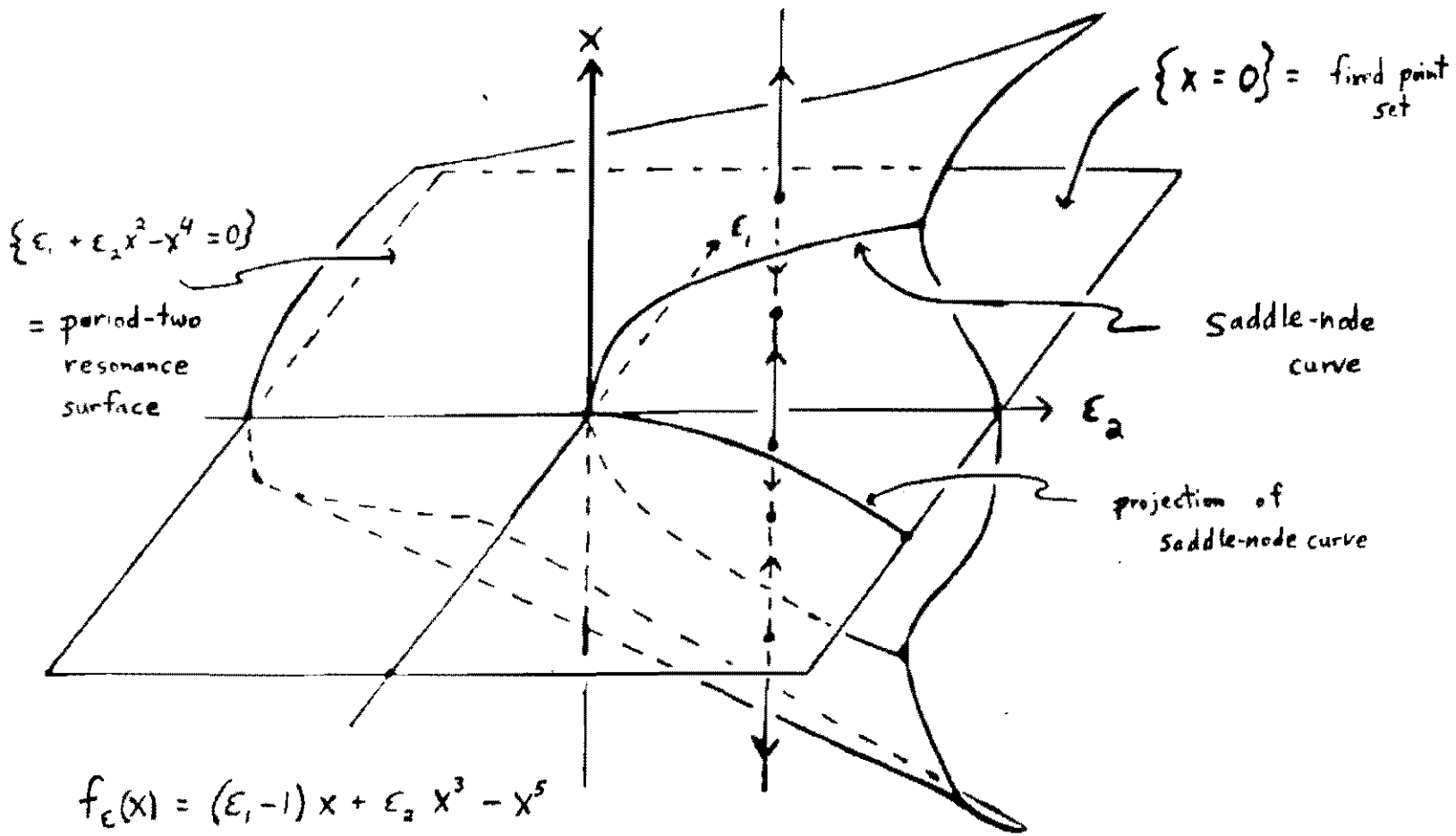
x
$\{x = 0\}$ = fixed point set
$\{\varepsilon_1 + \varepsilon_2 x^2 - x^4 = 0\}$
= period-two resonance surface
ε_1
saddle-node curve
ε_2
projection of saddle-node curve
$f_\varepsilon(x) = (\varepsilon_1 - 1)x + \varepsilon_2 x^3 - x^5$

Figure 2.5

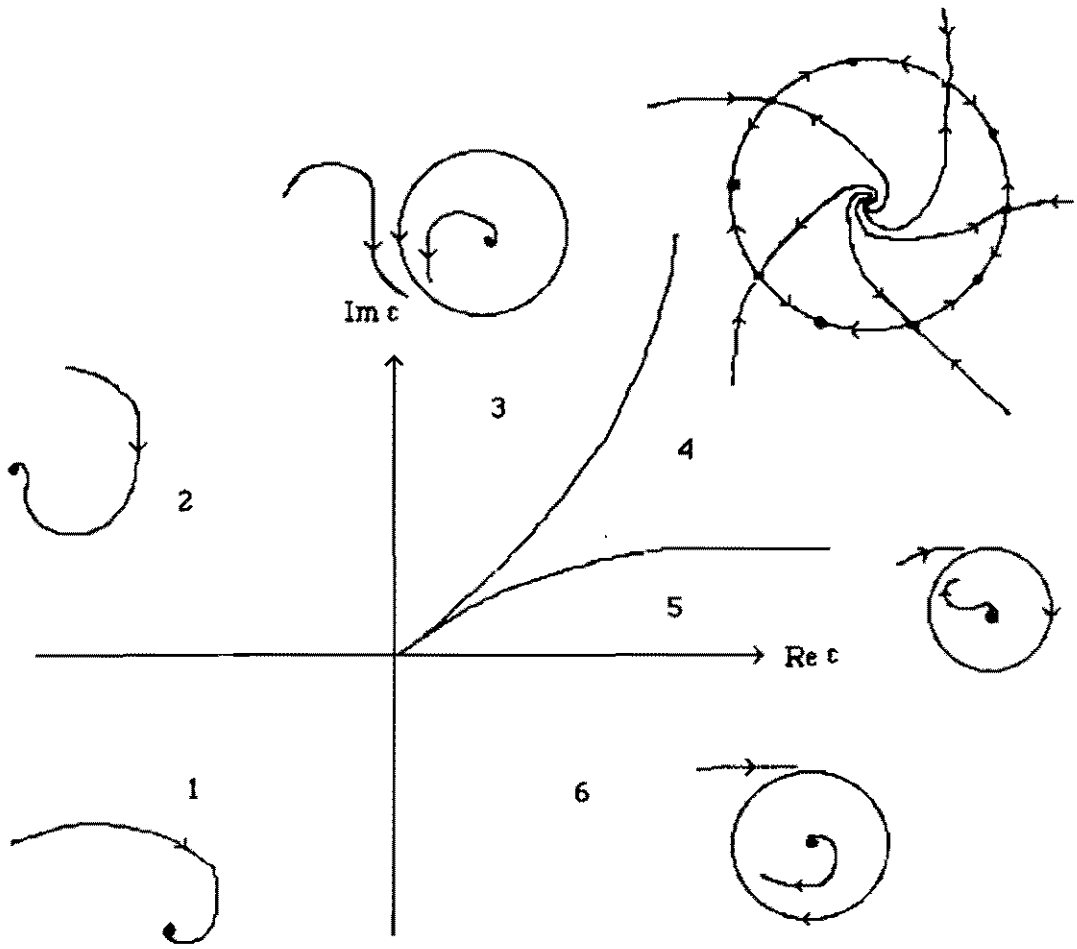

$$\dot{z} = cz + z\bar{z}^2 A(|z|^2) + B\bar{z}^{q-1}$$

Figure 2.6

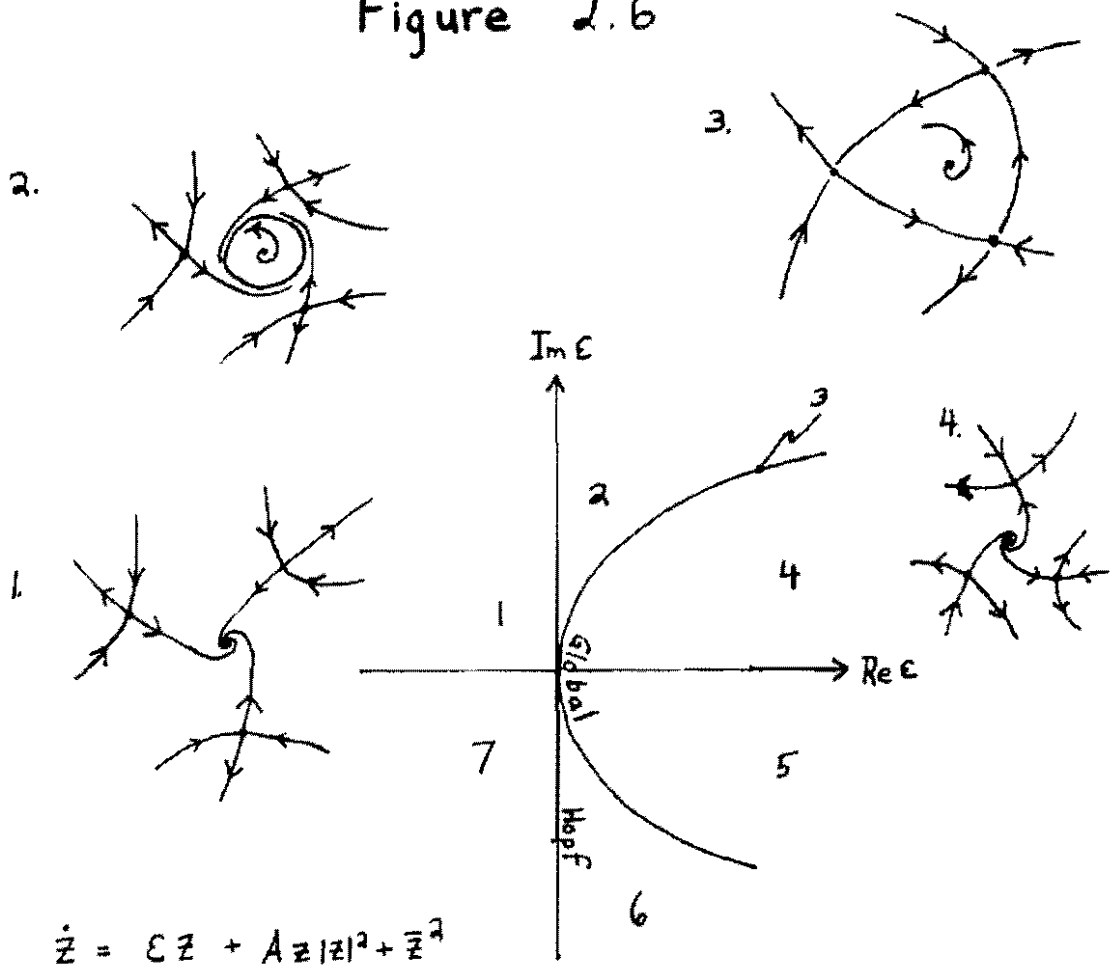
2.
3.
Im ε
1.
4.
2
3
4
1
Re ε
global
7
5
Hopf
6
$\dot{z} = \varepsilon z + A z|z|^2 + \bar{z}^2$
7.
6.
5.

Figure 2.7a

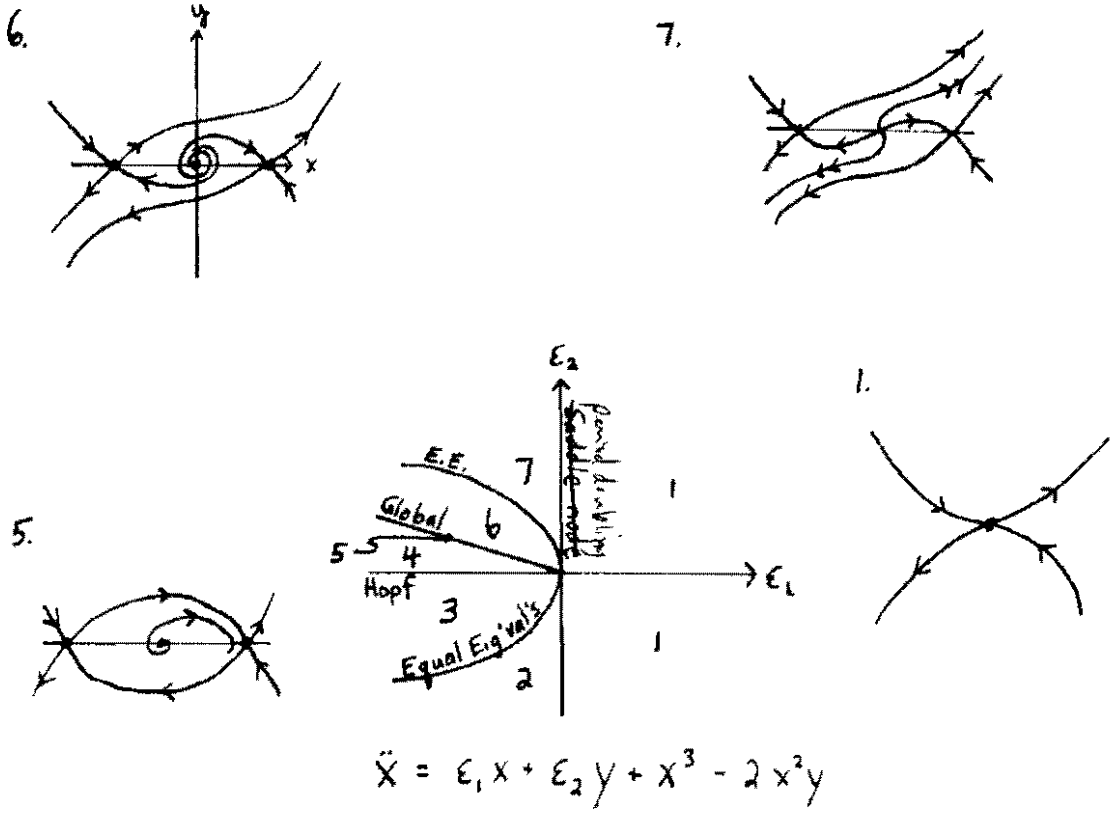
6.
y
x
7.
5.
ε_2
E.E.
7
Global
6
5
4
Hopf
3
Equal Eig'val's
2
Saddle-node
1
1
ε_1
1.
$\ddot{X} = \varepsilon_1 x + \varepsilon_2 y + x^3 - 2x^2 y$
2
4.
3.

Figure 2.7 b

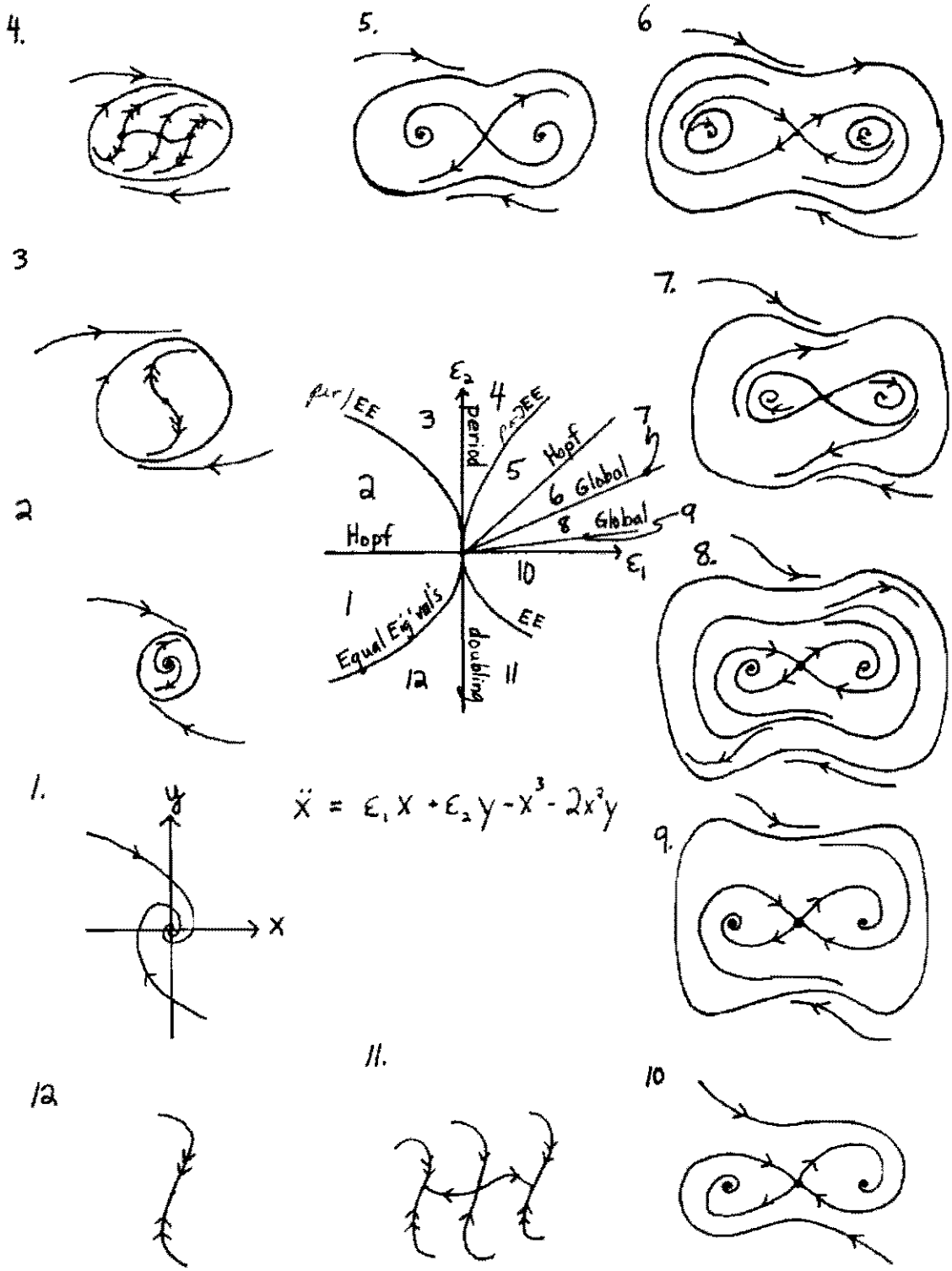
4.
5.
6
3
7.
2
8.
1.
$\ddot{x} = \varepsilon_1 x + \varepsilon_2 y - x^3 - 2x^2 y$
9.
11.
12
10
ε_2
ε_1
per/EE
3
4
per2EE
period
5
Hopf
6 Global
7
8
Global
9
Hopf
2
10
1
Equal Eg'vals
EE
12
doubling
11
y
x

Figure 2.8

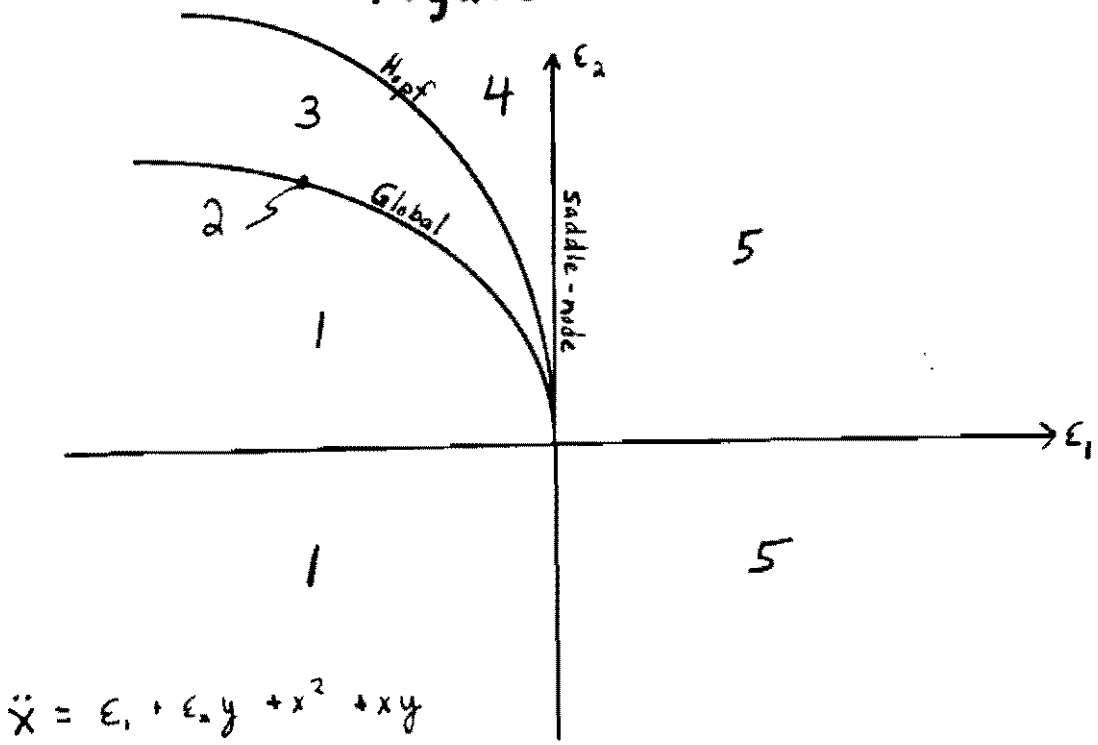

$$\ddot{x} = \varepsilon_1 + \varepsilon_2 y + x^2 + xy$$

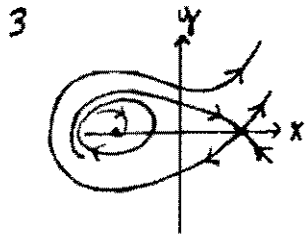

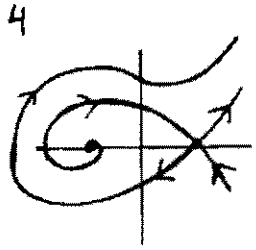

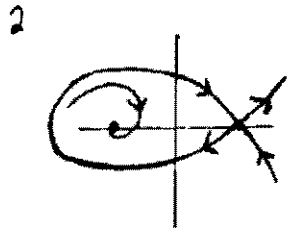

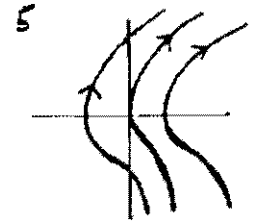

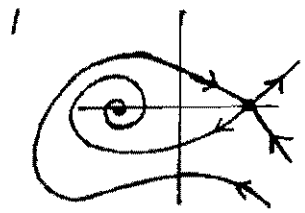

Figure 2.9

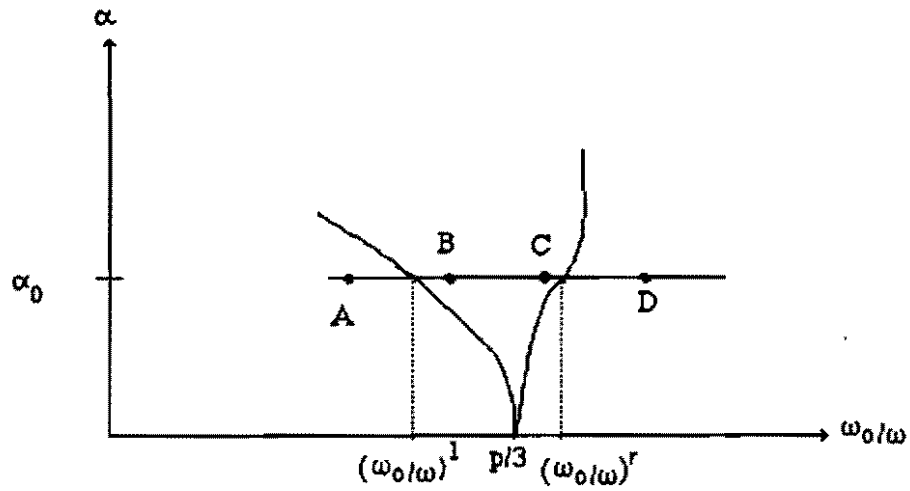

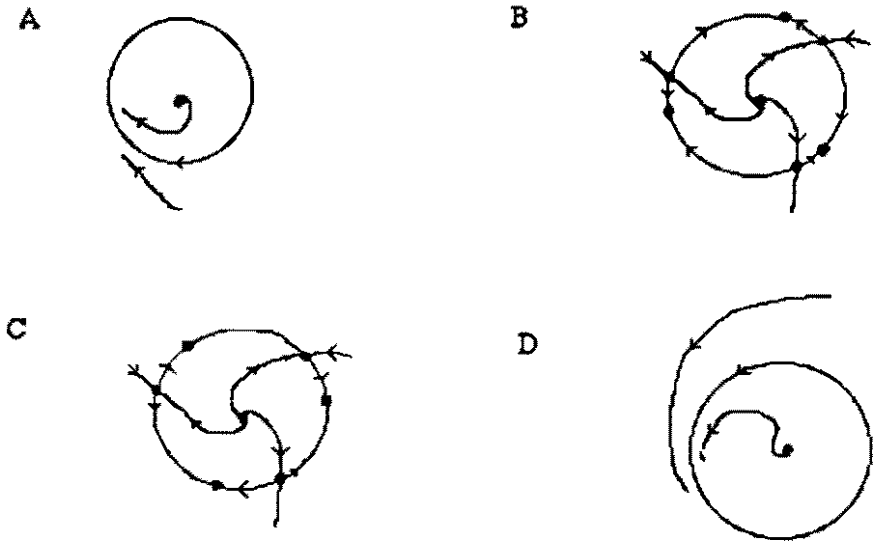

Figure 2.10

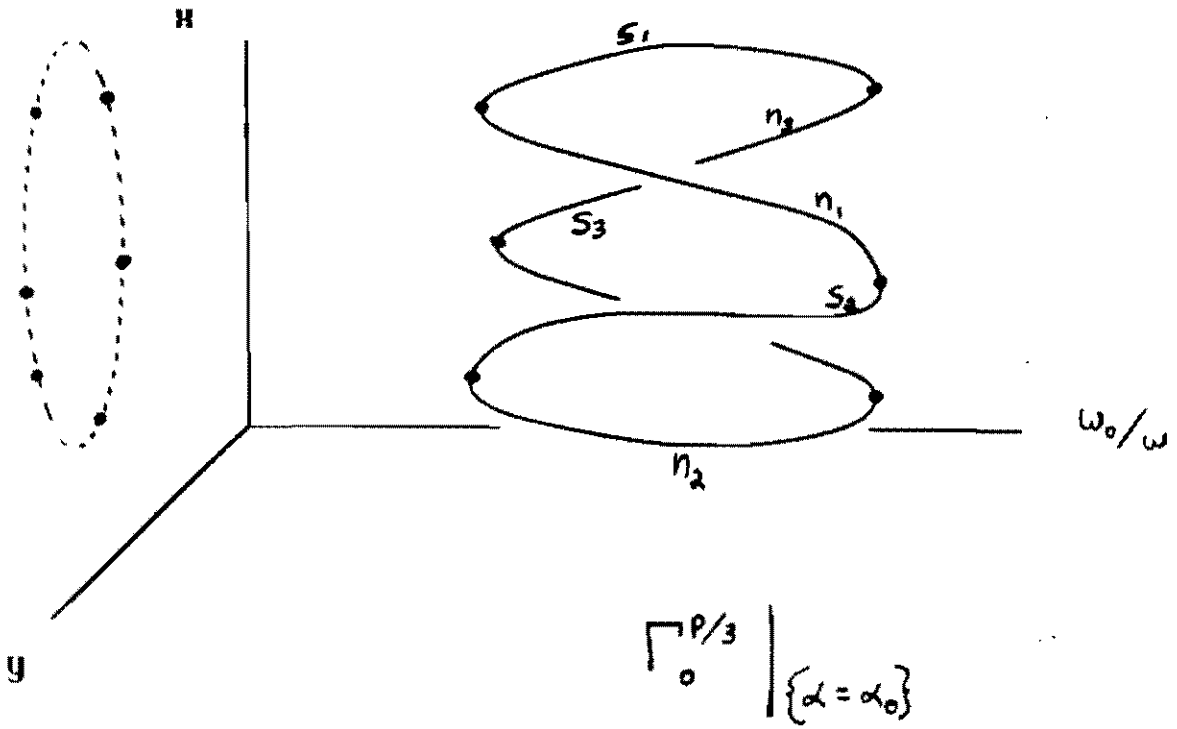
x
y
S_1
η_2
η_1
S_3
S_2
η_2
ω_0/ω
$\Gamma_0^{P/3}\Big|_{\{\alpha=\alpha_0\}}$

Figure 3.1

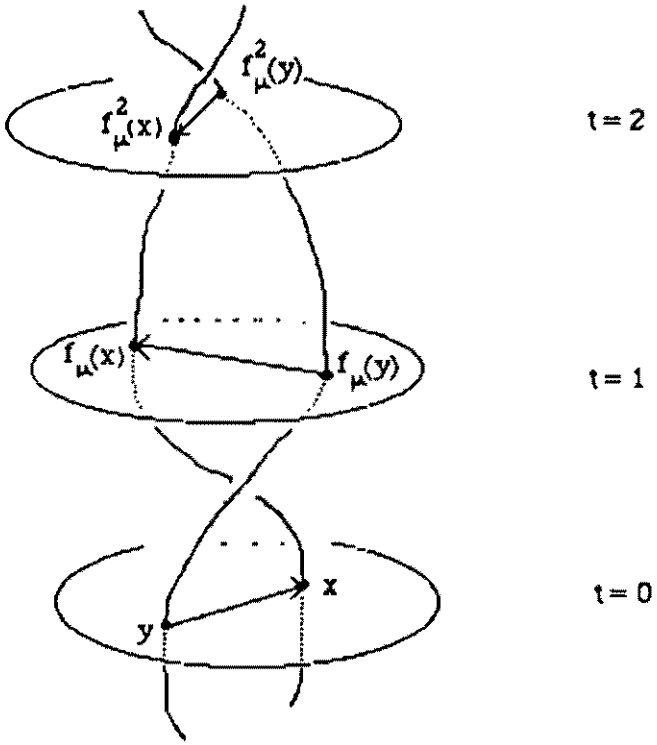

Figure 4.1

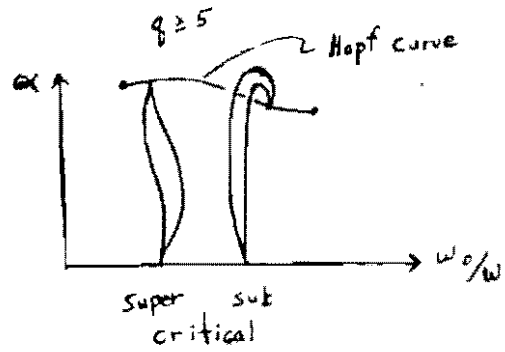

Figure 4.2

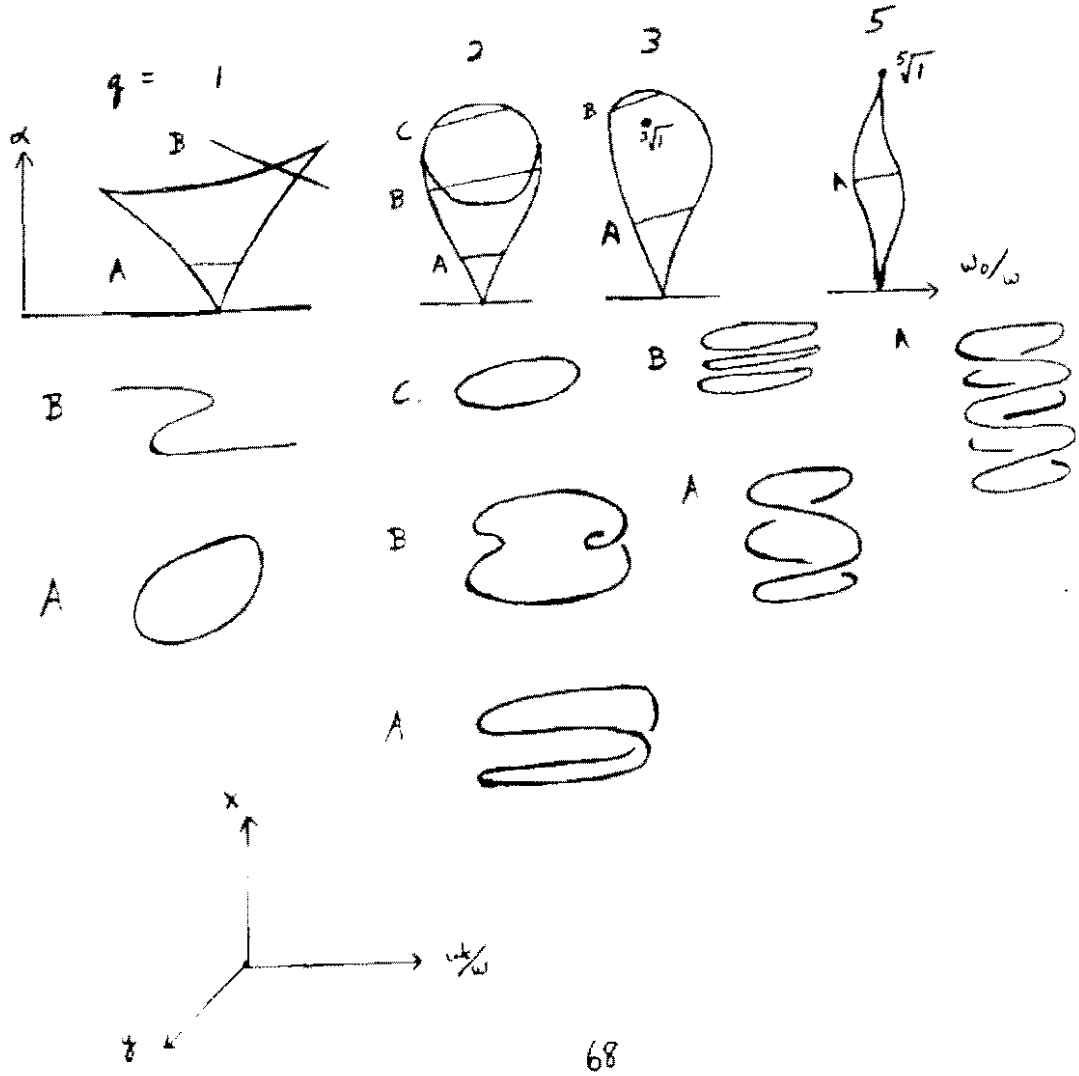

Figure 4.3

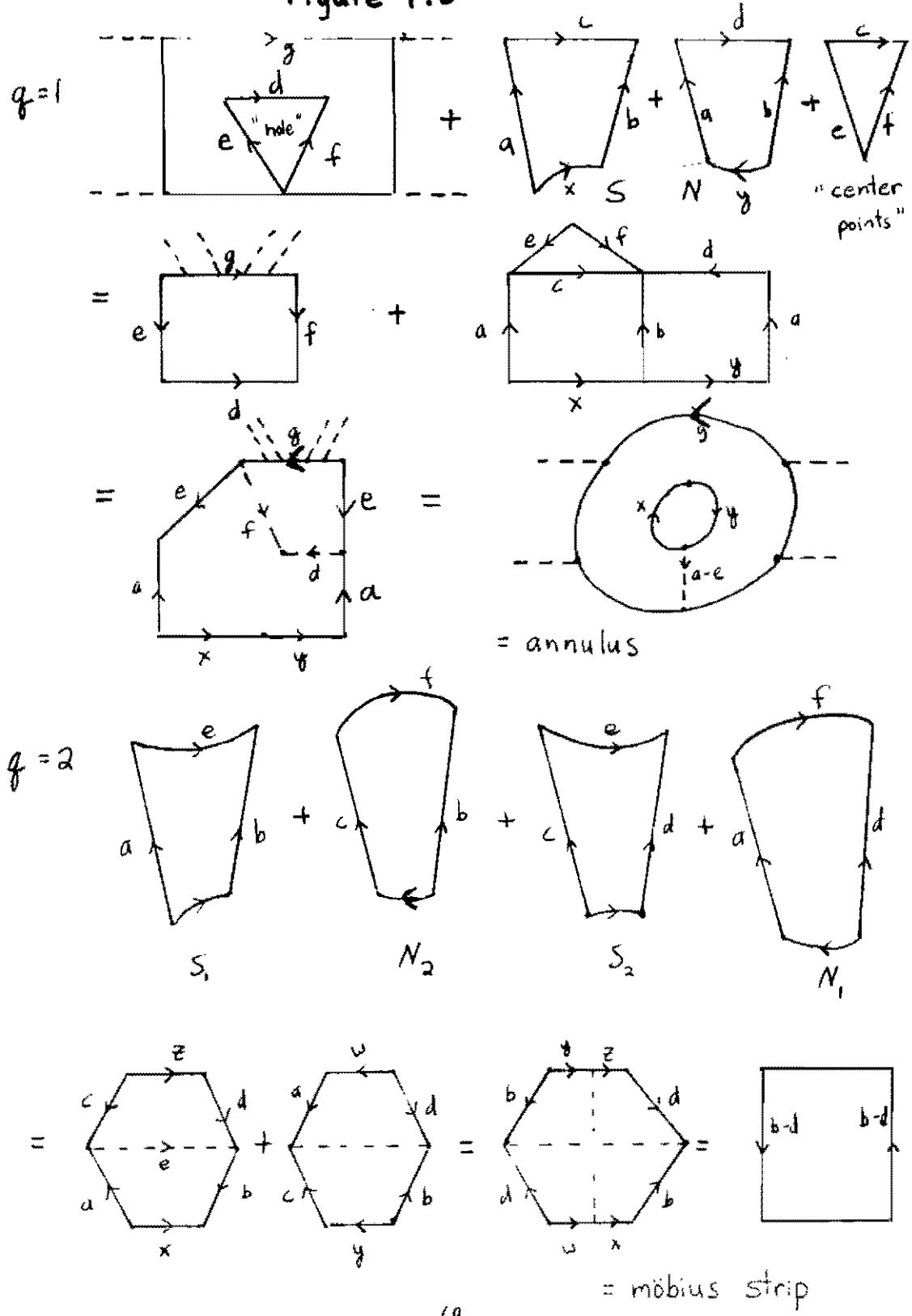

Figure 4.3 (cont.)

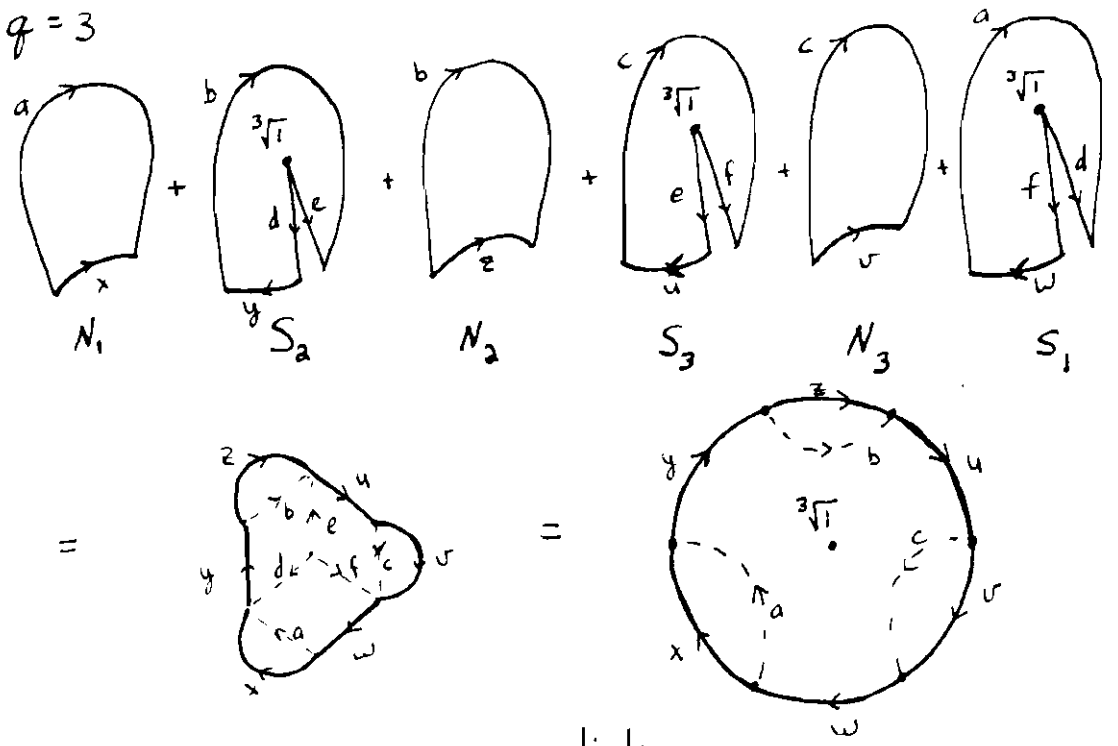

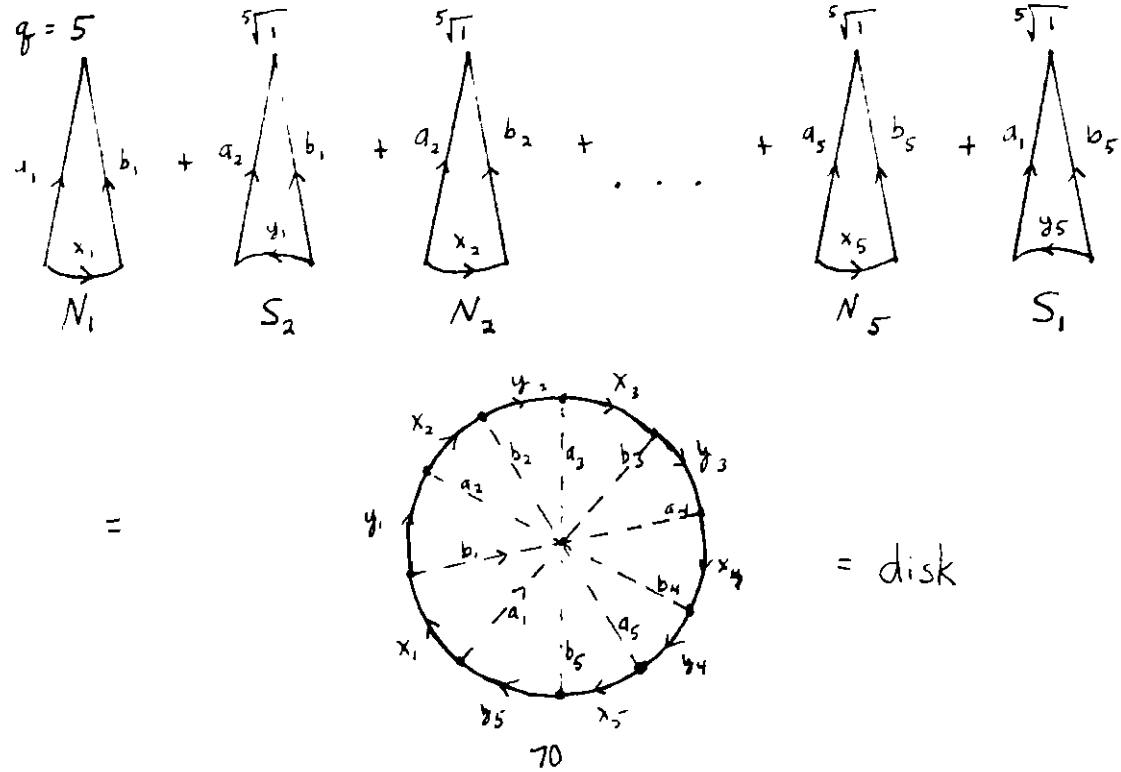

Figure 4.4

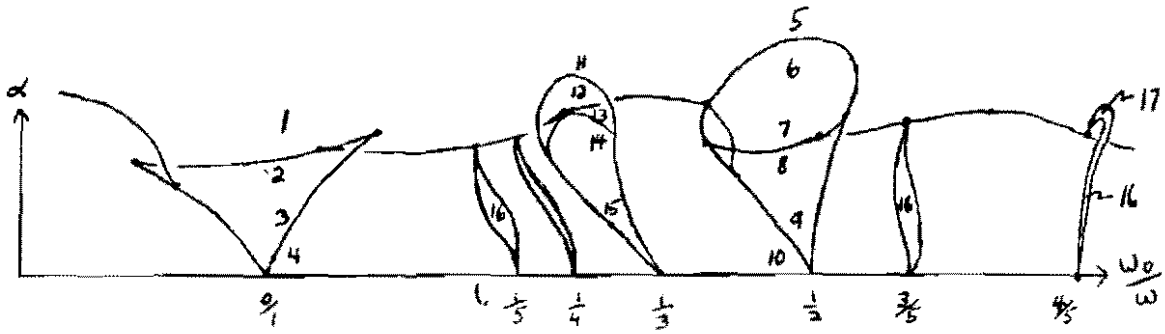

Manifolds and one-parameter families of orbits for f_{μ}^{q}

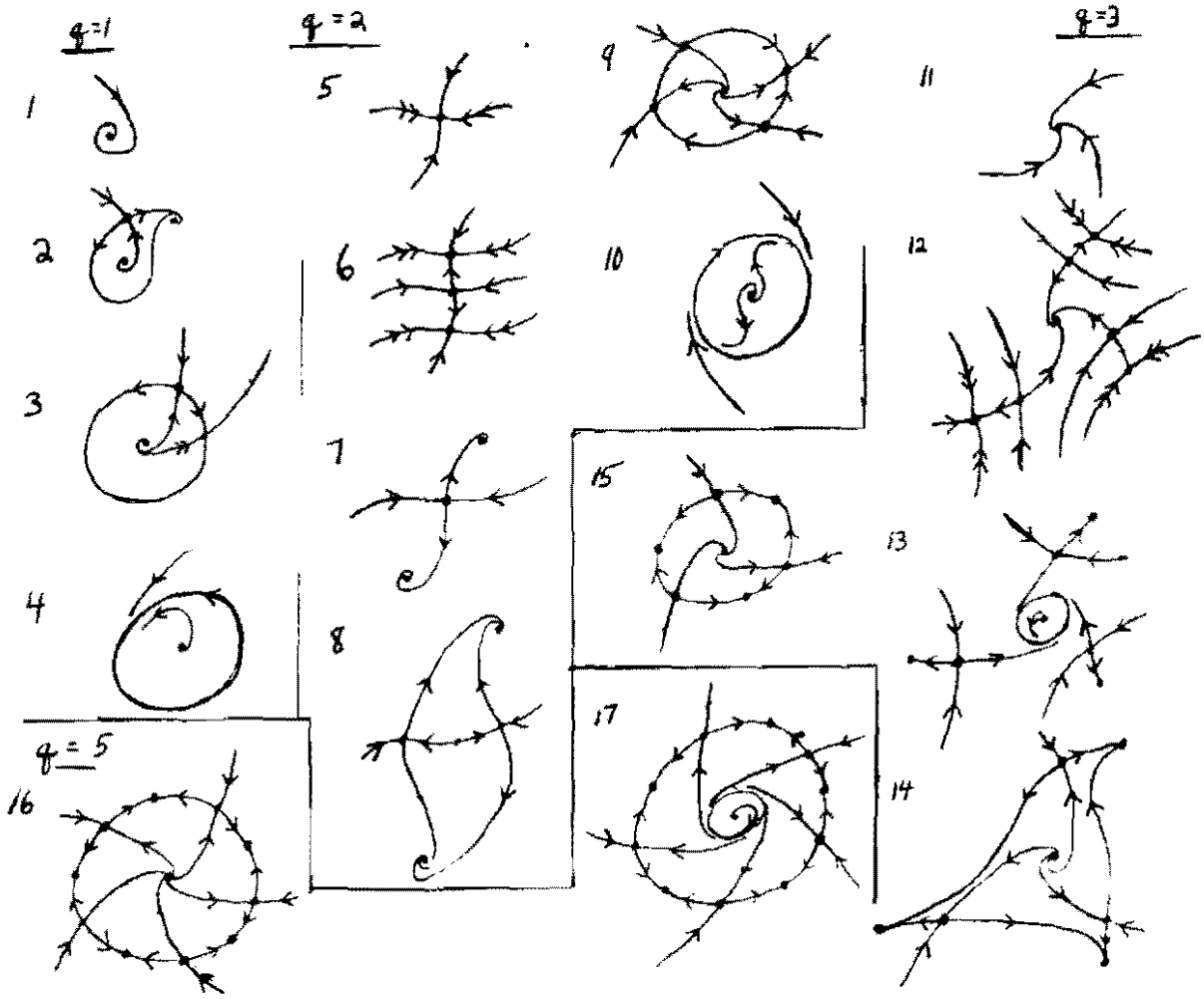

Figure 4.5

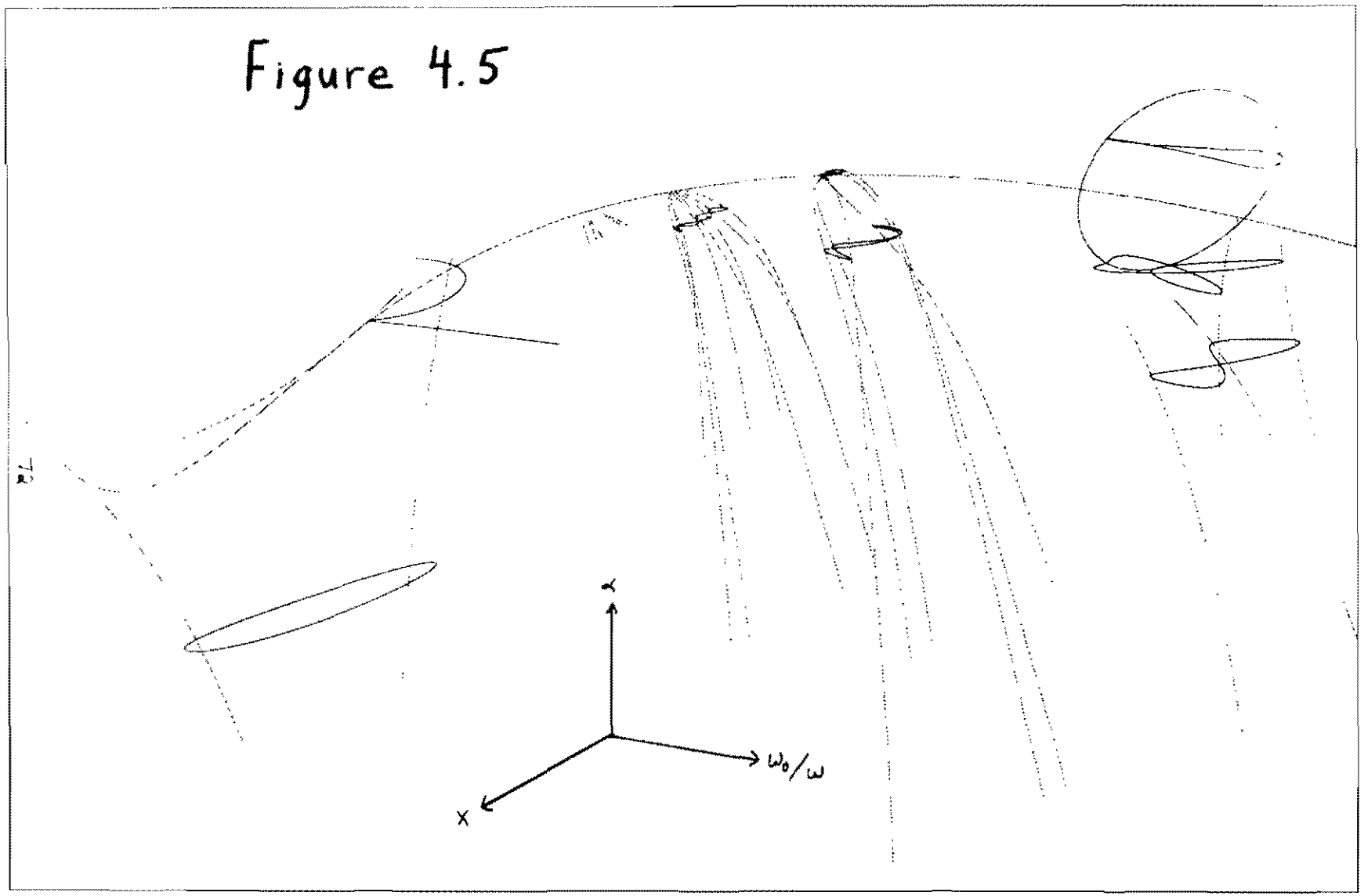

Figure 5.1

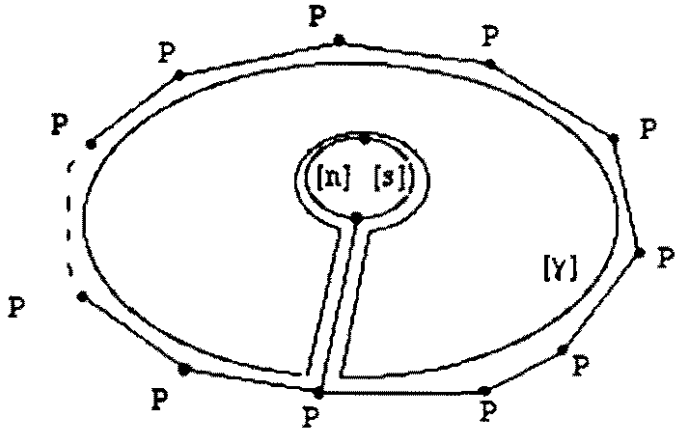

$[\Gamma_0^{p/q}]$

Figure 6.1

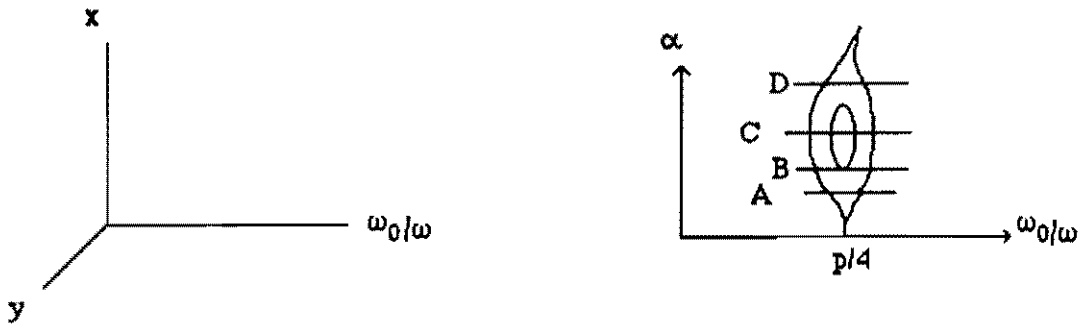

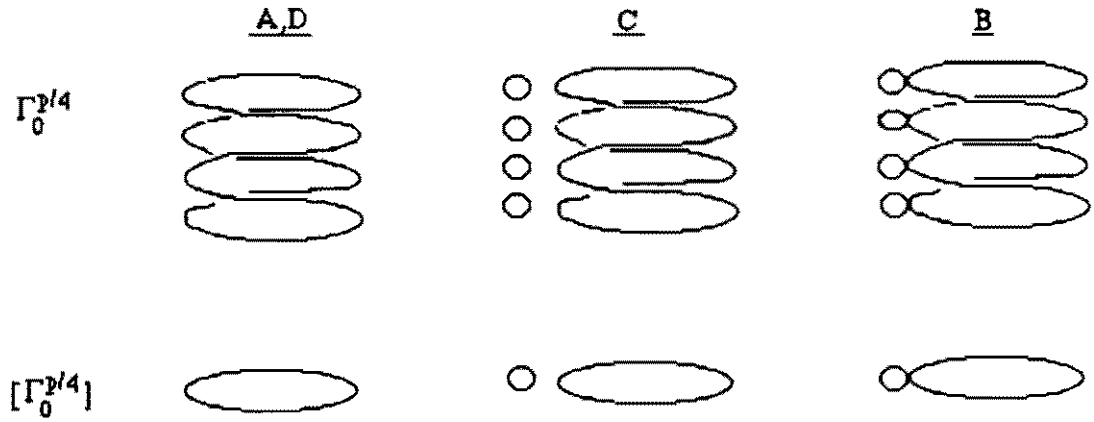

"Handle"

Figure 6.2

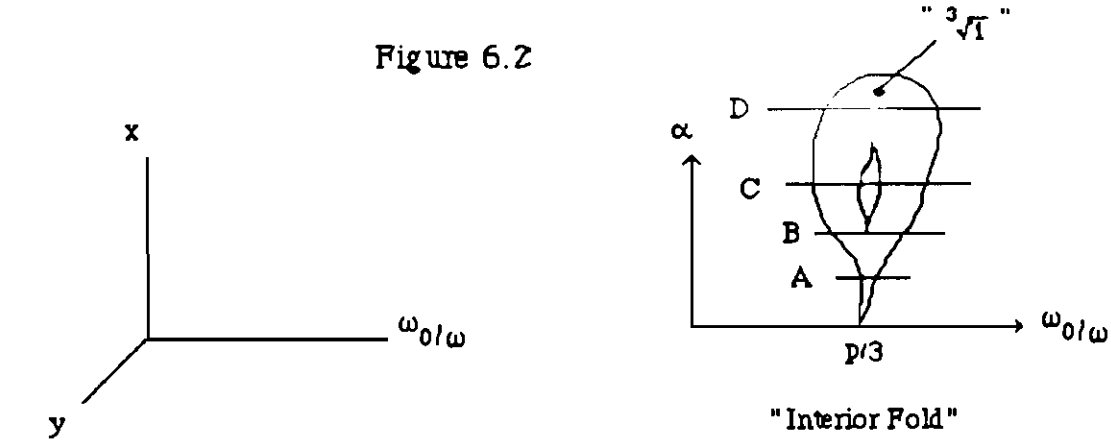

"Interior Fold"

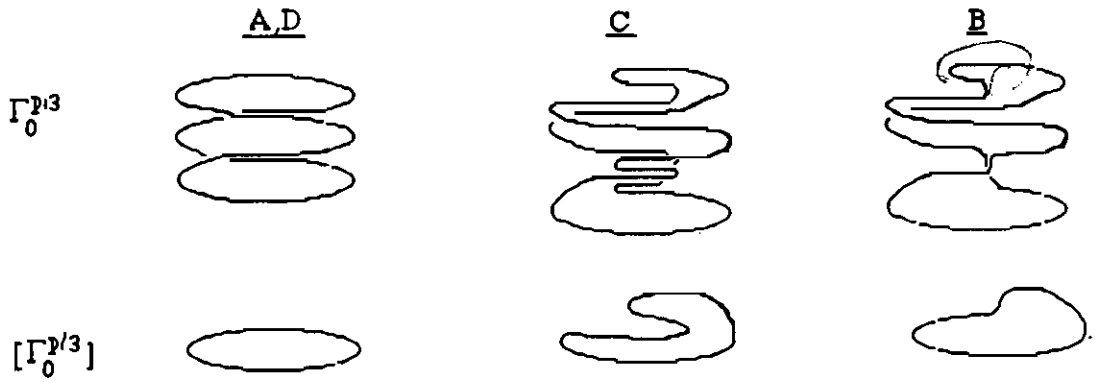

Figure 6.3

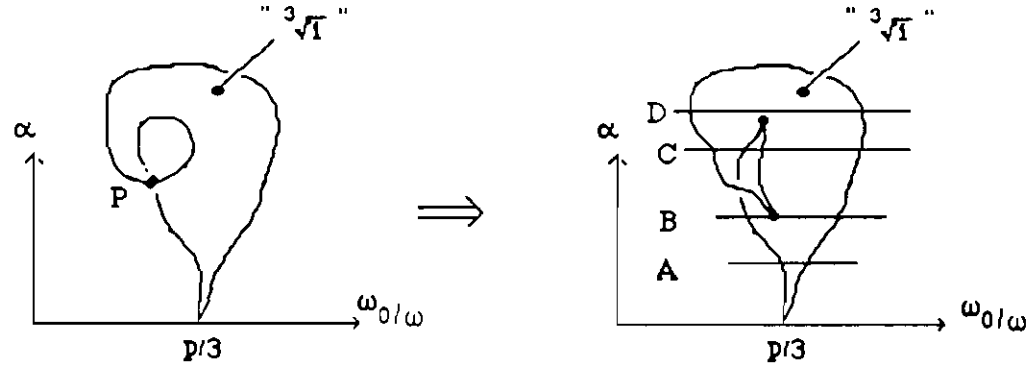

"Boundary Fold"

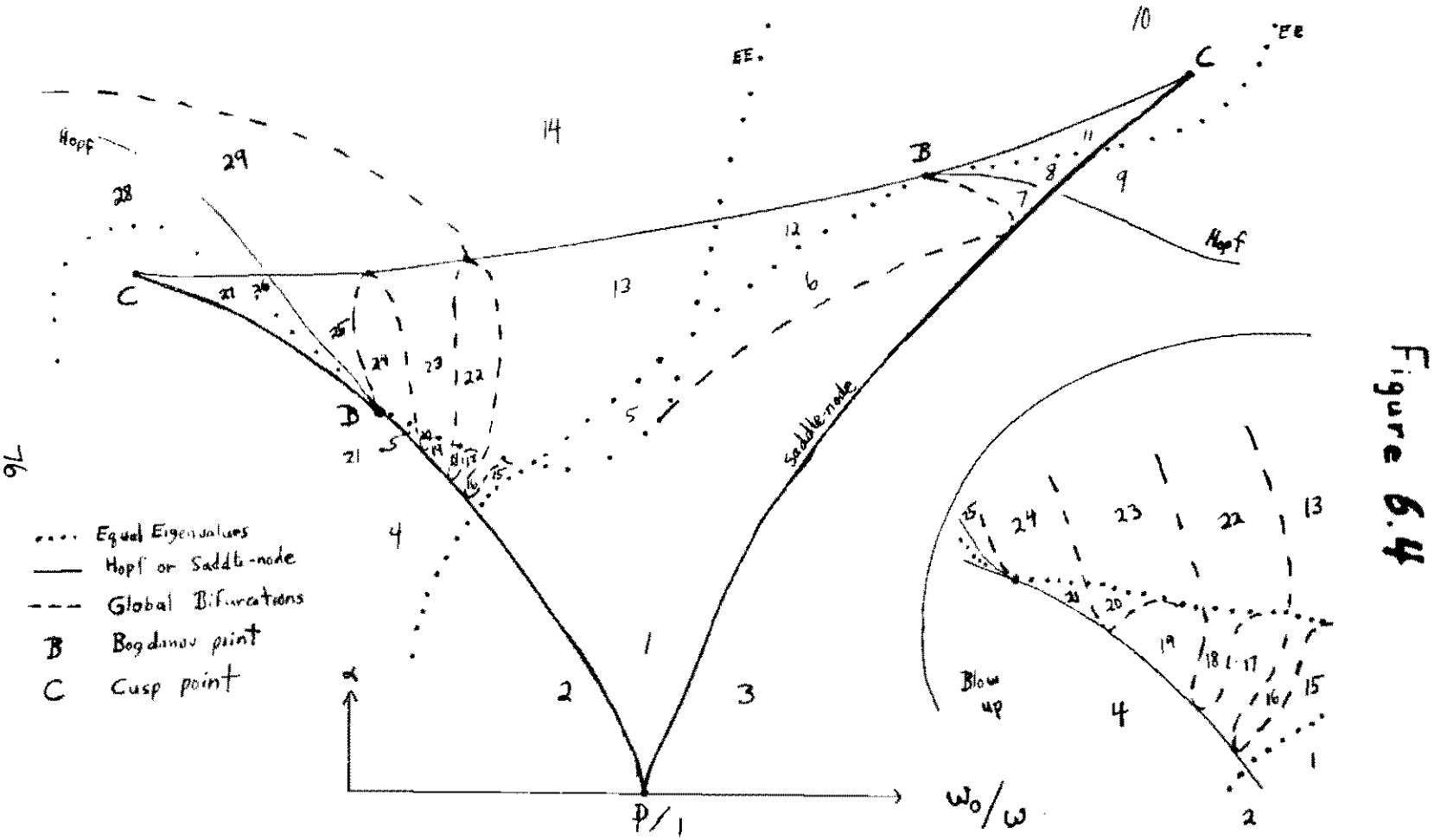

Figure 6.4

The "Period-one Resonance Horn"

Figure 6.4 (cont.)

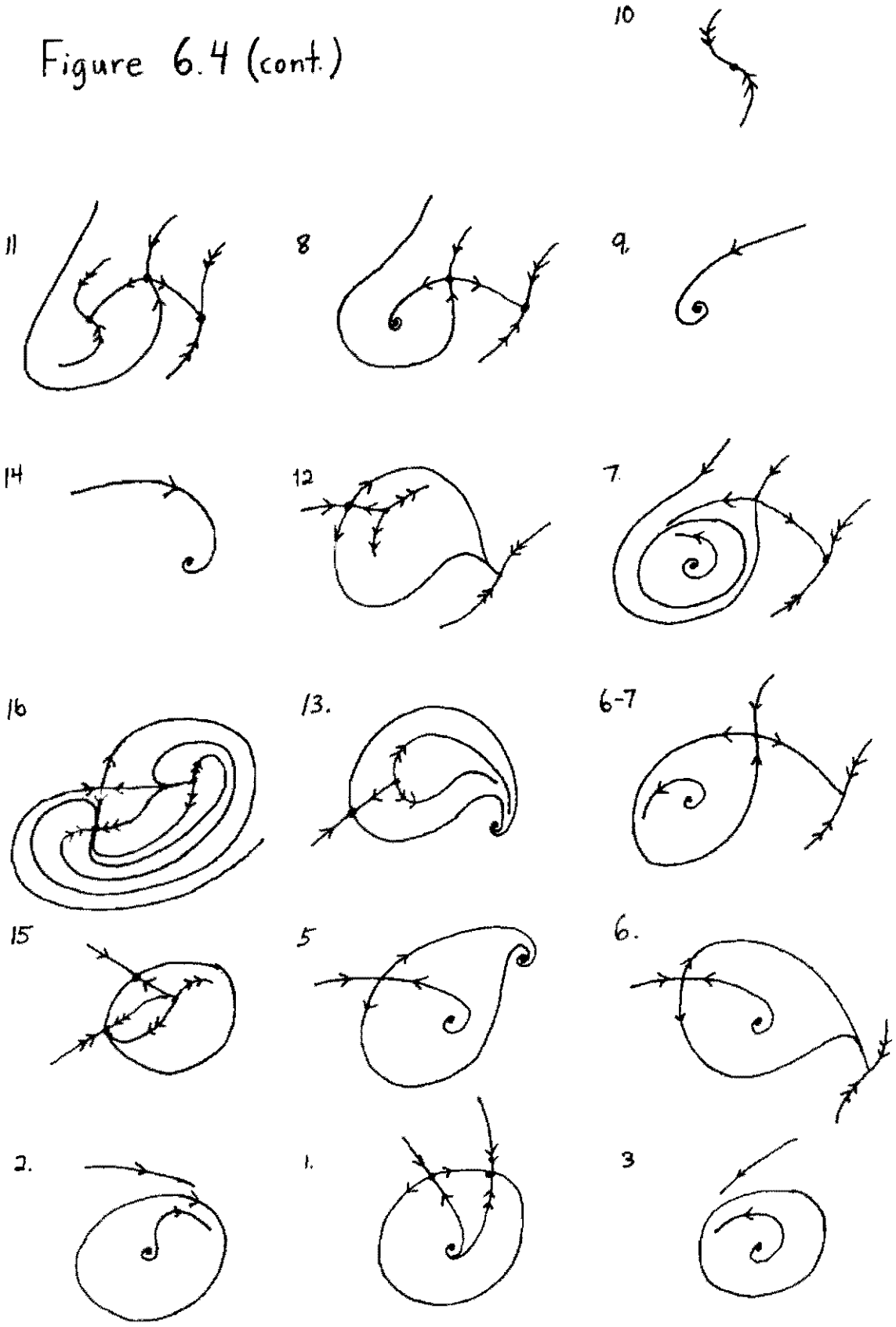

Figure 6.4 (cont.)

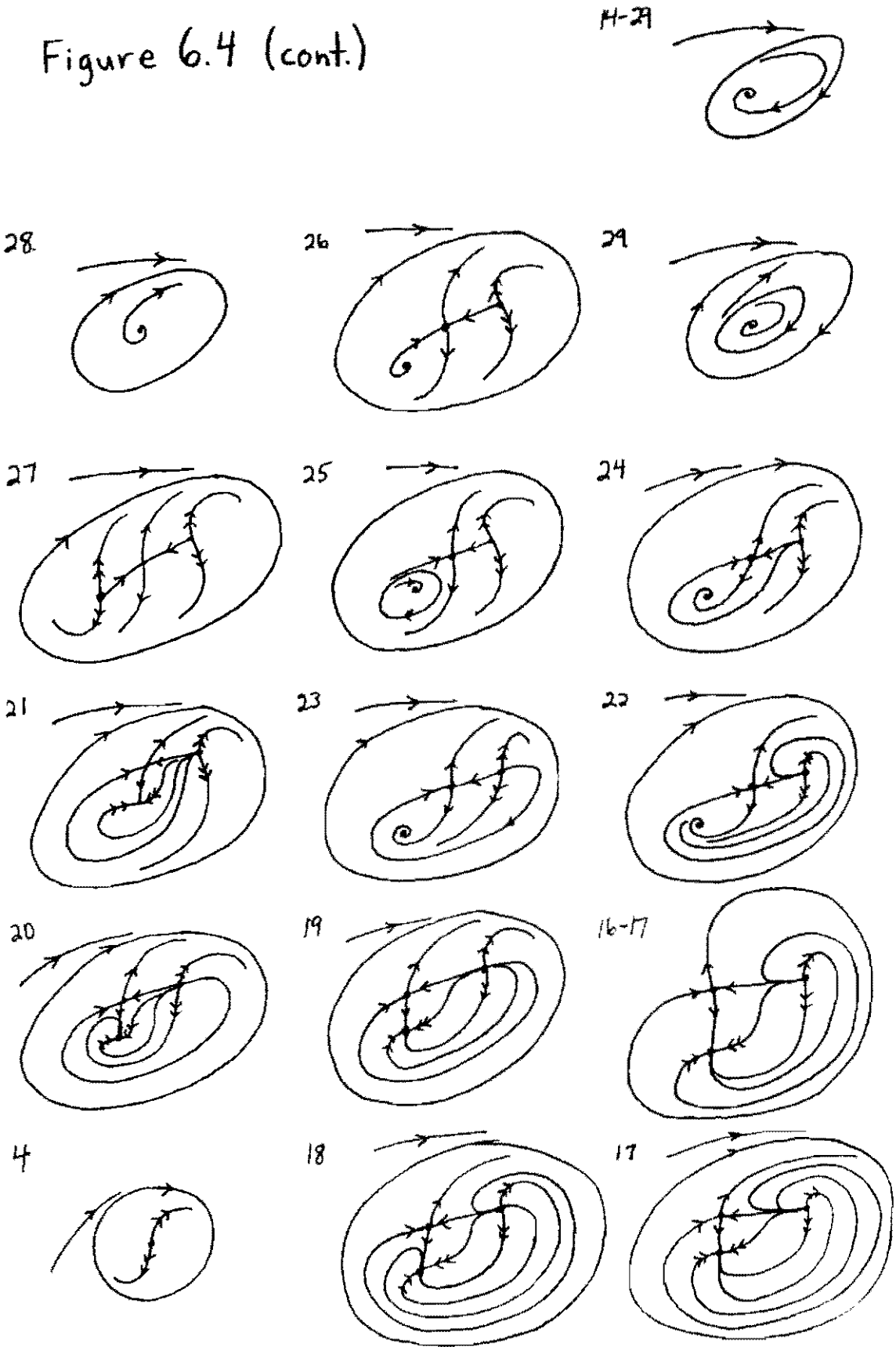

Figure 6.5

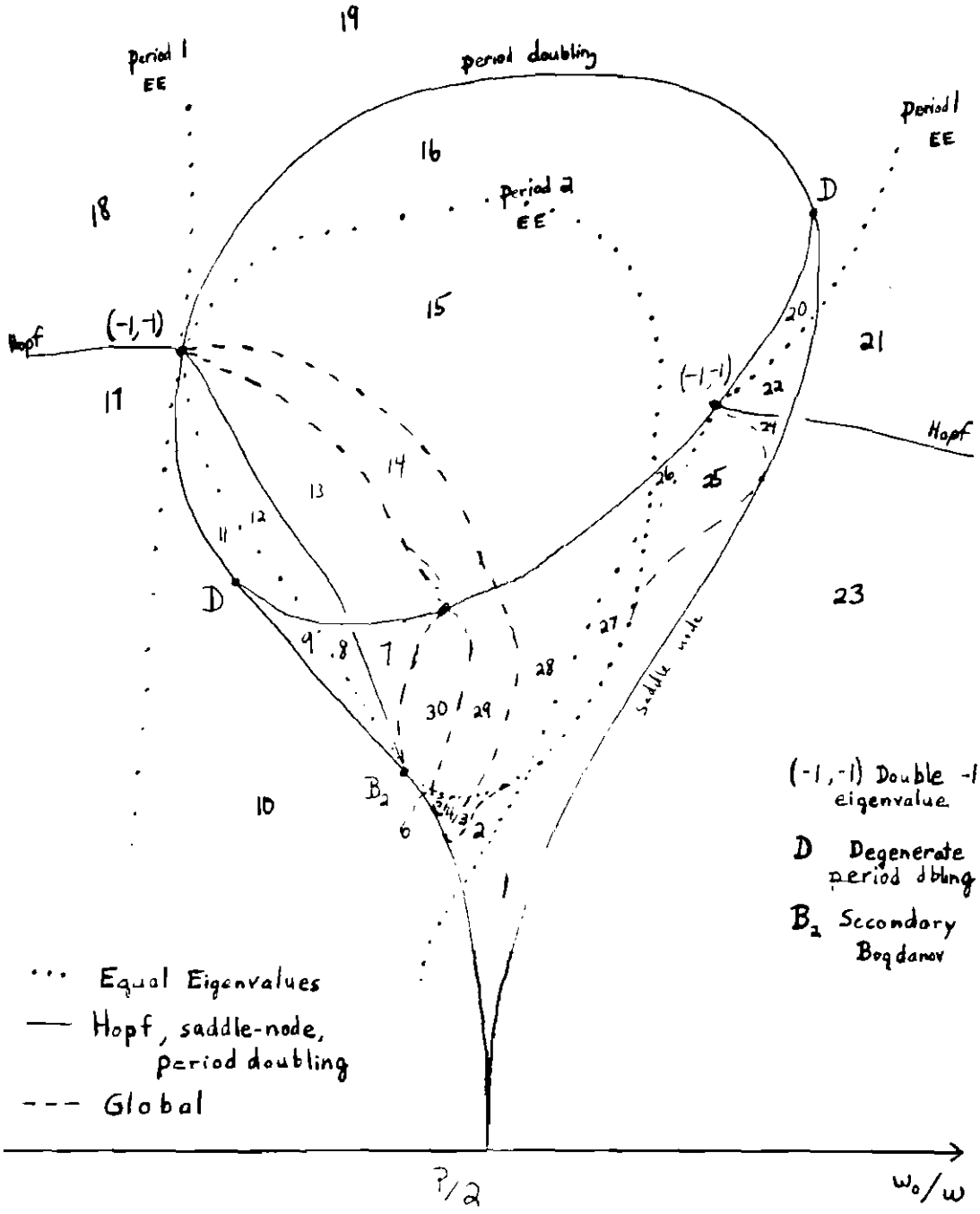

The Period-two Resonance Horn

Figure 6.5 (cont.)

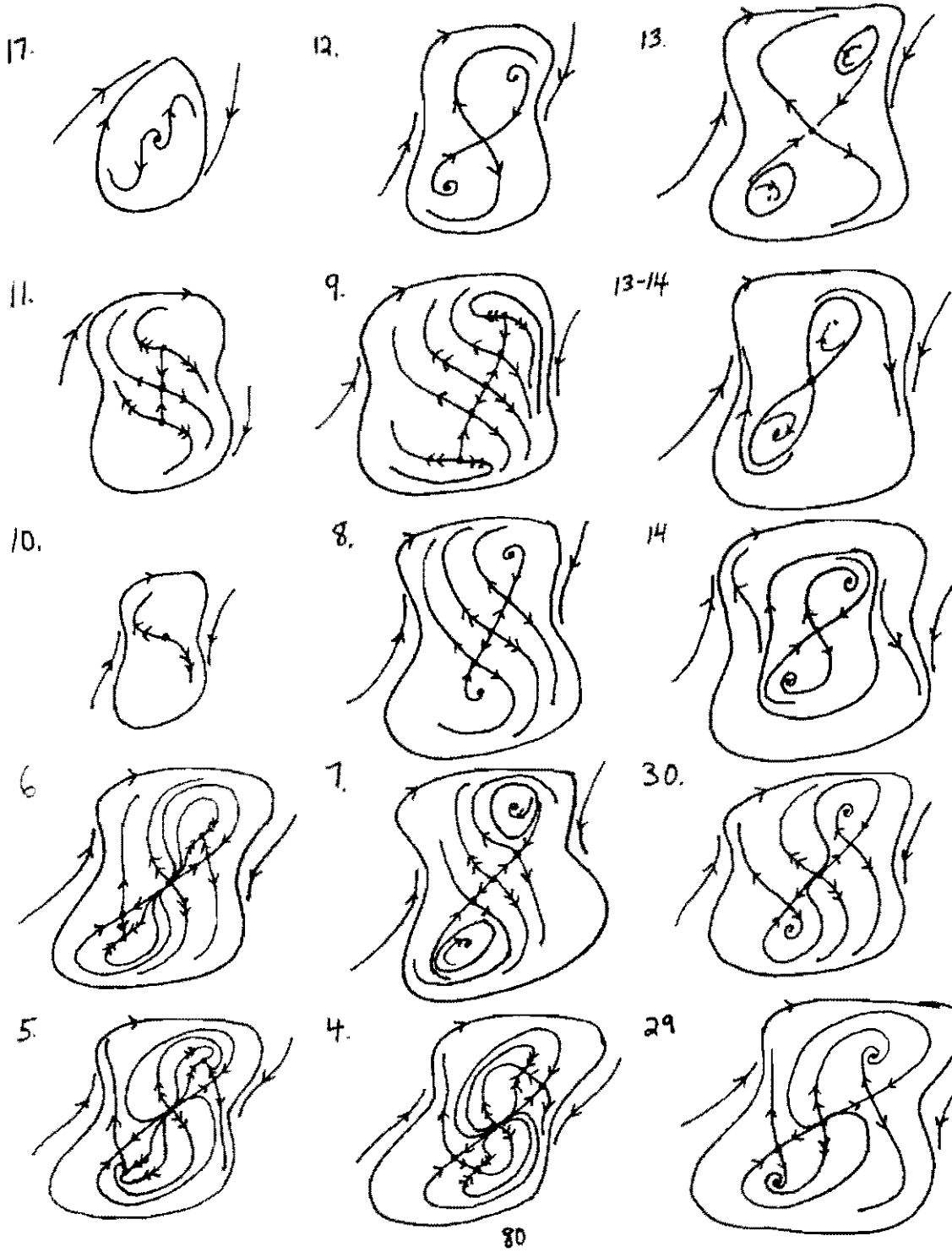

Figure 6.5 (cont.)

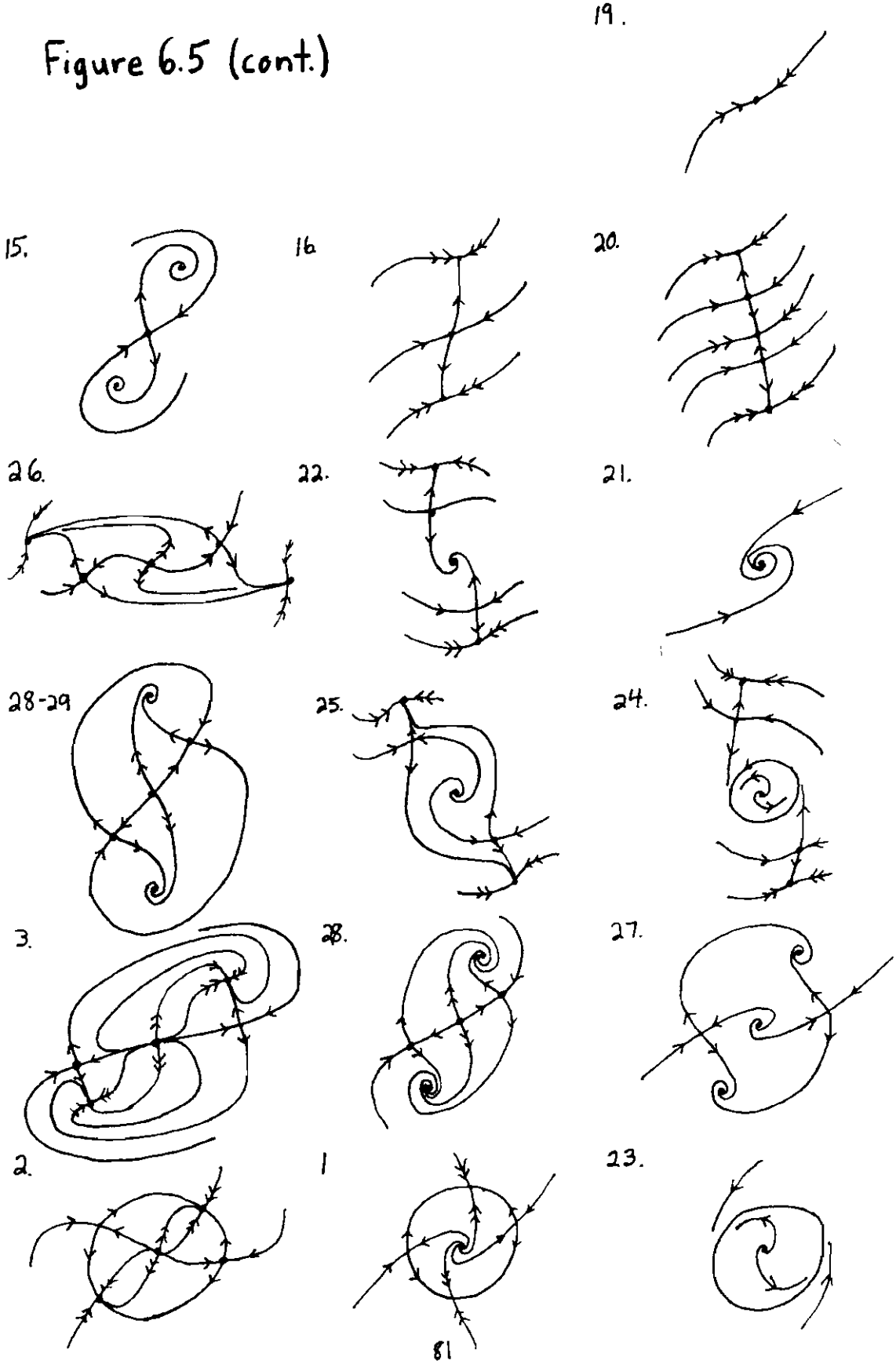

Figure 6.6

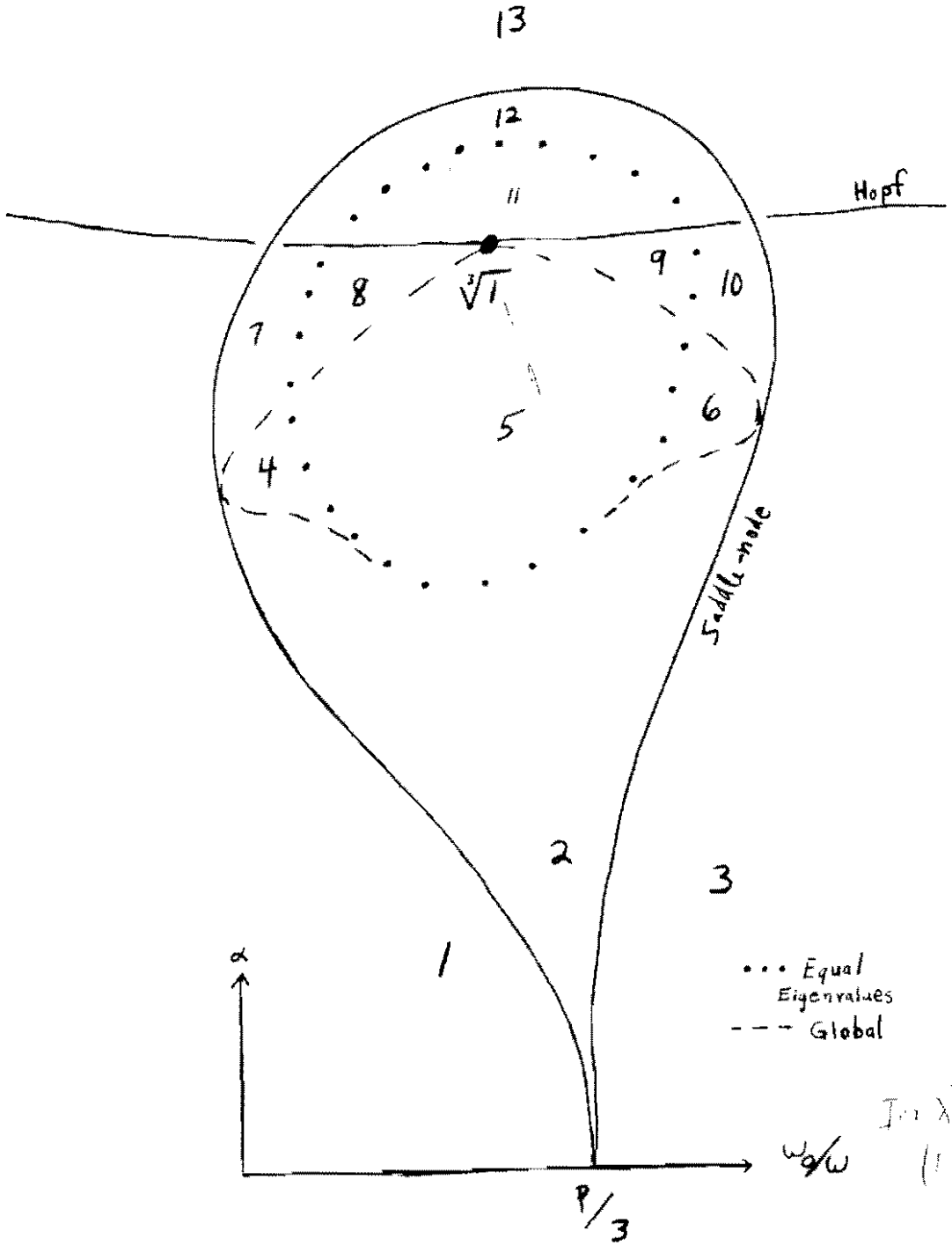

The Period-three Resonance Horn

Figure 6.6 (cont.)

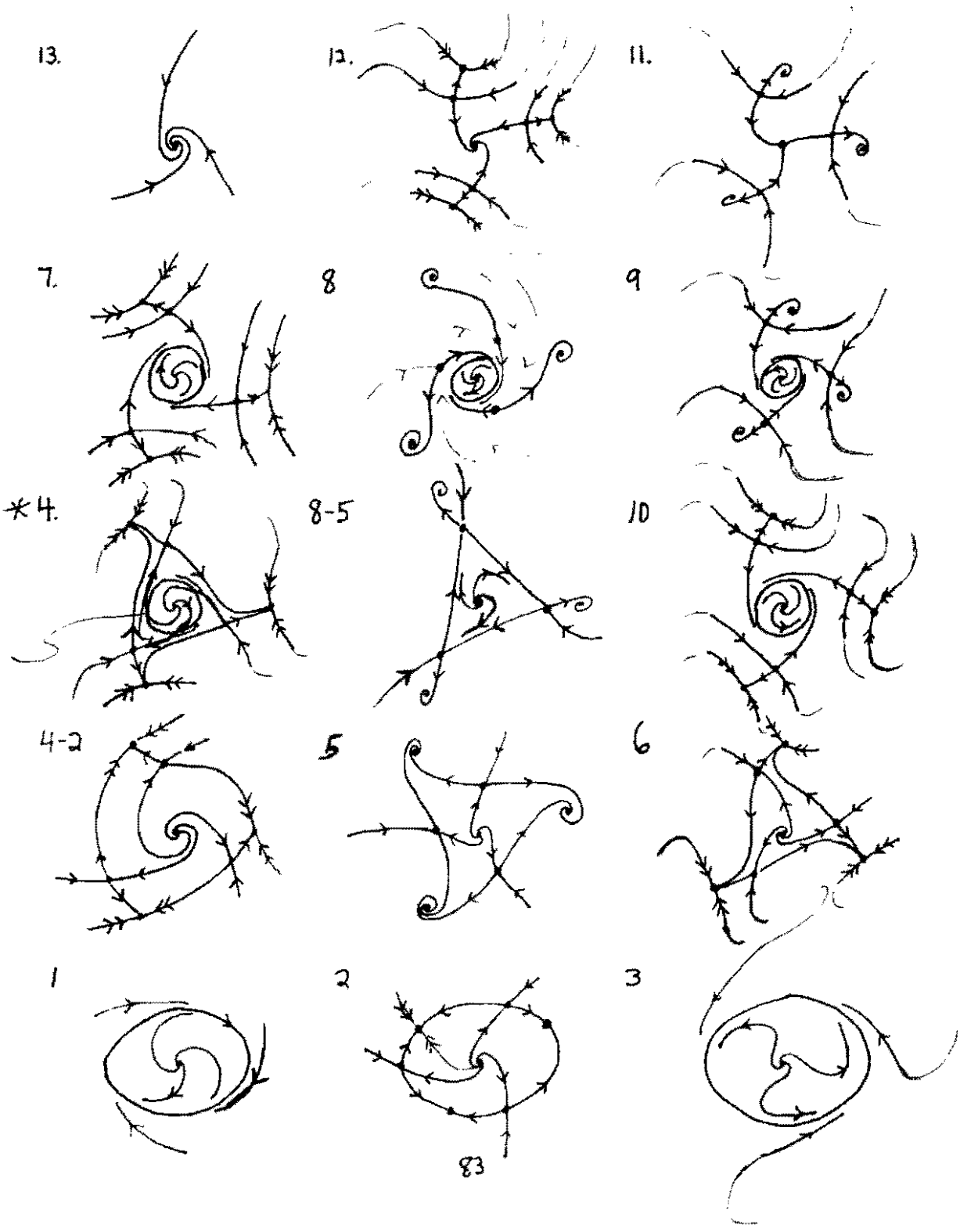

Figure 6.7

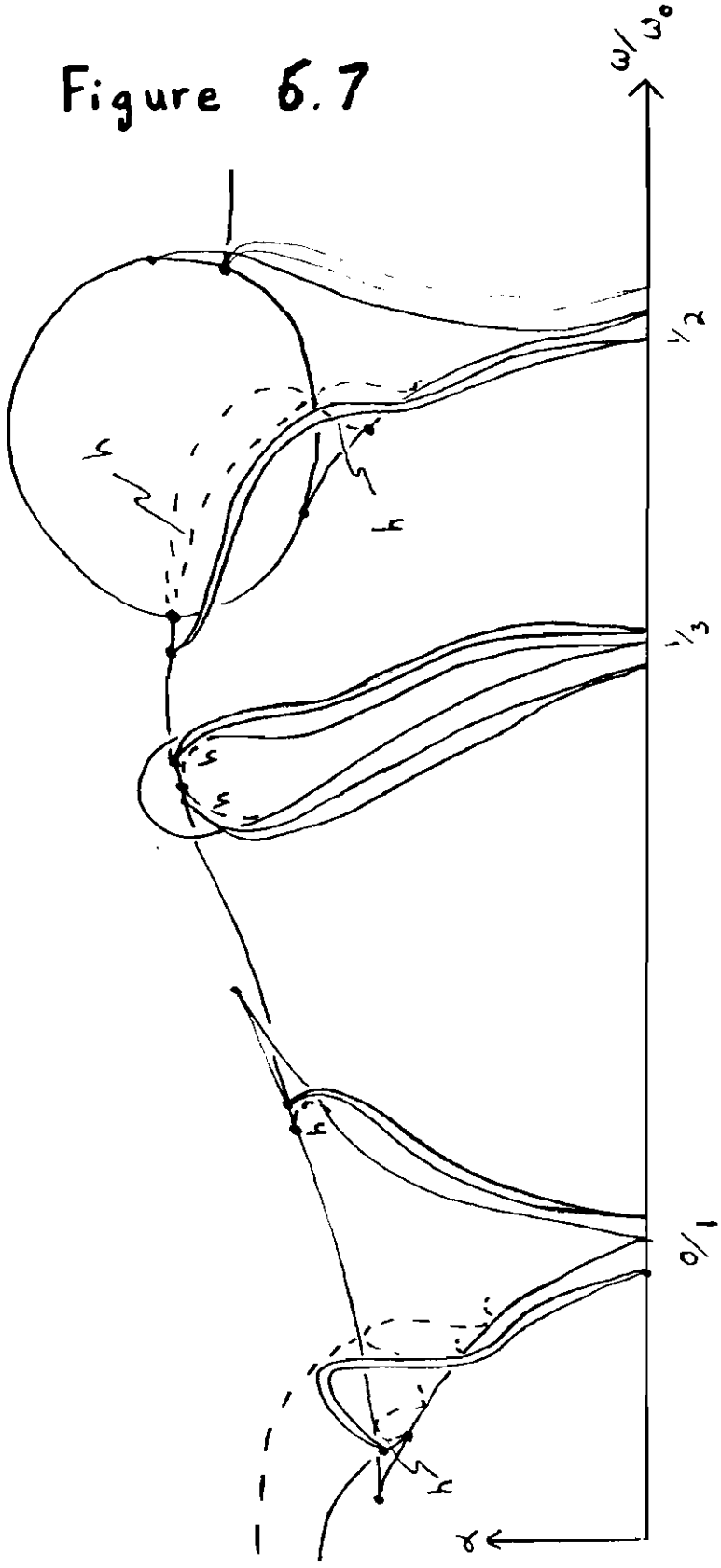

"Overlapping Resonance Horns"

REFERENCES:

Ar Arnol'd, V.I., *Geometrical Methods in the Theory of Ordinary Differential Equations*, Springer Verlag, New York, 1982.

AMKA Aronson, D. G., McGehee, R. P., Kevrekidis, I. G., Aris, R., "Entrainment Regions for Periodically Forced Oscillators," *Phys. Rev. A* **33** (3) 2190-2192, 1986.

ACHM Aronson, D. G., Chory, M. A., Hall, G. R., McGehee, R. P., "Bifurcations from an invariant circle for two-parameter families of maps of the plane: a computer assisted study," *Comm. Math. Phys.*, **83**, 303-354, 1980.

BW Birman, J. S. and Williams, R. F., "Knotted Periodic Orbits in Dynamical Systems - I: Lorentz's Equations," *Topology* **22** (1), 47-82, 1983.

Ch Chenciner, A.. "Bifurcation de points fixes elliptiques. II. Orbites periodiques et ensembles de Cantor invariants," *Inventiones mathematicae*, **80**, 81-106, 1985.

Do Doedel, E. J., "Numerical Analysis and Control of Bifurcation Problems," U. of Minnesota class notes, 1988.

DK Doedel, E. J. and Kernevez, J. P., "AUTO: Software for continuation and bifurcation problems in ordinary differential equations (including the AUTO 86 User Manual)," Report, *Applied mathematics, California Institute of Technology*, 1986.

GH Guckenheimer and Holmes,*Nonlinear Oscillations, Dynamical Systems and Bifurcations of Vector Fields*, Applied Mathematical Sciences, **42**, Springer Verlag, New York, 1983.

GS Golubitsky, M. and Schaeffer, D.,*Singularities and Groups in Bifurcation Theory, Volume I*, Applied Mathematical Sciences, **51**, Springer Verlag, New York, 1985.

Hale Hale, J., *Ordinary Differential Equations*, Wiley-Interscience, New York, 1969.

Hall Hall, G.R., "Resonance Zones in two-parameter families of circle homeomorphisms," *SIAM J. Math. Anal.* **15** (6), 1075-1081, 1984.

KAS Kevrekidis, I. G., Aris, R., Schmidt, L. D., "The Stirred Tank Forced," *Chem. Engng Sci.*, **41** (6), 1549-1560, 1986.

KT Kai, T., Tomita, K., "Stroboscopic phase portrait of a forced nonlinear oscillator," *Progr. Theor. Phys.*, **61** (1), 54-73, 1979.

MSA McKarnin, M., Schmidt, L., Aris, R., "Forced oscillations of a self-oscillating bimolecular surface reaction model," *Proc. R. Soc. Sond. A*, **417**, 363-388, 1988.

Ma Massey, W., *Algebraic Topology: An Introduction*, Harcourt, Brace and World, New York, 1967.

Mat Matsuoka, T., "The number and linking of periodic solutions of periodic systems," *Invent. Math.*, **70**, 319-340, 1985.

Mi Milnor, J., *Morse Theory*, Princeton university Press, Princeton, N. J., 1963.

Mu Munkres, J. R., *Topology, A First Course*, Prentice-Hall, Inc., Englewood Cliffs, New Jersey, 1975.

PK Peckham, B., Kevrekidis, I. G., "The Degenerate Period Doubling Bifurcation for Diffeomorphisms," in preparation.

SDCM Schreiber, I., Dolnik, M., Choc, P., Marek, M., "Resonance Behaviour in Two-Parameter Families of Periodically Forced Oscillators," *Physics Letters A*, **128**, 2, 66-70, 1987.

Ta Takens, F., "Singularities of Vectorfields," *Publ. Math. IHES*, **43**, 47-100, 1974.

Ta2 Takens, F., "Unfoldings of Certain Singularities of Vectorfields: Generalized Hopf Bifurcations," *Journal of Differential Equations*, **14**, 476-493, 1973.